

**POLY(ETHYLENE GLYCOL) HYDROGELS FOR SUSTAINED TOPICAL
DRUG DELIVERY TO THE EYES AND SKIN**

by

SIVA NAGA SREE PRIYA ANUMOLU

A Dissertation submitted to the

Graduate School-New Brunswick

Rutgers, The State University of New Jersey

In partial fulfillment of the requirements

For the degree of

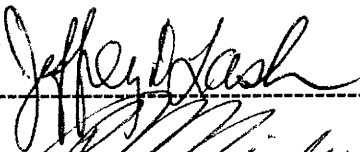
Doctor of Philosophy

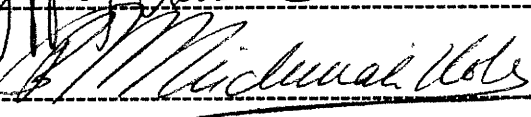
Graduate Program in Pharmaceutical Science

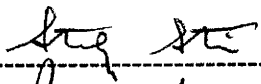
Written under the direction of

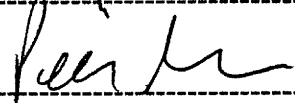
Professor Patrick J. Sinko, Ph.D.

And approved by









New Brunswick, New Jersey

January, 2010

ABSTRACT OF THE DISSERTATION
POLY(ETHYLENE GLYCOL) HYDROGELS FOR SUSTAINED TOPICAL
DRUG DELIVERY TO THE EYES AND SKIN

by **Siva Naga Sree Priya Anumolu**

Dissertation director: Patrick J. Sinko, Ph.D.

Sulfur mustard (SM) is a potent chemical warfare agent that mainly affects the eyes, lungs and skin. Inflammatory cytokines and Matrix Metalloproteinase-9 (MMP-9) have been identified as potential therapeutic targets for SM-induced tissue damage since they quantitatively increase over time in response to SM exposure. Doxycycline is a tetracycline antibiotic with anti-inflammatory properties that acts by inhibiting MMP-9. Currently, neither doxycycline nor doxycycline delivery systems have been investigated for treatment of SM injuries.

The objective of this thesis project is to design and fabricate sustained release topical doxycycline delivery systems and evaluate their wound healing efficacy. Fast forming hydrogels were prepared by crosslinking a poly(ethylene glycol) (PEG)-based polymer containing multiple thiol groups with different polymers or crosslinkers. The optical properties of the hydrogels were evaluated by spectrophotometry and the hydrogels that were transparent or close to transparent were chosen for drug delivery to the eye.

Physicochemical properties of the hydrogels evaluated by rheometry and swelling kinetics show that the hydrogels have good mechanical strength with a low degree of swelling (<8%).

In vitro release profiles of doxycycline-loaded hydrogels demonstrated biphasic release with an initial burst phase followed by a sustained phase. Permeation of doxycycline through vesicant wounded corneas was 2.5 to 3.4 fold higher than through unwounded corneas suggesting that the barrier function of the cornea is compromised after vesicant exposure. Doxycycline hydrogels showed a significant improvement in corneal epithelial healing compared to a similar dose of doxycycline solution in a vesicant-exposed rabbit corneal organ culture model.

The model vesicant, nitrogen mustard (NM) showed dose and time dependent wound progression in SKH-1 mice. The permeability of NM-exposed skin (5 μ moles) to different molecular markers increased significantly compared to the control suggesting that stratum corneum does not act as a barrier for transdermal drug absorption after vesicant exposure. From histology analyses, it is evident that doxycycline hydrogel treated groups showed significant wound healing efficacy compared to untreated or placebo hydrogel treated groups. In summary, *in situ* forming topical doxycycline-loaded PEG hydrogels showed superior wound healing efficacy offering a potential therapeutic option for mustard injuries in the eye and skin.

DEDICATION

**To my wonderful husband and best friend Ranjith,
for his love, endless support and motivation**

**To my parents Bipin Kumar and Devaki Devi,
who made numerous sacrifices over the years for me**

ACKNOWLEDGEMENT

I am very thankful for my loving family who supported and inspired me to make this dissertation possible. Without my husband's love, encouragement, and positive spirit it would have been much tougher to achieve my goal. I am deeply indebted to my parents for their endless patience and support. My dearest friend Ramakrishna, sister Suvarna and brother Harsha are a permanent source of motivation and strength.

I am extremely grateful to my research advisor Professor Patrick J. Sinko for giving me the opportunity to be a part of his achieving, high quality group. His guidance and excellent mentorship have made a tremendous impact in my scientific thought process. I thank my committee members Dr. Stanley Stein, Dr. Bozena Michniak-Kohn and Dr. Jeffrey Laskin for their time, suggestions and ideas that allowed me to advance my research proposal and project. I thank Dr. Marion Gordon's group and Dr. Donald Gerecke's group for being our collaborators and for their support with some crucial studies. A special thanks to Emmy for her advice and encouragement which made me look at life in a more positive perspective.

I am thankful to the past and present members in Dr. Sinko's lab for their help and support: Yash, Hill, Mahta, Sujata, Gao, Matt, Xiaoping, Sung-Hack, Bee and Peidi. I am grateful to Amy, Marianne, Sharana, Hui, Rita, Andrea and John for their timely assistance.

TABLE OF CONTENTS

ABSTRACT OF THE DISSERTATION.....	ii
DEDICATION.....	iv
ACKNOWLEDGEMENT.....	v
LIST OF TABLES.....	xiii
LIST OF FIGURES.....	xiv
1 INTRODUCTION.....	1
2 BACKGROUND AND SIGNIFICANCE.....	5
2.1 Effects of SM exposure on the eye and skin	5
2.1.1 SM.....	5
2.1.2 Effects of SM on eyes	6
2.1.3 Effects of SM on the skin.....	7
2.1.4 Molecular and cellular pathological effects caused by SM	8
2.2 Drug delivery to the eye.....	9
2.3 Drug delivery to the skin	11
2.4 Controlled drug delivery	13
2.5 Hydrogels for controlled topical drug delivery	14
2.5.1 Hydrogels.....	14
2.5.2 Classification of hydrogels	15
2.5.3 Characterization of hydrogels	16
2.5.3.1 Mechanism of drug release	16
2.5.3.2 Degree of swelling	19
2.5.3.3 Rheology.....	20

2.5.4	Optimization of in situ forming hydrogels.....	21
2.5.5	Hydrogels as wound dressings.....	22
2.5.5.1	Skin	22
2.5.5.2	Eye	24
2.5.5.3	Poly(ethylene glycol) (PEG) containing hydrogels	24
2.6	Summary.....	25
3	SPECIFIC AIMS.....	26
4	DESIGN AND EVALUATION OF NOVEL FAST FORMING PILOCARPINE LOADED OCULAR HYDROGELS FOR SUSTAINED PHARMACOLOGICAL RESPONSE	28
4.1	Introduction.....	28
4.2	Materials and methods	31
4.2.1	Materials	31
4.2.2	Copolymer synthesis and characterization.....	32
4.2.3	Hydrogel formation.....	33
4.2.4	Physicochemical characteristics of the hydrogel	33
4.2.4.1	pH titrations	33
4.2.4.2	OT	34
4.2.4.3	Rheological studies	34
4.2.4.4	Transmission Electron Microscopy (TEM)	34
4.2.4.5	Degree of swelling	35
4.2.5	In vitro release studies	35
4.2.5.1	Drug loading efficiency	35

4.2.5.2	In vitro release.....	36
4.2.6	In vivo studies	36
4.2.6.1	Eye irritation test.....	37
4.2.6.2	In vivo efficacy	37
4.3	Results and Discussion.....	39
4.3.1	Copolymer synthesis and characterization.....	39
4.3.2	Hydrogel studies	40
4.3.2.1	Influence of pH on gelation	41
4.3.2.2	OT	41
4.3.2.3	Rheology	41
4.3.2.4	Swelling kinetics.....	43
4.3.3	In vitro pilocarpine loading and release.....	44
4.3.4	In vivo studies	46
4.4	Conclusion	48
4.5	Tables	49
4.6	Figures.....	51
5	EVALUATION OF NITROGEN MUSTARD SKIN WOUND PROGRESSION AND BARRIER PROPERTY IN A MOUSE MODEL	60
5.1	Introduction.....	60
5.2	Materials and methods	62
5.2.1	Materials	62
5.2.2	Dose and time dependent effect of NM on mice skin.....	63
5.2.3	Measurement of inflammatory biomarkers.....	64

5.2.3.1	Measurement of edema	64
5.2.3.2	Measurement of mRNA levels.....	64
5.2.3.2.1	RNA isolation and reverse transcription.....	65
5.2.3.2.2	Real-time polymerase chain reaction.....	65
5.2.4	Evaluation of barrier property of skin by measurement of permeability of molecular markers through NM exposed skin	66
5.3	Results and Discussion.....	66
5.3.1	Dose and time dependent effects of NM on mouse skin	66
5.3.2	Measurement of inflammatory biomarkers.....	68
5.3.2.1	Measurement of edema	68
5.3.2.2	Measurement of mRNA levels.....	68
5.3.3	Permeation profiles of markers through NM exposed skin	69
5.4	Conclusion	72
5.5	Tables	73
5.6	Figures.....	74
6	DOXYCYCLINE LOADED POLY(ETHYLENE GLYCOL) HYDROGELS FOR OCULAR WOUND HEALING APPLICATION	81
6.1	Introduction.....	81
6.2	Materials and methods	84
6.2.1	Materials	84
6.2.2	Hydrogel formation.....	85
6.2.3	Optical Transmission (OT)	86
6.2.4	Rheology.....	86

6.2.5	Swelling studies	87
6.2.6	In vitro doxycycline loading and release	87
6.2.6.1	Drug loading efficiency	87
6.2.6.2	In vitro release.....	88
6.2.7	Ex vivo evaluation using Rabbit Cornea Organ Culture Model+	89
6.2.7.1	Permeation of doxycycline through vesicant exposed rabbit's cornea.	90
6.2.7.2	Wound healing efficacy of doxycycline loaded hydrogels on corneas exposed to CEES and NM	90
6.2.7.3	Detection of MMP-9 in vesicant exposed and treated corneas by immunofluorescence.....	91
6.3	Results and Discussion.....	92
6.3.1	Mechanism of hydrogel formation.....	92
6.3.2	OT	93
6.3.3	Rheology.....	93
6.3.4	Swelling studies	95
6.3.5	In vitro doxycycline loading and release	95
6.3.6	Ex vivo evaluation using Cornea Organ Culture Model.....	97
6.3.6.1	Permeability studies.....	97
6.3.6.2	Wound healing efficacy of doxycycline loaded hydrogels on corneas exposed to CEES and NM.	100
6.3.6.3	Detection of MMP-9 in vesicant exposed and treated corneas by immunofluorescence.....	102
6.4	Conclusions.....	103

6.5	Tables	105
6.6	Figures.....	108
7	DOXYCYCLINE HYDROGELS WITH REVERSIBLE CROSSLINKS FOR DERMAL WOUND HEALING APPLICATION	118
7.1	Introduction.....	118
7.2	Materials and methods	121
7.2.1	Materials	121
7.2.2	Synthesis and characterization of 8-arm-PEG-S-thiopyridyl	122
7.2.3	Hydrogel formation.....	123
7.2.4	Determination of physicochemical properties of the hydrogel.....	124
7.2.4.1	Swelling studies	124
7.2.4.2	Effect of formulation additives	124
7.2.4.2.1	Rheology	125
7.2.4.2.2	DSC.....	125
7.2.5	Reversible nature of hydrogels	126
7.2.6	In vitro release studies	126
7.2.6.1	Drug loading efficiency	126
7.2.6.2	In vitro doxycycline release	126
7.2.7	In vivo studies.....	127
7.2.7.1	Formation of wounds	127
7.2.7.2	Permeation of doxycycline through NM-exposed skin	128
7.2.7.3	In vivo wound healing efficacy of doxycycline hydrogels.....	128
7.2.7.3.1	Application of doxycycline hydrogels	128

7.2.7.3.2	Wound healing efficacy	129
7.3	Results and Discussion.....	129
7.3.1	Synthesis of 8-arm-PEG-S-TP	129
7.3.2	Hydrogel formation.....	130
7.3.3	Reversible nature of hydrogels	131
7.3.4	Degree of swelling	132
7.3.5	Effect of formulation additives	132
7.3.6	Rheology	133
7.3.7	DSC.....	134
7.3.8	In vitro doxycycline loading and release	135
7.3.9	Doxycycline permeation in NM exposed skin.....	138
7.3.10	In vivo wound healing efficacy of doxycycline hydrogels.....	140
7.4	Conclusions.....	143
7.5	Tables	145
7.6	Figures.....	148
8	SUMMARY AND CONCLUSIONS	164
9	REFERENCES.....	166
10	CURRICULUM VITA	188

LIST OF TABLES

Table 2.1. Physicochemical properties of SM.....	6
Table 2.2. Synopsis of SM pathology.....	6
Table 2.3. Ocular dose dependent effects of SM.....	7
Table 4.1. Estimation of diffusional exponent (n) and apparent diffusion coefficient (D) for various HBVS hydrogel formulations.....	49
Table 4.2. Comparison of pharmacological efficacy of 2 % pilocarpine administered ocularly as hydrogel and aqueous solution.....	50
Table 5.1. Permeability coefficients of different molecular markers through skin exposed to NM for 0, 24, 72 and 168 h.....	73
Table 6.1. Composition of 0.25% w/v doxycycline PEG hydrogel formulations evaluated for ocular wound healing efficacy.....	105
Table 6.2. Estimation of flux and diffusion exponent (n) for various NHS hydrogel formulations.....	106
Table 6.3. Estimation of lag time and permeation coefficient of doxycycline through vesicant-exposed corneas.....	107
Table 7.1. Composition of PEG hydrogel formulations evaluated for dermal wound healing.....	145
Table 7.2. Estimation of flux and diffusion exponents (n) for H ₂ O ₂ and S-TP hydrogel formulations.....	146
Table 7.3. Estimation of flux and permeability coefficients for doxycycline through NM exposed skin	147

LIST OF FIGURES

Scheme 4.1. Synthesis of PEG based copolymer	51
Figure 4.1. The GPC profile of crude polymerization reaction mixture obtained after 24 h.....	52
Figure 4.2. TEM images of 3 % (A) and 5 % (B) HBVS hydrogels prepared using copolymer and crosslinker in 1:1 stoichiometry.....	53
Figure 4.3. Optical transmissivities of 3, 4, 5 and 6 % HBVS hydrogels prepared using copolymer and crosslinker in 1:1 or 1:2 stoichiometries.. ..	54
Figure 4.4. Influence of strain (A) and frequency (B) on G' and G'' of HBVS hydrogels.....	55
Figure 4.5. Swelling kinetics of the HBVS hydrogels as a function of time.	56
Figure 4.6. Fractional release of pilocarpine as a function of time for 3, 4, 5 and 6 % w/v HBVS hydrogels prepared using 1:1 (A) and 1:2 (B) stoichiometries.	57
Figure 4.7. Decrease in pupil diameter vs. time for pilocarpine-loaded hydrogel and pilocarpine solution in PBS.	58
Figure 4.8. Correlation between in vitro pilocarpine release and pupillary constriction obtained in vivo.....	59
Figure 5.1. Dose dependent effects of NM exposure on mice skin visualized by H & E staining (10 x).....	74
Figure 5.2. The histology of time dependent effects of NM exposure on mice skin at 10 x magnification visualized by H & E staining.....	75

Figure 5.3. Time dependent inflammatory response of NM on mice skin measured by edema.....	76
Figure 5.4. Time dependent effect of NM exposure on mice skin measured from the mRNA levels of IL-1 β and TNF- α	77
Figure 5.5. Permeation profile of 3[H] mannitol (hydrophilic marker) through NM exposed mice skin.....	78
Figure 5.6. Permeation profile of FITC-dextran's (molecular weight markers) through NM exposed mice skin.....	79
Figure 5.7. Permeation profile of rhodamine 123 (lipophilic marker) through NM exposed mice skin.....	80
Scheme 6.1. NHS hydrogel formation.....	108
Scheme 6.2. Mechanism of formation of thioester bonds	109
Figure 6.1. Optical transmission of 5% (1:1), 7.5% (1:1), 7.5% (1:2), 10% (1:1), 15% (1:2), 15% (1:1), and 22.5% (1:2) NHS hydrogels.....	110
Figure 6.2. Influence of strain on G' (A) and G'' (B) of 5% (1:1), 7.5% (1:1), 7.5% (1:2), 15% (1:1), and 15% (1:2) NHS hydrogels.....	111
Figure 6.3. Influence of frequency on G' (A) and G'' (B) of 5% (1:1), 7.5% (1:1), 7.5% (1:2), 15% (1:1), and 15% (1:2) NHS hydrogels.....	112
Figure 6.4. Effect of polymer concentration and crosslinking density on the swelling kinetics of 5% (1:1), 7.5% (1:1), 7.5% (1:2), 10% (1:1), 15% (1:1), 15% (1:2), and 22.5% (1:2) NHS hydrogels.....	113
Figure 6.5. Cumulative amount of doxycycline released as a function of time for NHS hydrogels: 10% (1:1), 15% (1:2), 15% (1:1), and 22.5% (1:2).....	114

Figure 6.6. Cumulative amount of doxycycline permeated as a function of time through cornea exposed to different concentrations of CEES and NM.....	115
Figure 6.7. H & E staining to visualize the histology of CEES and NM-exposed corneas treated for 24 h with doxycycline in solution or in NHS hydrogel.....	116
Figure 6.8. Immunofluorescent staining of corneas exposed to CEES and NM and subsequently treated with doxycycline either in solution or NHS hydrogel.....	117
Scheme 7.1. H ₂ O ₂ hydrogel formation.....	148
Scheme 7.2. S-TP hydrogel formation.....	149
Scheme 7.3. Schematic representation of the reversible nature of hydrogels.....	150
Figure 7.1. DSC thermograms of 8-arm-PEG-SH and 8-arm-PEG-S-TP	15351
Figure 7.2. XPS analysis of 8-arm-PEG-S-TP	15452
Figure 7.3. Effect of the concentration of polymers on swelling kinetics of 4, 8 % H ₂ O ₂ hydrogels and 5, 8 % S-TP hydrogels.....	1533
Figure 7.4. Influence of strain (A) and frequency (B) on G' and G'' of 4 and 8 % H ₂ O ₂ hydrogels with and without formulation additives..	154
Figure 7.5. Influence of strain (A) and frequency (B) on G' and G'' of 5 and 8 % S-TP hydrogels with and without formulation additives.....	1555
Figure 7.6. The DSC thermograms for the 4 and 8 % H ₂ O ₂ hydrogels with and without formulation additives..	1566
Figure 7.7. The DSC thermograms for the 5 and 8 % S-TP hydrogels with and without formulation additives.....	1577

Figure 7.8. Cumulative amount of doxycycline released as a function of time for 4 and 8 % H ₂ O ₂ hydrogels and 5 and 8 % S-TP hydrogels.	15858
Figure 7.9. Cumulative amount of doxycycline permeated as a function of time through NM-exposed skin.....	159
Figure 7.10. Histology of mice skin exposed to NM and subsequently treated with H ₂ O ₂ /S-TP placebo or doxycycline hydrogels at 24 h.....	160
Figure 7.11. Histology of mice skin exposed to NM and subsequently treated with H ₂ O ₂ /S-TP placebo or doxycycline hydrogels at 72 h.....	161
Figure 7.12. Histology of mice skin exposed to NM and subsequently treated with H ₂ O ₂ /S-TP placebo or doxycycline hydrogels at 168 h.....	162
Figure 7.13. Histology of mice skin exposed to NM and subsequently treated with H ₂ O ₂ /S-TP placebo or doxycycline hydrogels at 240 h.....	163

1 INTRODUCTION

Sulfur Mustard (SM) is a potent chemical warfare agent and is the most abundantly produced and stockpiled vesicant worldwide [1]. Injuries produced by SM are more pronounced in the eyes, lungs and skin [1]. The eyes are most sensitive to SM and symptoms such as conjunctivitis, grittiness under the eyelid, tearing, corneal edema, photophobia, severe blepharospasm, corneal damage, ulceration and perforation occur depending on the dose and time of exposure [2]. SM rapidly penetrates the skin causing edema, erythema, blisters, lesions, ulceration and necrosis depending on temperature, moisture, and anatomical location of the site of exposure and also on the absorbed dose [3]. The specific pathogenic and molecular mechanisms responsible for SM induced injury remains unclear, but alkylation of resident proteins is considered to be responsible for disruption of the tissue organization both in the eyes and skin [1]. In recent years, the targeting of civilian populations by groups willing to employ chemical warfare agents has intensified our need to develop countermeasures. The most devastating aspect of SM exposure is that wound healing occurs over a prolonged time period as compared to other blister-forming injuries resulting from, for example ultraviolet (UV) exposure. The current research project focuses on developing countermeasures for the treatment of SM-exposed eyes and skin.

Although the molecular mechanisms of SM induced injury are unclear, SM can alkylate DNA, RNA, and proteins causing inflammation, tissue damage and cell death [3]. MMPs are a family of proteases that enhance the action of many activating factors during the

inflammatory response and contribute to tissue degradation [4-16]. MMP-9 quantitatively increases over time in response to SM exposure and is a potential target of therapy for SM damage [12, 13]. Clinically impaired corneas resulting from SM exposure were characterized mainly by chronic inflammation and increased MMP activity [17]. The level of MMP-9 decrease was correlated with accelerated wound healing [18, 19]. Intervention strategies targeting the inflammatory response and increased protease expression could provide an approach for treating SM-induced injuries in both the eye and skin.

Doxycycline is an inexpensive, Food and Drug Administration (FDA) approved antibiotic that could potentially promote wound healing by reducing inflammation and protease activity at the wound site. Doxycycline belongs to the tetracycline class of antibiotics with anti-inflammatory properties resulting from the inhibition of MMP-9. Doxycycline was found to inhibit MMP-9 activity in skin keratinocytes [20], endothelial cells [21], human corneal epithelial cells [22, 23], prostate cancer cells [24, 25], and corneal epithelial cells of experimental dry eye [26]. Doxycycline treatment has been shown to be beneficial in the attenuation of acute and delayed ocular injuries [27, 28] and respiratory tract lesions [29] caused by SM exposure.

Eye drops (i.e., solutions) are conventional dosage forms used for ocular drug delivery. However, they are rapidly cleared from the eye resulting in short residence time and reduced drug bioavailability. A drug delivery system that prolongs the contact time with the cornea and provides sustained drug release might help in accelerating the wound

healing process. This is especially true if the barrier properties are compromised and residence time is very short. Traditional wound dressings of the skin include topical formulations and wound dressings. Many synthetic wound dressings have been developed during the mid 1990's to prevent bulk loss of tissues or non healing wounds such as trauma, burn, diabetic and venous stasis ulcers [30]. However most of the wound dressings only protect the damaged tissue and do not play a significant role in healing of wounds. An ideal wound dressing for the skin should be easily applicable and removable, protect the wound from bacterial contamination and provide a sustained drug release that will improve wound healing.

Hydrogels are an attractive class of biocompatible polymers that are increasingly being used for controlled release applications. Hydrogels are a crosslinked network of hydrophilic polymers that have the ability to absorb large amount of water and swell, while maintaining their three-dimensional structure. Molecules of different sizes can diffuse into and out of the hydrogel network, which allows for their possible use as a drug-depot for controlled release applications. Hydrogels show minimum tendency to adsorb protein from body fluids due to their low interfacial tension and they also closely resemble living tissue due to their high water content, and soft/rubbery characteristics [31]. As a result of these favorable properties, hydrogels are used as scaffolds in tissue engineering and drug delivery systems in various biomedical and pharmaceutical applications. Since hydrogels require minimal regulation, they are designated as Class I devices by FDA [32]. Hydrogels containing PEG are most widely used for their good

hydrophilicity, strength, easy processability, high stability to temperatures and pH, minimum cell adhesion and protein absorption [33, 34].

Therefore, a PEG based hydrogel system loaded with doxycycline, an MMP-9 inhibitor, may possibly provide sustained drug release at the site of SM injury and accelerate wound healing.

2 BACKGROUND AND SIGNIFICANCE

The concepts that relate to the significance of developing a PEG based hydrogel drug delivery system for topical application to the eyes and skin for treatment of mustard wounds are discussed in this chapter. The references cited throughout the chapter provide more detailed insight to each topic that is presented.

2.1 Effects of SM exposure on the eye and skin

2.1.1 SM

Although SM was first synthesized in 1822, it was identified and used as a chemical warfare agent during World War I [1, 35]. The synonyms used for SM are Hun Stoff distilled (HD), mustard gas, yellow cross, Yperite, lost and pyro. It is the most abundantly produced and stockpiled vesicant worldwide, because it is cheap and easy to synthesize [1]. SM injured over 100,000 Iranians during the Iran-Iraq war (1983-1988) [36, 37]. SM exposure mainly affects the eyes, lungs and skin. The Central nervous system (CNS), endocrine system, gastrointestinal tract (GIT) and hematopoietic system are also affected by SM exposure [38-40].

SM is a pale yellow to brown oily liquid that has poor solubility in water but good solubility in organic solvents. The physicochemical properties of SM are summarized in Table 2.1 [1].

Chemical formula	$C_4H_8Cl_2S$
Appearance	Oily liquid, light yellow to dark brown
Odor	Mustard, garlic and onion
Molecular weight	159.08
Liquid density	1.27 (specific gravity)
Freezing point	13°C-14°C
Boiling point	215°C-217°C
Volatility (mg/m ³ , 20°C)	610
Solubility	Poor in water, high in ethanol

The pathological effects of SM are due to the formation of a cyclic sulfonium ion that alkylates nucleophilic cellular sites in the tissue [41]. Acute toxic effects after SM exposure have been observed after a variable length of latency period depending on the dose, form (vapor/ liquid), time of exposure and individual's susceptibility [42, 43].

Table 2.2. gives a synopsis of SM pathology [1].

Gross pathology	Histopathology and cytopathology	Molecular pathology
Erythema Pain Blisters Pseudomembranes Ulcers Impaired wound healing	Cellular infiltrate Separation of cellular layers Apoptosis Necrosis	Cytokines (IL-1, IL-6, IL-8 and TNF- α) Prostaglandins Matrix metalloproteinases Serine proteases Caspase activation DNA adducts Cell cycle arrest Oxidative stress Intracellular Ca ⁺⁺ increase Impaired energy metabolism

2.1.2 Effects of SM on eyes

The eyes are most sensitive to SM with a very short (30 - 60 min) latency period after exposure as compared to other organ systems [2]. High concentrations may cause eye

pain within 30 minutes [44]. The ocular dose dependent effects of SM are summarized in Table 2.3.

Dose of SM (mg·min/m³)	Ocular effects
12-70 50-100 > 200	Mild ocular irritation Conjunctivitis, grittiness under the eyelid, and tearing. Eyelid and corneal edema, impairment of vision, photophobia, and severe blepharospasm

The high susceptibility of the eyes to SM is due to the presence of a thin cornea continuously covered by tear fluid. The presence of moisture favors the formation of reactive SM intermediates [45]. Thus, SM easily penetrates through the ocular epithelia. Conjunctival and corneal edema is observed several hours after SM exposure. Conjunctival goblet cells disappear over time leading to decreased production of mucus. Severe endothelial damage results from occlusion of conjunctival vessels [46]. Ocular pain and blepharospasm occurs as a result of damaged nerve endings in the cornea. The cornea detaches from the stroma resulting in the formation of small vesicles. Severe exposure to SM causes extended destruction of the limbal blood vessels [2], chemical anterior uveitis, corneal necrosis, and lens opacification [47].

2.1.3 Effects of SM on the skin

The skin's susceptibility to SM exposure mainly depends on temperature, moisture, and anatomical location. Body areas which are moist with thin epidermal layers are highly sensitive to SM exposure. The onset of symptoms depends on the vapor concentration and exposure time. Higher doses are known to shorten the symptom free latency period. Itching and erythema are observed 4 - 8 h after SM exposure at a vapor dose of 100–300

mg·min/m³ and liquid dose of 10–20 µg/cm². At much higher doses (vapor: 1000–2000 mg·min/m³, liquid: 40–100 µg/cm²) blister formation occurs [3]. Initially small blisters (vesicles) are formed in the erythemic area which coalesce to form large blisters (bullae) [48]. A positive Nikolsky sign (increased friction aggravates local damage) is observed in skin sites exposed to SM. Blisters can occur several weeks after exposure, despite any further contact with SM [1, 49].

SM mainly affects the epidermis which is the outermost layer of skin. Edema, inflammation and cell death are observed mainly at the basal keratinocyte layer. The rapidly proliferating keratinocytes of the basal layer are the main target of SM exposure. Histopathologically this layer shows highest cell damage like karyolysis and pyknosis [50, 51]. Blister formation occurs between the epidermis and dermis and is observed several hours after SM exposure [52, 53]. The dermis is comparatively less affected and shows signs of discrete necrosis, decreased number of fibroblasts and histiocytes. Biopsies at the exposed areas often have no epidermis, exhibit necrosis, massive cellular infiltration, capillary engorgement and thrombosis [51]. Cell death, separation of cellular layers, and cellular infiltrate are the common histopathological changes that occur both in the eyes and skin after SM exposure.

2.1.4 Molecular and cellular pathological effects caused by SM

SM induced cytotoxicity is caused by the reaction of SM with proteins, RNA, DNA and phospholipids [1, 54]. High SM concentrations induce enhanced production of reactive oxygen species by depleting the antioxidant defense systems in the body, especially

glutathione levels [55, 56]. SM alkylation of DNA mainly at the N7 of guanine forming 7-(2-hydroxyethylthioethyl) guanine (7-HETEG) [57-59] plays an important role in the delayed wound healing of SM injuries [60]. SM activates PARP-1 resulting in depletion of NAD^+ and ATP, inhibition of cellular energy metabolism, protease release and necrotic cell death [61-63].

SM injury causes activation of several proteases and proinflammatory cytokines. Of the proteases, MMPs are the main players in skin pathology of SM-induced blisters [12, 13] and in junctional epidermolysis bullosa (JEB) [16]. Studies with the mouse ear model suggest that MMP-9 is the most upregulated MMP in SM-exposed skin [13]. Several proinflammatory mediators are released shortly after SM exposure, the most important of them being IL - $1\alpha/\beta$, IL - 6, IL - 8, TNF - α , GM-CSF and iNOS [12, 64-68]. The release of cytokines can induce a strong chemotactic response that attracts neutrophils and macrophages. The number of infiltrating cells is dependent on dose and time of SM exposure [69]. SM induces the cyclooxygenase (COX) pathway resulting in the production of eicosanoids (prostaglandins, thromboxanes, and leukotrienes) from phospholipids. SM induced inflammation has been shown to be reduced by COX inhibition [70].

2.2 Drug delivery to the eye

Ocular tissues are protected from toxic substances in the environment and the bloodstream by tear secretions that continuously flush its surface, an impermeable corneal epithelium and membrane transporters actively clearing the retina of agents that

can potentially disturb the visual process [71]. However, the same protective mechanisms act as barriers to ocular drug delivery. The annular tight junctions completely surround and effectively seal the corneal epithelial cells by providing a diffusional barrier to drug absorption into the anterior chamber of the eye [72]. Hence, the corneal epithelium is the rate limiting barrier to ocular penetration of topically applied drugs [73, 74].

Physiological barriers to the diffusion and absorption of topically applied ocular drugs exist in the precorneal and corneal spaces. Solution drainage, lacrimation and tear dilution, tear turnover, conjunctival absorption and corneal epithelium are the main factors that limit the ocular contact time and bioavailability of topical solution dosage forms resulting in a short duration of pharmacological response [75, 76]. The residence time of most conventional ocular solutions ranges between 5-25 minutes [77-79]. Only 1-10 % of topically applied drug is absorbed [80], which also includes absorption from the GIT due to drainage through the nasal-lacrimal duct [81]. As a result, a frequent dosing regimen is necessary to achieve therapeutic efficacy [82]. However, frequent instillation of eye drops containing drugs like pilocarpine result in local side effects such as headaches due to ciliary muscle spasm, decreased vision in poor illumination due to miosis, and accommodative myopia [83]. Ocular delivery systems with prolonged ocular residence time such as ointments and suspensions have been developed to overcome these challenges and increase ocular drug bioavailability [84, 85]. There are, however, several limitations that reduce patient compliance. For example, ointments are greasy and produce blurred vision [86, 87]. Similarly, non-erodible inserts such as Ocusert are difficult to administer and remove, have problems with retention, unnoticed loss of the

unit from the eye and rupture of its membrane causing excessive bolus drug release [88, 89]. The major goal in ocular drug delivery is to circumvent these structural obstacles and protective mechanisms and to obtain desired pharmacological response [71].

2.3 Drug delivery to the skin

Skin is the largest organ of the body. The stratum corneum which is the outermost layer of the skin particularly determines its barrier function by protecting the body from intrusion of toxins and also drugs released from topically applied formulations [90, 91]. However, the barrier properties of skin are expected to compromise during burns, wounds and ulcers. Therefore, technologies that are developed to overcome the barrier function of skin and effectively deliver drugs transdermally will be of little relevance to the proposed thesis project.

Topical wound healing agents include liquid and semi-solid formulations as well as dry dressings. Topical formulations are prepared as liquids (solutions, suspensions and emulsions) and semi-solids (ointments, pastes and creams). Antimicrobial agents such as silver, povidone-iodine [92], and polyhexamethylene biguanide [93] are sometimes incorporated into dressings to control or prevent infection [94]. Physiological saline solution has also been used traditionally for cleansing of wound and dead tissue removal [95, 96]. Liquid dosage forms have a short wound contact time, and are not particularly useful when there is a measurable degree of exuding wound fluid. Semi-solid preparations have been used to increase wound residence time. However, they are not very effective for highly exuding wounds as they rapidly absorb fluid, become mobile

and lose their rheological characteristics [94]. Skin wound dressings mainly include cotton, lint, wool, gauzes and bandages. Unlike the topical formulations, these dressings are dry and do not provide a moist wound environment. They may be used as primary or secondary dressings, or form part of a composite of several dressings [94].

Wound dressings recently developed represent an improvement over traditional wound healing agents that essentially retain and create a moist environment around the wound to facilitate wound healing. Modern dressings are classified according to the materials from which they are produced including hydrocolloids, alginates and hydrogels that generally occur in the form of gels, thin films or foam sheets [94]. Hydrocolloid dressings are used for light to moderately exuding wounds such as pressure sores, minor burns, abrasions, lacerations, post-operative wounds and traumatic injuries. Because of their occlusive outer cover, hydrocolloid dressings prevent water vapor exchange between the wound and are not suitable for infected wounds that require a certain amount of oxygen to heal rapidly [95, 97]. Alginate dressings are useful for medium to heavily exuding wounds. Because they are so absorptive, alginate dressings cannot be used for dry wounds or those covered with hard necrotic tissue as they dehydrate the wound and delay healing [94]. Foam dressings are porous making them suitable for partial and full thickness wounds, as well as for wounds with moderate to heavy exudates. Foam dressings are not suitable for dry epithelializing wounds as they rely on exudates to achieve an optimum wound healing environment [98]. Hydrogel wound dressings will be elaborated in the forthcoming sections.

An ideal wound dressing for the skin should be easily applicable and removable, protect the wound from bacterial contamination, provide a moist environment around the wound, provide effective oxygen circulation to aid regenerating cells and tissues and provide a sustained release of drug that will help accelerate wound healing.

2.4 Controlled drug delivery

The advantages of controlled drug delivery are reduction in dosage frequency, predictable, and reproducible drug release rates for extended periods, uniform pharmacological response, reduction in GI irritation, and other dose and drug related side effects and increased patient compliance [99]. Controlled delivery dressings can provide an excellent means of delivering drugs to wound sites in a consistent and sustained fashion over long periods of time without the need for frequent dressing change. Synthetic, semi-synthetic and naturally derived polymeric dressings are potentially useful in the treatment of wounds. They result in increased local concentration of drugs while avoiding high systemic doses [100] thus reducing patient exposure to an excess of drug beyond that required at the wound site [101]. The ideal drug delivery system should be inert, biocompatible, mechanically strong, comfortable for the patient, capable of achieving high drug loading, safe from accidental release, simple to administer and remove and easy to fabricate.

2.5 Hydrogels for controlled topical drug delivery

2.5.1 *Hydrogels*

Hydrogels are polymeric networks with a three-dimensional configuration capable of imbibing large amounts of water or biological fluids without dissolving [102, 103]. The affinity to absorb water results from presence of hydrophilic groups such as $-\text{OH}-$, $-\text{CONH}-$, $-\text{CONH}_2-$, and $-\text{SO}_3\text{H}$ in the polymers used for the preparation of hydrogels [104]. A hydrophilic polymer is hydrated to a greater extent (up to 95 %) than a hydrophobic polymer (< 5-10 %) depending on the nature of the aqueous environment and polymer composition [105]. The hydrogels resemble living tissues more so than any other class of synthetic biomaterials, which is due to their high water content, soft and robbery consistency and low interfacial tension with water or biological fluids [106]. As a result of these favorable properties, hydrogels are increasingly being used as scaffolds in tissue engineering [107] and drug delivery systems for various biomedical [108] and pharmaceutical [31, 109-111] applications.

Hydrogels can be comprised of (i) natural polymers such as chitosan, dextran, agarose, alginate and cellulose derivatives, (ii) synthetic polymers and copolymers such as PEG, derivatives of PEG, hydroxyethyl methacrylate (HEMA) and poly(glutamic acid) and (iii) combinations of natural and synthetic polymers such as collagen acrylate, alginate acrylate and P(PEG-co-peptides) [112]. Hydrogels made from natural polymers may not provide sufficient mechanical strength that is important to maintain their physical integrity *in vivo* and to prevent burst drug release. Natural polymeric hydrogels may also contain pathogens that evoke immune/inflammatory responses. However, they are

biodegradable and have biologically recognizable moieties that support cellular activities. Synthetic hydrogels, do not possess these inherent bioactive properties, but usually have well-defined structures that can be modified to yield tailorable degradability and functionality [113]. The crosslinks in the hydrogels are physical (entanglements or crystallites) or chemical (tie-points and junctions) [103, 114-118]. These crosslinks are formed by covalent bonds, hydrogen binding, van der Waals interactions, or physical entanglements [119, 120].

2.5.2 Classification of hydrogels

Preparation of hydrogels is mainly by physical [121, 122] and chemical crosslinking [123, 124]. Physical crosslinking of polymer chains can be achieved using a variety of environmental triggers such as pH, temperature, ionic strength and a variety of physicochemical interactions such as hydrophobic interactions, charge condensation, hydrogen bonding, stereo complexation or supramolecular chemistry [125]. The disadvantage with physical crosslinking is that the crosslinking network may be deformed or damaged at applied stresses lower than those required to disrupt covalent crosslinks [126]. The strength of a physically crosslinked hydrogel is directly related to the chemical properties of the constituent gelators and hence it is difficult to decouple variables such as gelation time, degradation time, pore size and chemical functionalization which restricts the design flexibility of these hydrogels [125]. Chemical crosslinking is achieved by using a crosslinking agent, which can condense with the reactive side or terminal groups of the polymer chain. A desired crosslinking ratio may be achieved by suitably varying the amount of polymer and crosslinking agent used in the

reaction, and the chemical reactions do not involve elaborate procedures or equipment [127].

Hydrogels can further be classified as preformed [128, 129] or *in situ* forming [130-132] based on their physical state at the time of their application. Preformed hydrogels are simple viscous solutions [128] or hydrogel films [129], which gel outside the site of application and do not undergo any modification after administration. *In situ* forming hydrogels are liquids upon instillation and undergo a phase transition to form a viscoelastic gel in response to environmental changes like temperature [130, 132], pH [133], and electrolyte composition [134]. *In situ* forming hydrogels are attractive as drug delivery systems because of facile dosing as a liquid, which insures rapid and complete coverage at the site of action. They also allow for accurate and reproducible quantities to be administered in contrast to pre-gelled formulations [77]. Also *in situ* forming drug delivery systems are widely accepted, since they serve as a depot for the sustained release of the entrapped compound without invasive surgical placement [135]. However, *in situ* hydrogels are often unstable and reversible. One of the drawbacks of *in situ* gelation is the high risk of a significant burst effect due to the lag time for gelation [136]. The burst effect is dependent to some extent on the nature of the drug incorporated in the hydrogel with hydrophilic drugs exhibiting a greater burst effect than hydrophobic drugs [136].

2.5.3 Characterization of hydrogels

2.5.3.1 Mechanism of drug release

The fundamental goal of sustained drug delivery systems is to achieve a constant release rate over a prolonged period of time. Various factors controlling the rate of drug release from hydrogels include method of preparation of the hydrogel, molecular weight of the polymer and crosslinking density. Additionally, size of the drug molecule, drug solubility, drug loading, and the type and strength of the interactions between the crosslinker and polymer chains that form the hydrogel network are important in controlling drug release [108, 137].

Understanding the mechanisms and identifying the key parameters that govern drug release from hydrogels represents the first step towards predicting the release profile. Drug release from a delivery system encompasses both dissolution of drug in the release medium and diffusion of drug from the polymer matrix. It may occur by diffusion, chemical reaction or solvent activation [31]. Drug diffusion within highly swollen hydrogels is best described by Fick's law of diffusion or Stefan–Maxwell equations [138]. Diffusion controlled hydrogel delivery systems can be either reservoir or matrix systems [139]. In both systems the drug migrates from its initial position in the polymer system to the outer surface prior to being released [136].

For a reservoir system where the drug depot is surrounded by a polymeric hydrogel membrane, Fick's first law of diffusion can be used to describe drug release through the membrane:

$$J_A = -D \frac{dC_A}{dx} \quad (1)$$

For a matrix system where the drug is uniformly dispersed throughout the matrix, unsteady state drug diffusion in a one-dimensional slab-shaped matrix can be described using Fick's second law of diffusion:

$$\frac{dC_A}{dt} = D \frac{d^2C_A}{dx^2} \quad (2)$$

Where, J_A is the flux of drug A, D is the drug diffusion coefficient, C_A is drug concentration and x is the time. For computational simplicity, Fick's law of diffusion as described above are based on the assumption that the diffusion coefficient (D) is independent of concentration and that diffusion occurs in one dimension.

Hydrogels are regarded as swelling controlled systems, since the absorption of water from the environment changes the dimension and physical properties of the system and drug release [31]. Thus, drug release is typically Non-Fickian occurring via a combination of convective transport and diffusion, depending on the state of the hydrogel. Drug release from hydrogels in the equilibrium swollen state follows Fick's second law of diffusion. However, in hydrogels that contain different phases in various degrees of hydration (glass core surrounded by a swollen phase), drug release occurs via a combination of Fickian diffusion and convective transport [136].

The relative importance of diffusion and polymer relaxation on the mechanism of drug release can be determined by fitting the experimental data to the Ritger-Peppas equation [140] and determining the exponent n . Equation 3 can only be applied to the first 60 % of the total amount of drug released.

$$\frac{M_t}{M_\infty} = kt^n \quad (3)$$

Where, k is a structural/geometric constant for a particular system and n is designated as release exponent representing the release mechanism.

Drug release from the hydrogel can be classified into four types based on the relative rates of diffusion and polymer relaxation [31, 136].

Case I (Fickian diffusion), which occurs when the rate of diffusion is significantly less than that of polymer relaxation ($n = 0.5$).

Case II (Relaxation controlled transport), which occurs when diffusion is rapid compared with the polymer relaxation process ($n = 1$).

Non-Fickian (Anomalous diffusion), which occurs when the diffusion and polymer relaxation rates are comparable ($0.5 < n < 1$).

Super Case II transport, which occurs when the polymer undergoes relaxation as the hydrogel swells ($n > 1$).

The drug release mechanism from a hydrogel mainly depends on the method of hydrogel formation, type of polymer, concentration of polymer, concentration of crosslinker, crosslinking density, pore size, solubility of the drug in the release medium, and molecular size and weight of the drug. By modifying the above factors, drug release from a hydrogel can be tailored as required.

2.5.3.2 Degree of swelling

The equilibrium degree of swelling of the hydrogel directly influences the rate of water sorption, the permeability to drugs and the mechanical strength of the hydrogel. There is a direct relationship between hydrogel swelling and solute permeability. Specifically, as the hydrogel swelling is reduced, the mobility of solute becomes restricted due to a smaller average pore size of the hydrogel network. Therefore, reducing the degree of swelling of the hydrogel by increasing the crosslinking of the network will reduce the molecular weight cut off for the hydrogel. This effect has been exploited in an attempt to control drug release from hydrogels.

The crosslinking ratio and the chemical structure of the polymer control the degree of swelling of the hydrogel [31]. Tighter hydrogels with a lower degree of swelling are produced by increasing the crosslinking ratio [141]. Modifying the hydrophilic or hydrophobic nature of the polymer also affects the degree of swelling of the hydrogel with hydrophilic groups resulting in greater swelling [142].

2.5.3.3 Rheology

The mechanical strength and viscoelastic properties of the hydrogels can be investigated using rheological measurements to assess their retention behavior and physical integrity *in vivo* [143, 144]. Analysis of the rheological behavior of hydrogels can be used to study the effects of the type of polymer and crosslinker, concentration of polymer and crosslinker as well as crosslinking density on the viscoelastic properties of hydrogels as determined by strain sweep test and frequency sweep test. The strain sweep test allows for the determination of linear viscoelastic (LVE) regime of the hydrogel and can be used

to determine the subsequent choice of strain value to be used in the frequency sweep test. The frequency sweep test provides a ‘fingerprint’ of a viscoelastic system under non destructive conditions [145, 146]. Both the strain sweep test and frequency sweep test are used to obtain rheological parameters such as the storage/elastic modulus (G'), loss/viscous modulus (G'') and loss tangent/phase angle ($\tan\delta = G''/G'$). G' represents the elastic storage of energy and is a measure of the well structuredness of the hydrogel. G'' represents the viscous energy dissipation and changes depending on the viscosity of the hydrogel. In the presence of a gel structure, G' and G'' are independent of frequency and $\tan\delta$ is small. For concentrated solutions, G' and G'' are dependent on frequency and the $\tan\delta$ is variable [147].

2.5.4 Optimization of in situ forming hydrogels

Successful optimization of *in situ* hydrogels includes several factors. The concentration of the polymers and crosslinkers used to prepare the hydrogel influences both the diffusion based drug release kinetics and the degradation time of the hydrogel. However, the concentration of polymers or their functionalized derivatives is often limited by the aqueous solubility of the gel precursors or the resulting high viscosity of the solutions, although the concentration can be increased when lower molecular weight gel precursors are used. The rate of *in situ* crosslinking is determined by the underlying chemical kinetics of the crosslinking reaction, the ease of diffusion of the polymer precursors through the partially viscous pre-gel solution, and the concentration of polymers and crosslinkers used to prepare the hydrogel. The crosslinking density in the hydrogels can be controlled by the amount of polymer and crosslinker added and/or the density of

reactive functional groups on the polymers. Higher crosslinking densities result in hydrogels with smaller pore sizes, thereby reducing the release rate of entrapped drugs. Also higher crosslinking densities can increase the mechanical strength of the hydrogel. However, the high degree of chemical modification required to form hydrogels with high crosslink densities can significantly alter the physical properties of the base hydrogel, particularly in terms of the drug–hydrogel affinity. Thus, trade-offs must be made in the hydrogel design according to the targeted application of the hydrogel.

2.5.5 Hydrogels as wound dressings

2.5.5.1 Skin

The advantages of hydrogels compared to other wound dressings for skin are fluid absorption, hydration of the wound bed, cooling of the wound surface which may lead to a marked reduction in pain and therefore high patient acceptability. Hydrogels are permeable to water vapor and oxygen, but do not leak liquid water [148]. Depending on the state of hydration of the tissue, the hydrogel can absorb or donate water to the wound environment [149]. Hydrogels leave no residue, are malleable and improve reepithelization of wounds. Amorphous hydrogels have been demonstrated to be useful in treating sloughy and necrotic wounds [150-153]. Also, hydrogels are transparent or semitransparent, permitting some visual observation of the wound without removing the dressing [154].

The maintenance of a moist wound bed is widely accepted as the most ideal environment for effective wound healing [155]. This is due to the fact that renewed skin, instead of

eschar (dry scab or slough), forms during healing in a wet environment [156-158]. Also, in the absence of adequate hydration, the wound bed undergoes necrosis which can lead to a destructive cycle. Various enzymes involved in autolytic debridement function only in moist environment including the peptide growth factors and other molecules that mediate cellular repair [32, 159]. Depending on the composition of the hydrogel and the level of hydration of the wound to which it is applied to, the nature of the hydrogel enhances autolytic debridement [160, 161].

Countless clinical studies attest to the benefits of moist wound healing [162] and demonstrate that hydrogel dressings lead to faster healing, reduced pain and cost savings when compared to saline wet-to-dry dressings [32, 163]. Debridement of the wound surface was shorter in the hydrogel group and cost-effectiveness analysis showed that the higher cost of the hydrogel dressing was justified by its healing advantage [164]. The ability of hydrogel dressings to hydrate the wound surface and resist drying made them excellent replacements for saline moistened gauze [32]. Hydrogel dressings have a cooling influence on the wound that engenders an analgesic effect due to their high water content. Reduced wound pain has been noted when hydrogel dressings are used in burns, venous ulcers, dermabrasion wounds and in lactating women with deepithelized nipples and areolae [165]. The hydrogel covers the exposed nerve endings, reducing the pain and thus resulting in a moist wound healing environment [166].

2.5.5.2 *Eye*

In the eye, hydrogels act by providing viscosity, increased oncotic pressure, and possibly some ill-defined demulcent action [167]. A few reports have indicated that hydrogels containing hydroxy propyl methyl cellulose (HPMC) [167], methyl cellulose [167, 168], and carboxymethyl cellulose [169] enhance healing of wounds in the cornea. It was hypothesized that the prolonged effect on reepithelization is due to continuous low levels of epithelial growth factor (EGF) receptor stimulation resulting in accelerated wound healing when the above mentioned hydrogels were used [167]. Pratoomsot et al, investigated the suitability of a PLGA-PEG-PLGA hydrogel as a potential bandage for corneal wound repair and their studies suggest that hydrogels could be employed for treatment of conditions arising from superficial chemical or thermal corneal burns [170].

2.5.5.3 *Poly(ethylene glycol) (PEG) containing hydrogels*

The term PEG is often used to refer to polymer chains with molecular weights below 20000 Da, while polyethylene oxide (PEO) refers to higher molecular weight polymers. PEG hydrogels contain PEG units which make it water soluble, non toxic, biocompatible and non-immunogenic [171]. PEG exhibits rapid clearance from the body, (depending on the size of PEG and route of administration) and has been approved for a wide range of biomedical applications. Because of these favorable properties, PEG is FDA approved and hydrogels prepared from PEG are excellent candidates as biomaterials. PEG-modified surfaces are protein rejecting thus inhibiting non-specific protein adsorption on the surface of the biomaterial. As a result, they display reduced immunogenicity and antigenicity [170]. Hydrogels containing PEG are most widely used for their

hydrophilicity, strength, easy processability, high stability to temperatures and pH, minimum cell adhesion and protein absorption [33, 34]. PEG may transfer its properties to another molecule when it is covalently bound to that molecule resulting in toxic molecules becoming non-toxic or hydrophobic molecules becoming soluble when coupled to PEG [137, 172, 173].

PEG hydrogels have been used in drug delivery, wound healing, and a variety of other biomedical applications [172, 174]. These hydrogels are often used in combination with other polymers to produce an appropriate biomaterial [137]. PEG has formed a basis for some commercial products including Vigilon™, which is formed by radiation crosslinking of high molecular weight PEO chains. This product is used as a sheet wound covering material [137, 175]. Hypol™, a crosslinked PEG foam is used for wound healing and drug delivery materials [176]. PEG hydrogels have been used as controlled release devices [137, 177, 178] and the rate of drug release was found to be dependent not only on the method of preparation, but also on the crosslinking density, molecular weight of the PEG/PEO chains, and drug solubility.

2.6 Summary

PEG hydrogels are valuable topical drug delivery systems to eyes and skin as they are easy to apply and capable of sustained drug release for prolonged periods, while increasing delivery at the site of application. PEG hydrogel delivery systems incorporating doxycycline can potentially intervene the hazardous effects of SM injuries by inhibiting MMP-9 and other inflammatory mediators.

3 SPECIFIC AIMS

Sulfur mustard is a potent vesicant and chemical warfare agent that mainly affects the eyes, lungs and skin. Currently there are no effective drugs or delivery systems to treat SM wounds. Doxycycline acts by inhibiting inflammatory cytokines and MMP-9, which quantitatively increase over time in response to SM exposure. Drugs delivered orally have limited bioavailability in the eyes/skin because typical systemic concentrations are low and diffusion into the eyes/skin from the systemic circulation is slow. However, when higher doses are administered orally, systemic toxicity may result. Therefore, therapy involving local drug administration limits systemic toxicity while increasing the drug concentration at the site of injury. The overall hypothesis of the proposed research is that a topical doxycycline delivery system, which can be easily applied and removed, is beneficial for the treatment of SM wounds. Such a delivery system can provide sustained doxycycline release and accelerate wound healing by inhibiting both MMP-9 and inflammatory mediators. The proposed strategy utilizes a fast forming hydrogel drug delivery system to deliver controlled amounts of doxycycline at the wounded site for at least one week.

The specific aims of this dissertation are as follows:

1. To investigate the potential of PEG hydrogels for sustained delivery of a model drug, pilocarpine.

Hypothesis: Pilocarpine release from the hydrogel is sustained for at least 1 week and results in improved pharmacological response (i.e., pupillary constriction) in rabbit eyes compared to a solution delivery system.

2. To evaluate dermal wound progression after nitrogen mustard (NM) exposure in a mouse model and to investigate the barrier properties of skin after vesicant exposure by using different markers of permeability.

Hypothesis: The NM-induced wound progresses in a dose- and time- dependent manner and the permeability of molecular markers increase through NM-exposed skin.

3. To design, characterize and evaluate doxycycline hydrogels for wound healing efficacy in a vesicant-exposed rabbit cornea organ culture model system.

Hypothesis: Doxycycline hydrogels demonstrate a significant improvement in wound healing as compared to similar dose of doxycycline in solution.

4. To design and develop doxycycline hydrogel dressings with reversible crosslinks for dermal wound healing of mustard injuries.

Hypothesis: Doxycycline hydrogels show improved healing of NM dermal wounds compared to untreated wounds or wounds treated with placebo hydrogels.

4 DESIGN AND EVALUATION OF NOVEL FAST FORMING PILOCARPINE LOADED OCULAR HYDROGELS FOR SUSTAINED PHARMACOLOGICAL RESPONSE

4.1 Introduction

Controlled drug delivery to the eye remains a challenging task due to normal ocular protective mechanisms such as blinking and tear drainage that promote rapid clearance and reduced bioavailability resulting in a short duration of pharmacological response [179]. The residence time of most conventional ocular solutions ranges between 5-25 minutes [78, 79]. Only 1-10 % of topically applied drug is absorbed [80], which also includes absorption from the gastrointestinal tract due to drainage through the nasal-lacrimal duct [81]. As a result, a frequent dosing regimen is typically necessary to achieve therapeutic efficacy [82]. However, frequent instillation of eye drops results in local side effects such as headaches due to ciliary muscle spasm, decreased vision in poor illumination due to miosis, and accommodative myopia [83]. Ocular delivery systems with prolonged ocular residence time such as ointments and suspensions have been developed to overcome these challenges and increase ocular drug bioavailability [84, 85]. There are, however, several limitations that reduce patient compliance. For example, ointments are greasy and produce blurred vision [86, 87]. Similarly, non-erodible inserts such as Ocusert also have limitations. These are due, in part, to the fact that most glaucoma patients are geriatric and find weekly insertion and removal of Ocusert difficult. Furthermore, when pilocarpine is administered continuously, tachyphylaxis occurs, further diminishing the potential of this technology. Other limitations are difficulty with retention, unnoticed loss of the unit from the eye and rupture of its membrane causing excessive bolus drug release [88, 89]. Ocusert, however, is still

considered a technical breakthrough, even though it has achieved only limited success in the market due to these limitations [180].

Current research efforts are focused towards the design and evaluation of ocular delivery systems that are easy to administer, require decreased administration frequency, and provide controlled and possibly sustained drug release in order to increase therapeutic efficacy and patient compliance. Hydrogels are a crosslinked network of hydrophilic polymers that have the ability to absorb large amounts of water and swell, while maintaining their three-dimensional structure. Molecules of different sizes can diffuse into and out of the hydrogel network, which allows their possible use as a drug-depot for controlled release applications. Hydrogels show minimum tendency to adsorb protein from body fluids due to their low interfacial tension. They closely resemble living tissue due to their high water content, and soft/rubbery characteristics. As a result of these favorable properties, hydrogels are increasingly being used as scaffolds in tissue engineering [107] and drug delivery systems in various biomedical [108] and pharmaceutical [31, 109-111] applications. As ocular drug delivery systems, hydrogels are expected to provide prolonged corneal contact time, reduced precorneal drug loss, and convenience in administration as compared to eye drops, suspensions or ointments. The viscoelastic properties of hydrogels should allow for sufficient mechanical strength to resist clearance due to blinking resulting in prolonged ocular residence time.

Hydrogels can be preformed [128, 129] or prepared *in situ* [130-132]. Preformed hydrogels are simple viscous solutions [128] or hydrogel films [129], which gel outside of the eye and do not undergo any modification after administration. Viscous solutions do

not have the mechanical strength to resist ocular clearance mechanisms and only offer a transient improvement in ocular residence time. *In situ* forming hydrogels are liquids upon instillation and undergo a phase transition to form a viscoelastic gel in response to environmental changes like temperature [130, 132], pH [133] and electrolyte composition [134]. *In situ* forming hydrogels are attractive as ocular drug delivery systems because of facile dosing as a liquid, which insures rapid and complete ocular coverage. They also allow for accurate and reproducible quantities to be administered to the eye in contrast to pre-gelled formulations. The above-mentioned *in situ* hydrogels are often unstable and reversible. The currently examined hydrogels are produced *in situ* at physiological pH by covalent intermolecular crosslinking of polymer chains through irreversible thioether bonds resulting in stable viscoelastic hydrogels.

Pilocarpine has been widely used topically in the eye for controlling elevated intraocular pressure associated with glaucoma [181, 182]. When administered as a solution, it has good water solubility but suffers from low ocular bioavailability of 0.1- 3 % [78, 183] due to its low lipophilicity and the short residence time of aqueous solutions in the eye. In the present work, pilocarpine-loaded hydrogels were prepared at physiological pH by the intermolecular crosslinking of a thiol-containing copolymer with the bifunctional crosslinker, HBVS (1, 6-hexane-bis-vinylsulfone). The hydrogels were prepared using different copolymer/crosslinker concentrations and pH to optimize hydrogel formation, drug loading, and release properties. It was further evaluated in rabbits for controlled ocular delivery of pilocarpine and pupillary constriction.

4.2 Materials and methods

4.2.1 Materials

Polyoxyethylene bis(amine) [PEO, MW ~3350 Da], pilocarpine hydrochloride (hereafter referred to as pilocarpine), Ellman's reagent [5,5'-dithiobis(2-nitrobenzoic acid)], mercaptosuccinic acid, trityl chloride, 4-dimethylaminopyridine, p-toluenesulfonic acid monohydrate, trifluoroacetic acid, and triisopropyl silane were obtained from Sigma-Aldrich (St. Louis, MO). N, N-dimethylformamide, dichloromethane, diethyl ether, acetonitrile and HPLC grade solvents were obtained from Fisher Scientific (Pittsburgh, PA). HBVS was obtained from Pierce (Rockford, IL). The Spectra/Por RC 7 dialysis membrane (MWCO: 50,000 Da) was obtained from Spectrum Laboratories Inc (Rancho Dominguez, CA). Gel permeation chromatography (GPC) was carried on a Waters Breeze GPC system (Milford, MA) equipped with dual-absorbance UV and refractive index detectors using an Ultrahydrogel 1000 size-exclusion column (7.8 x 300 mm). PEO/PEG molecular weight standards kit was obtained from Polymer Standards Service-USA Inc. (Warwick, RI). A DSC Q100 (TA Instruments, New Castle, DE) was used for DSC. The optical transmission (OT) of the hydrogel was determined using a UV 1201 UV-Vis spectrophotometer (Shimadzu, Columbia, MD). Rheological data were obtained on a SR-2000 rheometer from Rheometric Scientific Inc (Piscataway, NJ) and analyzed by RSI orchestrator software. TEM studies were carried out on a Philips CM12 transmission electron microscope at 100Kv using an AMT digital camera. Waters HPLC system equipped with a UV detector and reverse phase (RP) C₁₈ column (Waters, Novapak, 3.9 x 150 mm) was used to analyze pilocarpine concentration.

4.2.2 Copolymer synthesis and characterization

The copolymer was synthesized using a solution polymerization technique as previously reported by our group [184]. PEO-bis-amine (1 g, 0.298 mM) was dissolved in anhydrous dichloromethane (20.0 mL). S-tritylmercaptosuccinic acid (1 equiv., 116.9 mg), 4-dimethylaminopyridine (1 equiv., 36.4 mg), and p-toluenesulfonic acid monohydrate (1 equiv., 56.6 mg) were added to the solution under anhydrous conditions. The solution was cooled to 0° C and 1, 3-diisopropyl carbodiimide (4 equiv., 184 μ L) was added. The reaction mixture was then stirred at RT for 24 h. Crude copolymer was obtained by precipitation from cold ether (4 x 25 mL) and subsequent drying. Dialysis was performed to remove low molecular weight impurities. The copolymer was dissolved in water (~50.0 mL), transferred to a dialysis membrane and suspended in stirring water (2.0 L). Dialysis was performed for 24 h. After dialysis, the copolymer solution was transferred to polypropylene tubes and freeze-dried (Yield. 835 mg). Copolymer was finally treated with acid to remove the trityl groups. Copolymer (800 mg) was suspended into the trifluoroacetic acid solution (10.0 mL) containing 5 % each of triisopropyl silane and water. The reaction mixture was placed on a shaker for 5 h and free thiol-containing copolymer was obtained after precipitation from cold ether. The copolymer was obtained as white flakes after vacuum drying for 1-2 h (Yield. 510 mg).

The weight-average (Mw) and number-average molecular weight (Mn) and polydispersity index of the copolymer were estimated by GPC. Polymer standards (50 μ L, 2mg/mL) with molecular weight (Mw) of 1490, 4270, 6950, 12400, 20100, 41300 and 70400 respectively were injected to generate a calibration curve. Finally, an aqueous solution of copolymer was injected and molecular weights were estimated by using the

GPC software. To measure glass transition temperature (T_g) by DSC, copolymer samples were weighed into aluminum pans that were sealed and perforated. The samples were heated from 0-200 °C under a nitrogen atmosphere, cooled to -50 °C, and re-heated to 200 °C at a sweep rate of 10 °C/min. T_g was determined by Universal Analysis software from the first heating cycle and T_m was determined from the average of the melting points calculated from the first and second heating and the cooling cycles.

4.2.3 Hydrogel formation

Hydrogels were prepared by mixing the copolymer and crosslinker solutions in sodium phosphate buffer (20 mM, pH = 7.4) at RT. Hydrogels were prepared from 3, 4, 5 and 6 % w/v copolymer solutions using copolymer to crosslinker stoichiometries of 1:1 or 1:2. Pilocarpine (2 %, w/v) was mixed with the copolymer solution prior to mixing of copolymer and crosslinker solutions. Hydrogel formation was determined by the “inverted tube method” and hydrogels were considered to have formed once the solution ceased to flow from the inverted tube. Hydrogels used for optical transmission, degree of swelling, drug loading and *in vitro* release studies were 300 μ L in volume, 10 mm in diameter, and 0.3 mm in thickness.

4.2.4 Physicochemical characteristics of the hydrogel

4.2.4.1 pH titrations

4 % w/v hydrogels as described above were prepared in aqueous sodium phosphate buffer solutions (20 mM) with pH values of 6.5, 6.9, 7.4 and 7.9 to investigate the influence of pH on hydrogel formation.

4.2.4.2 OT

Hydrogels (300 μ L) were placed in a quartz cuvette containing distilled water and transmission of light was measured at 480 nm [185]. Cuvette containing only distilled water was used as reference. Eight hydrogels were used for the OT measurements. All OT studies were done in triplicate and the mean \pm standard error (SEM) is reported. The statistical significance between groups was measured using student's t-test.

4.2.4.3 Rheological studies

Rheological measurements were performed using a rheometer with a cone plate geometry at 37 °C (plate diameter: 25 mm, gap: 3 mm, 2° angle) [143, 144]. Hydrogels were prepared from 3 and 5 % w/v copolymer solutions using a copolymer to crosslinker stoichiometry of 1:1. The hydrogel samples were equilibrated on the plate for 5 min to reach the running temperature before each measurement. Rheological test parameters, storage/elasticity (G') and loss (G'') moduli were obtained under dynamic conditions of non-destructive oscillatory tests. All rheological studies were performed in triplicate and the mean \pm SEM is reported.

Dynamic strain sweep test: Experiment was performed at a constant frequency of 1 Hz with percent strain ranging from 10^{-1} to 10^3 .

Dynamic frequency sweep test: Experiment was carried out at a constant strain of 1 % (linear viscoelastic region) with frequency ranging from 10^{-1} to 10^1 Hz.

4.2.4.4 Transmission Electron Microscopy (TEM)

Hydrogel samples (3 and 5 % w/v, 1:1 stoichiometry) were prepared by placing the solution on a 400 mesh copper grid coated with carbon mica [186]. The excess hydrogel was removed after 1 min. The grids were stained negatively with 1 % phosphotungstic acid solution (PTA) and electroscoped.

4.2.4.5 Degree of swelling

The effect of the copolymer concentration (3, 4, & 6 %, w/v) and copolymer to crosslinker ratios (1:1 and 1:2) on the degree of hydrogel swelling were evaluated. Hydrogels were placed in a vial and weighed to obtain the initial weight. They were next immersed in simulated tear fluid (4.0 mL) and placed in a shaking incubator (37 °C, 60 rpm). The tear fluid was prepared by dissolving sodium chloride (0.67 %, w/v), sodium bicarbonate (0.2 % w/v) and calcium chloride dihydrate (0.008 % w/v) in water and pH adjusted to 7.4 [130]. The tear fluid was removed at predetermined time intervals and the weights of vial with swollen hydrogels were recorded. The simulated tear fluid was replaced after every measurement and swelling experiments were continued until equilibrium hydration has been reached. The increase in the weight of the hydrogel in the vial was correlated to the tear fluid uptake by the hydrogel. All measurements were made in triplicate for each hydrogel and the mean \pm SEM of the values is reported.

4.2.5 In vitro release studies

4.2.5.1 Drug loading efficiency

The pilocarpine-loaded hydrogels containing 2 % w/v of pilocarpine were dissected into small pieces (300 μ L) and suspended into the simulated tear fluid (4.0 mL). The suspension was sonicated for 30 min to completely extract pilocarpine from the hydrogel.

The amount of pilocarpine extracted was quantified by RP HPLC analysis. After extraction, the suspension containing the hydrogel was stored for several days at 37 °C and then re-analyzed to ensure the complete extraction of pilocarpine from the hydrogel. Pilocarpine was stable under the conditions used (37 °C), as determined by HPLC analysis.

4.2.5.2 *In vitro* release

The hydrogels (300 µL) loaded with 2 % w/v of pilocarpine were suspended in vials containing simulated tear fluid (4.0 mL). The vials containing the tear fluid were placed in a shaking incubator (37 °C, 60 rpm) during the duration of the study (8-days). Aliquots (200 µL) were collected from the vials at predetermined intervals and replaced with equal volume of tear fluid medium to maintain sink conditions through out the study. The concentration of pilocarpine in the release medium was determined using RP HPLC at a wavelength of 220 nm. Water containing 0.1 % trifluoroacetic acid (solvent A) and 100 % acetonitrile (solvent B) were used as mobile phase. The retention time for pilocarpine was 15 min. The cumulative amount of pilocarpine released from the hydrogel was determined using a calibration curve. All release experiments were done in triplicate and the results are reported as mean \pm SEM.

4.2.6 *In vivo* studies

Four female New Zealand albino rabbits weighing 3.5-4.0 kg (Charles River Laboratories, Wilmington, MA) were obtained and acclimatized for 3-days prior to use. They were fed a normal diet and exposed to alternating 12 h light and dark cycles. Animals were treated according to the Principles of Animal Care by National Institutes of

Health and animal protocol approved by the Rutgers University Institutional Animal Care and Use Committee.

4.2.6.1 Eye irritation test

Acute eye irritation/corrosion [187] and ocular irritation potential of the hydrogel or its components (copolymer and HBVS) was tested prior to the approval of the protocol by the Rutgers University Institutional Animal Care and Use Committee. The irritation test was performed according to the Organization for Economic Cooperation and Development (OECD/OCED) test guideline 405. Hydrogels (25 μ l) were prepared from 4 % w/v copolymer solutions (copolymer/crosslinker: 1:2) with no drug and placed in the conjunctival sac of one of the rabbit's eye; the untreated eye served as control. The ocular irritation potential was evaluated for 21-days by scoring lesions of conjunctiva, cornea and iris at specific time intervals. Experiments were done in triplicate.

4.2.6.2 In vivo efficacy

All rabbits were acclimatized to laboratory testing conditions for 30 min before the study. The right and left pupil diameters were alternatively measured four times within 30 min, using a standard pupillary diameter gauge held at a fixed distance from each rabbit to establish baseline values for both eyes. For each pair of readings, the differences in pupil diameter (control minus test eye) were determined. These predosing differences were averaged, and the mean was used to convert post administration data to the baseline-corrected values. This process minimized both animal and day variation.

Both the aqueous and hydrogel formulations were tested in each rabbit. A minimum of 1 week elapsed between tests in the same rabbit. Hydrogel prepared from 4 % w/v

copolymer solutions using copolymer to crosslinker stoichiometry of 1:2 was chosen for this study. 25 μ l of a hydrogel solution containing 2% pilocarpine was placed in the lower conjunctival sac of the right eye. To avoid experimental bias, the left eyes received 25 μ l of a hydrogel solution with no drug (control). The eyes were checked frequently and no inflammation was observed in any experiment. After one week, the above procedure was repeated using 2% pilocarpine solution in phosphate buffered saline (PBS, pH 7.4), hereafter referred to as drops. 25 μ l of pilocarpine drops were placed in the lower conjunctival sac of the right eye and 25 μ l of PBS with no drug was placed in the left eye of the rabbits and pupil diameter was measured.

After administration of both the control vehicle and the pilocarpine containing copolymer solutions, the pupil diameters of both the eyes were measured at predetermined time intervals (0.25, 0.5, 0.75, 1, 1.5, 2, 2.5, 3, 4, 5, 6, 12 and 24 h). For each time point, the difference in pupil diameter (control minus test eye) was calculated and data was converted to a baseline-corrected value (i.e., the pharmacological response of pilocarpine) by subtracting the average baseline difference in pupil diameter for each experiment on the basis of the readings obtained before dosing. To assess the extent of total pharmacological response of the various formulations, areas under the decrease in pupil diameter vs. time profiles in 24 h (AUC_{0-24}) were calculated using the GraphPad Prism 4 software. The mean \pm SEM of four determinations is reported. Two way analysis of variance (ANOVA) was used to determine the overall statistical significance, while student's t-test was used for individual comparison between groups.

4.3 Results and Discussion

4.3.1 Copolymer synthesis and characterization

The synthesis of the copolymer poly[poly(ethylene oxide)-alt-poly(mercaptosuccinic acid)] has been reported earlier by our group [184]. Briefly, a polycondensation reaction was carried out between polyoxyethylene bis(amine) **1** and S-tritylmercaptosuccinic acid **2** to obtain copolymer **3** containing alternating units of poly(oxyethylene glycol) and S-tritylmercaptosuccinic acid. The thiol-containing copolymer **4** was obtained after removing the trityl group with acid (Scheme 4.1). The copolymer was characterized by GPC and DSC analysis. The GPC profile of crude copolymer (Figure 4.1) showed the presence of a predominantly high molecular weight peak at 6.91 min (copolymer) along with peaks at 11.77 and 16.05 min, which correspond to low molecular weight impurities (monomeric PEG/other reagents). The relative proportion of copolymer in the crude reaction mixture was calculated as $\geq 50\%$ from AUC. Low molecular weight impurities were removed by dialysis (MWCO = 50,000). The M_w and M_n for purified copolymer were estimated as 64435 and 57289 Da, respectively and the polydispersity index of the copolymer was calculated as 1.15. The T_g of copolymer as measured by DSC, was found below $-40\text{ }^\circ\text{C}$ whereas the T_m was found as $45 \pm 1\text{ }^\circ\text{C}$. The extrapolated on set and end set of melting points were found to be $37 \pm 1\text{ }^\circ\text{C}$ and $49 \pm 1\text{ }^\circ\text{C}$ respectively. The entropy/heat of fusion (ΔH), which is defined as the heat required for melting the copolymer was calculated to be $110 \pm 5\text{ J/g}$. The thiol contents of copolymer were estimated as $183\text{ }\mu\text{M}$ / $1.2 \times 10^{-5}\text{ mM}$ by the Ellman's assay.

The advantage of using this copolymer is that it contains PEG units, which are water soluble, non-toxic and biocompatible [188]. They have been widely used in various pharmaceutical products administered by parenteral, topical and oral routes [189, 190]. The advantage of using mercaptosuccinic acid is that it provides reactive thiol functionalities that can be utilized for intermolecular crosslinking of copolymer or to anchor drugs, targeting and/or signaling moieties on to the copolymer.

4.3.2 Hydrogel studies

A thiol-containing copolymer was crosslinked with the bifunctional crosslinker HBVS resulting in the formation of a hydrogel network through thioether bonds. The thiol groups are known to react with mutually reactive groups such as thiol, maleimide, and vinyl sulfone to form disulfide and thioether bonds [191]. The disulfide bonds are cleavable (reversible) under reducing conditions whereas the thioether bonds are highly stable (irreversible) in the biological environment.

Different copolymer concentrations (w/v) and stoichiometric amounts of crosslinker (1:1) were used to prepare the hydrogels. It was observed that 2 % w/v copolymer solution did not form a hydrogel whereas 3, 4, 5 and 6 % copolymer solutions resulted into hydrogels in 4.0, 2.5, 2.0 and 1.8 min respectively. Copolymer solutions beyond 6 % w/v were too viscous and hence not investigated. When prepared using 1:2 stoichiometries, the 3-6 % hydrogels were formed in 3.0, 2.0, 1.4 and 1.2 min respectively. Thus, an increase in copolymer/crosslinker concentration decreased the time required for hydrogel formation by producing more rapid and intense crosslinking. Hydrogels were further characterized using TEM (Figure 4.2) [186]. The micrographs of hydrogels prepared from 3 and 5 %

copolymer solutions clearly showed that an increase in copolymer concentration leads to the formation of denser crosslinked polymer networks.

4.3.2.1 Influence of pH on gelation

The influence of buffer pH on hydrogel formation was evaluated and 4 % copolymer solution was found to form hydrogels in 5.2, 2.8, 2.5 and 1.0 min at pH 6.5, 6.9, 7.4 and 7.9. The decrease in gelation time is due to enhanced thiol reactivity at elevated pH [192].

4.3.2.2 OT

Delivery systems for the eye should ideally be transparent. Optical Transmission (OT) is defined as the ratio of the amount of light passing through the hydrogel to the amount of light incident on it (expressed as percentage). Since human eyes are most responsive around 480 nm, the OT of hydrogels was measured at this wavelength [185]. Hydrogels with optical transmission ≥ 90 % are classified as transparent, ≤ 90 % but ≥ 10 % as translucent, and ≤ 10 % as opaque [185]. Figure 4.3 shows the percentage of copolymer (w/v) containing crosslinker in the ratio of 1:1 or 1:2 plotted vs. % OT. The groups that showed a statistically significant difference ($p < 0.05$ or $p < 0.01$) are indicated by * and **, respectively. All hydrogels used in the present study were either transparent ($OT > 90$ %) or nearly transparent ($OT > 78$ %). An increase in copolymer concentration decreased the transparency of the hydrogel whereas an increase in crosslinker concentration has little influence. These results indicate that the optical properties of the hydrogels make them suitable as ocular drug delivery systems.

4.3.2.3 Rheology

The mechanical strength and viscoelastic properties of the hydrogels were investigated using rheological measurements [143, 144] to assess their retention behavior and physical integrity *in vivo*. Viscoelastic properties were investigated because hydrogels with good mechanical strength are expected to maintain their integrity and help to prevent physical drug loss from blinking [147]. The strain sweep test (Figure 4.4A) was performed on 3 % and 5 % hydrogels in order to establish the regime of linear viscoelasticity (LVE) and to determine if the elasticity of the formulations differed, as expressed by the storage/elastic modulus (G'). The strain sweep test results suggest that G' dominates in both the formulations and this is supported by the results obtained from the frequency sweep test (Figure 4.4B). Since G' was one order of magnitude greater than G'' (loss modulus), this suggests that the hydrogel system is more elastic than viscous in the investigated frequency range. This is in direct contrast to reversible gels, which have poor mechanical strength leading to reduced corneal residence time. Figures's 4.4A and 4.4B also show that the G' is independent of frequency and strain whereas the G'' is weakly dependent on them. The hydrogels containing higher copolymer concentrations (5 %) showed a higher and constant storage modulus under increasing frequency, suggesting that the hydrogels have the ability to resist structural changes under strain. The loss tangent ($\tan\delta$) values calculated as G''/G' indicate that the storage modulus is the dominant feature in all of the hydrogels, as a small $\tan\delta$ indicates an elastic material. There is little variation in the $\tan\delta$ values, and the curves are similar for the different hydrogels, which further supports the strain sweep test results suggesting that the variations in hydrogel formulations in the current study do not result in extreme variations in rheological parameters. The rheological data show that the hydrogels have good mechanical

properties, which might help prolong their ocular contact time. An increased contact time in turn may lead to an increased duration of pharmacological response.

4.3.2.4 *Swelling kinetics*

The swelling behavior of hydrogel influences its surface and mechanical properties as well as the drug release kinetics (solute diffusion coefficients). Also since hydrogels are swelling controlled systems, the degree of swelling is a measure of the crosslinking density in the hydrogel and is important for regulating the pore size of the hydrogel. The effect of copolymer concentration and the copolymer to crosslinker ratios on the degree of swelling was determined. The degree of swelling for each hydrogel was determined by using the equation below:

$$\%Swelling = \frac{(W_s - W_o)}{W_o} \times 100 \quad (1)$$

Where W_s is the weight of the swollen hydrogel at time t and W_o is the initial weight. Figure 4.5 shows the degree of swelling expressed as percent swelling plotted against time for 3, 4 and 6 % hydrogels prepared using 1:1 and 1:2 copolymer/crosslinker ratios. Initially, the hydrogels swelled rapidly and then gradually reached the equilibrium. Compared to hydrophilic hydrogels reported in the literature [123, 124], a relatively lower degree of swelling ($< 8\%$) was observed in this case. Furthermore, the degree of swelling decreased with an increase in copolymer (3 - 6 %, w/v) and crosslinker (1: 2) concentrations. Hydrogel swelling is caused by the presence of hydrophilic groups in the network, due to which polymer chains are hydrated to different degrees (sometimes, more than 90 % wt), depending on the nature of the aqueous environment and polymer

composition [112]. Although PEG is highly hydrophilic and is expected to swell significantly, the controlled degree of hydrogel swelling in the present case is due to the incorporation of the less hydrophilic mercaptosuccinic acid in the copolymer chain. Further, the decrease in hydrogel swelling with increasing crosslinker concentration is due to the smaller pore size and the fact that higher crosslinking reduces the exposure of copolymer chains to water [193, 194].

4.3.3 *In vitro* pilocarpine loading and release

Pilocarpine-loading efficiency results show that 3, 4, 5 and 6 % w/v hydrogels with 1:1 stoichiometries entrapped 70.0, 72.5, 66.5, and 68.0 % of loaded pilocarpine. Similarly, the 3 – 6 % w/v hydrogels prepared using 1:2 stoichiometries resulted in pilocarpine loading efficiencies of 73.6, 72.9, 71.6, and 70.8 %. The hydrogels prepared using 1:2 stoichiometry showed up to 5 % higher pilocarpine loading compared to hydrogels prepared using 1:1 stoichiometry, which might be due to an increase in crosslinking density between the copolymer chains.

The pilocarpine release profiles from different hydrogels were studied *in vitro* using simulated tear fluid as dissolution medium. The plot of fractional release of pilocarpine (M_t/M_∞) as a function of square root of time (Figure 4.6) demonstrates that pilocarpine entrapment in the hydrogel slows down the drug release and there is a sustained release for about 192 h (8 days). The percentage of pilocarpine released from 3, 4, 5 and 6 % hydrogel formulation prepared using 1:1 stoichiometry decreased from 100 to 86 % whereas same hydrogels prepared using 1:2 stoichiometry released 98 to 85 % of pilocarpine. Neither difference was considered significant. Thus, most of the loaded

pilocarpine was released in all of the hydrogel formulations evaluated. It is also evident from the plot that increase in copolymer/crosslinker concentration results in slower pilocarpine release, which might be due to the formation of a tighter hydrogel network and decreased pore size.

The relative influence of diffusion and polymer relaxation on the mechanism of pilocarpine release was determined by fitting the experimental data (first 60 % of the total amount released) to the Ritger-Peppas equation [140].

$$\frac{M_t}{M_\infty} = kt^n \quad (2)$$

In Equation 2, M_t/M_∞ is the fractional release of the drug, k is the proportionality constant, n is the diffusional exponent and t is the time. The diffusional exponent was calculated from the slope of the natural logarithmic values (\ln) of the fractional release as a function of time (Table 4.1). The release mechanism for all of the hydrogels was found to be non-fickian or anomalous involving both diffusion and polymer relaxation ($0.5 < n < 1$). Pilocarpine release was dependent on two simultaneous processes, water migration into the hydrogel and drug diffusion through continuously swelling hydrogels. The apparent diffusion coefficients at the early stage of controlled release ($M_t/M_\infty < 0.6$) were determined using an equation derived from Fick's second law of diffusion [195].

$$\frac{M_t}{M_\infty} = 4\left(\frac{Dt}{\pi h^2}\right)^{1/2} \quad (3)$$

In Equation 3, M_t/M_∞ is the fractional release of the drug, D is the diffusion coefficient, t is the time, and h is the thickness of the hydrogel. The apparent diffusion coefficient was calculated from the slope of the fractional release as a function of square root of time/thickness of the hydrogel (Table 4.1). The diffusional exponents and the apparent diffusion coefficients decreased with an increase in copolymer and crosslinker concentrations. This indicates a decrease in swelling and pore size of the hydrogels. The *in vitro* release studies show that by changing the copolymer/crosslinker concentrations, drug release from hydrogels can be optimized.

4.3.4 *In vivo studies*

The possibility of eye irritation due to the hydrogel administration was evaluated in rabbits. Three veterinarians independently graded the rabbits for ocular lesions and no symptoms of ocular irritation such as tearing, redness, inflammation or swelling were observed after hydrogel administration. Furthermore fluorescein staining did not indicate corneal or conjunctival epithelial defects.

The pharmacological response (i.e., decrease in pupil diameter) vs. time profiles of a 4 % w/v hydrogel formulation prepared using copolymer and crosslinker in a 1:2 ratio and drops containing 2 % pilocarpine were compared next (Figure 4.7). The miotic effect of the hydrogels is significantly greater than drops ($p < 0.001$) as shown by ANOVA. The time points that showed a statistically significant difference ($p < 0.05$ or $p < 0.01$) were indicated by * and **, respectively. At all times post administration, the decrease in pupil diameter was greater for the hydrogel formulation compared to drops, although the pharmacological profile was similar for up to 3 h. Five indicators of pharmacological

efficacy are summarized in Table 4.2: (1) I_{max} , the peak miotic intensity (2) T_{max} , the time to reach the peak miotic intensity (3) AUC, the area under the decrease in pupil diameter vs. time curve (4) the duration of miotic response and (5) the slope of the linear portion of the decrease in pupil diameter vs. time curve. I_{max} , T_{max} and duration of miotic responses were determined by linear interpolation between the data points, while AUC was calculated using Graph Pad Prism 4 software.

It can be seen from Table 4.2 that I_{max} for the hydrogel formulation is 1.3 times higher than the drops even though T_{max} for both formulations is similar (15 min). Also, the duration of miotic response is 8-fold greater for the hydrogel formulation (24 h) than the drops (3 h), indicating a more sustained release due to greater diffusional resistance. The AUC_{0-24h} values indicate approximately a 5-fold increase in total miotic response for the hydrogel formulation relative to drops. In addition, pupillary response is greater for hydrogel formulation than drops, shown by a 1.7-fold higher slope for the hydrogel formulation. The higher efficacy of pilocarpine loaded hydrogel formulation compared to drops, is possibly due to the increased residence time in cul-de-sac, sustained drug release, and decreased clearance by tears.

Figure 4.8 shows a linear correlation between the *in vitro* release of pilocarpine and *in vivo* pharmacological response in the eye. As the amount of pilocarpine available for absorption increases, there is a corresponding decrease in pupil diameter. The *in vivo* results coupled with the *in vitro* results suggest that the hydrogel formulation significantly prolongs the pilocarpine contact time and pharmacological response, which

makes it a superior formulation for sustained ocular pilocarpine delivery compared to conventional drops.

4.4 Conclusion

The *in situ* PEG hydrogels prepared and evaluated in the current study are stable, show resistance to external forces, give high pilocarpine loading, and provide sustained pilocarpine release. These hydrogel formulations are administered into the eye as a solution, rapidly forming a hydrogel that is able to withstand the shear forces in the cul-de-sac of the eye. The *in vivo* results show that compared to drops, the hydrogel formulations provide prolonged pharmacological response as measured by a decrease in pupil diameter with no visible irritation. Overall, the results support the rationale behind using PEG-based hydrogels as ocular drug delivery systems.

4.5 Tables

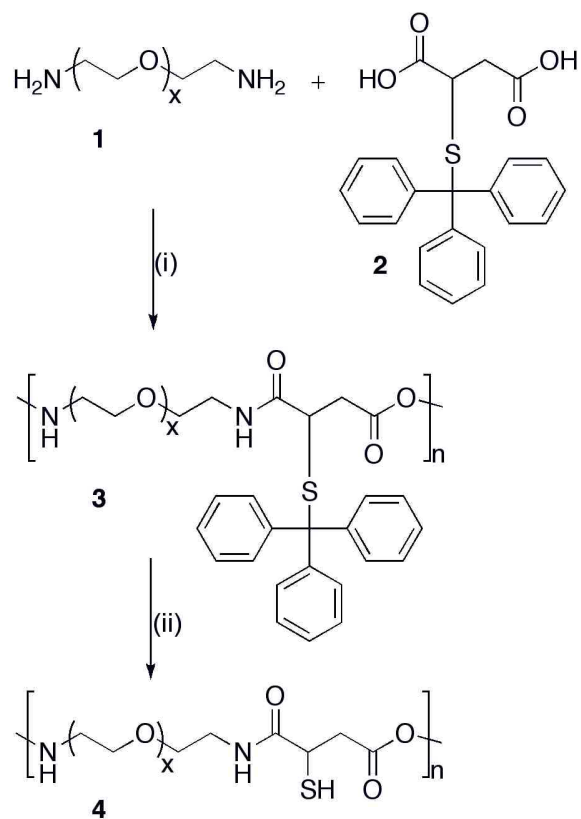
Table 4.1. Estimation of diffusional exponent (n) and apparent diffusion coefficient (D) for various hydrogel formulations.

% Hydrogels (copolymer : crosslinker)	Diffusional exponent (n)	Apparent diffusion coefficient ($\text{cm}^2 \text{sec}^{-1}$) $\times 10^{-6}$
3 % (1:1)	0.98	7.44
4 % (1:1)	0.88	7.10
5 % (1:1)	0.81	6.23
6 % (1:1)	0.63	5.87
3 % (1:2)	0.89	5.05
4 % (1:2)	0.81	4.19
5 % (1:2)	0.74	2.91
6 % (1:2)	0.57	1.91

Table 4.2. Comparison of pharmacological efficacy of 2 % pilocarpine administered ocularly as hydrogel and aqueous solution.

Ocular Delivery System	I_{max} (mm)	T_{max} (h)	AUC (mm/h)	Duration (h)	Slope
Hydrogel	3.125	0.25	22.19	24	-0.26
Drops	2.375	0.25	4.45	3	-0.44

4.6 Figures



Scheme 4.1. Copolymer synthesis, (i) N, N-dimethylaminopyridine, p-toluene sulfonic acid monohydrate, N, N-diisopropylcarbodiimide/dichloromethane, RT, 24 h; (ii) trifluoroacetic acid, triisopropyl silane/water, RT, 5 h.

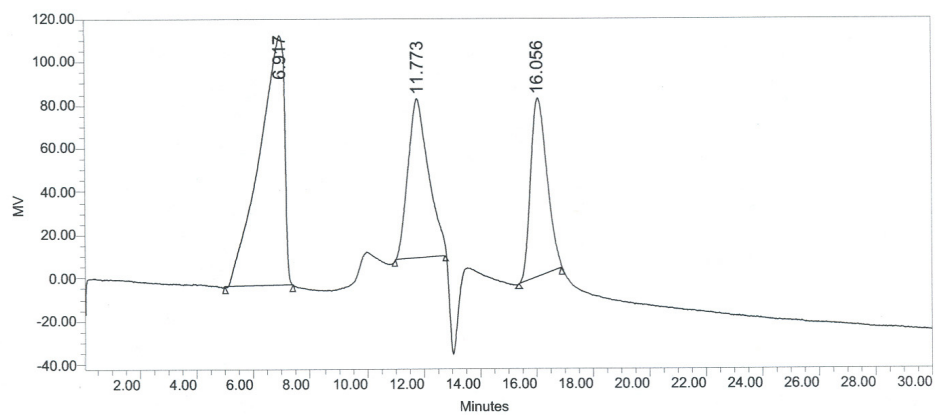


Figure 4.1. The GPC profile of crude polymerization reaction mixture obtained after 24 h. The high molecular weight copolymer peak appears at 6.91 min whereas the low molecular weight fragments appear at 11.77 and 16.05 min.

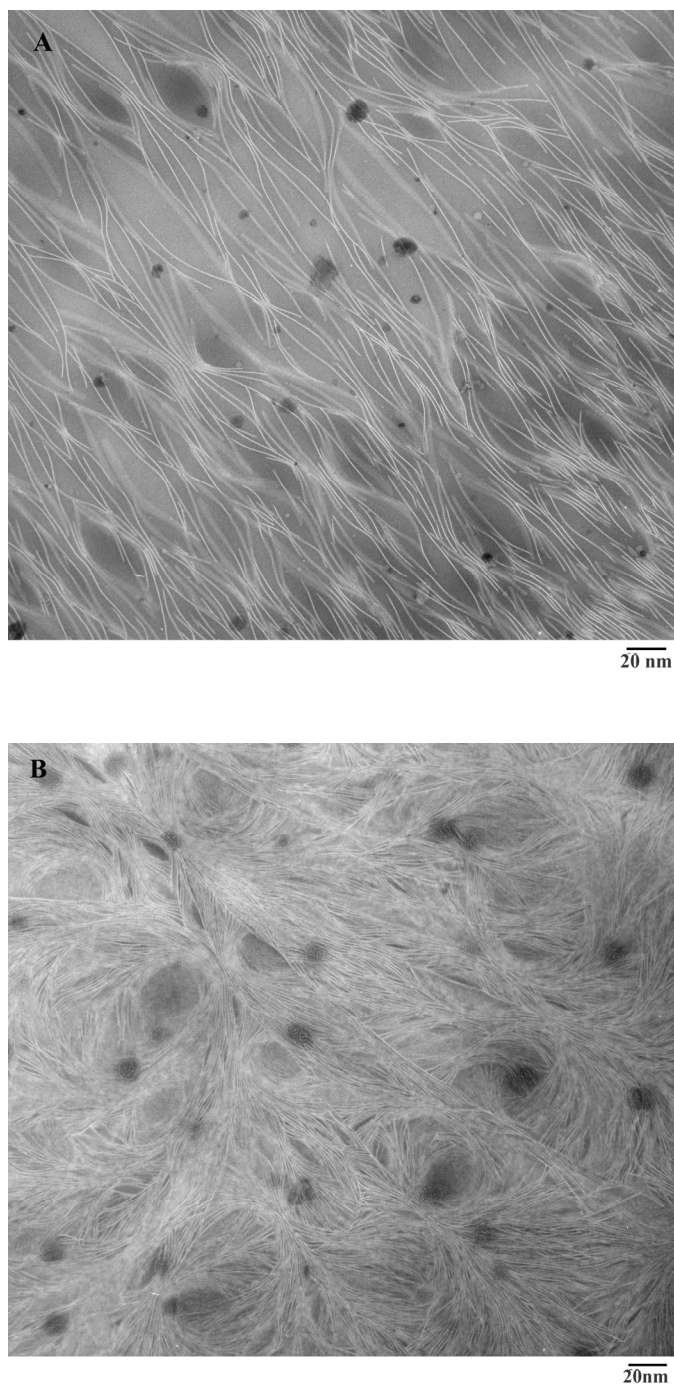


Figure 4.2. TEM images of 3 % (A) and 5 % (B) hydrogels prepared using copolymer and crosslinker in 1:1 stoichiometry. The crosslinking networks are clearly visible; the network density increases with increase in copolymer concentration.

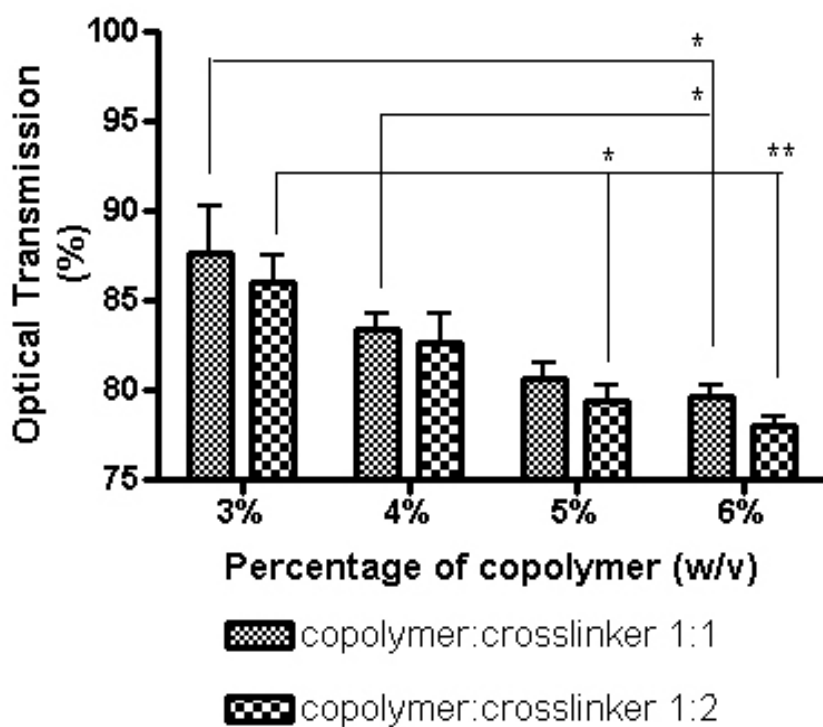


Figure 4.3. Optical transmissivities of 3, 4, 5 and 6 % hydrogels prepared using copolymer and crosslinker in 1:1 or 1:2 stoichiometries. The statistically significant different groups are denoted by * ($p < 0.05$) and ** ($p < 0.01$). The optical transmissivities of the hydrogel decreases with increase in copolymer and crosslinker concentration. All the hydrogels were found to be transparent or close to transparent.

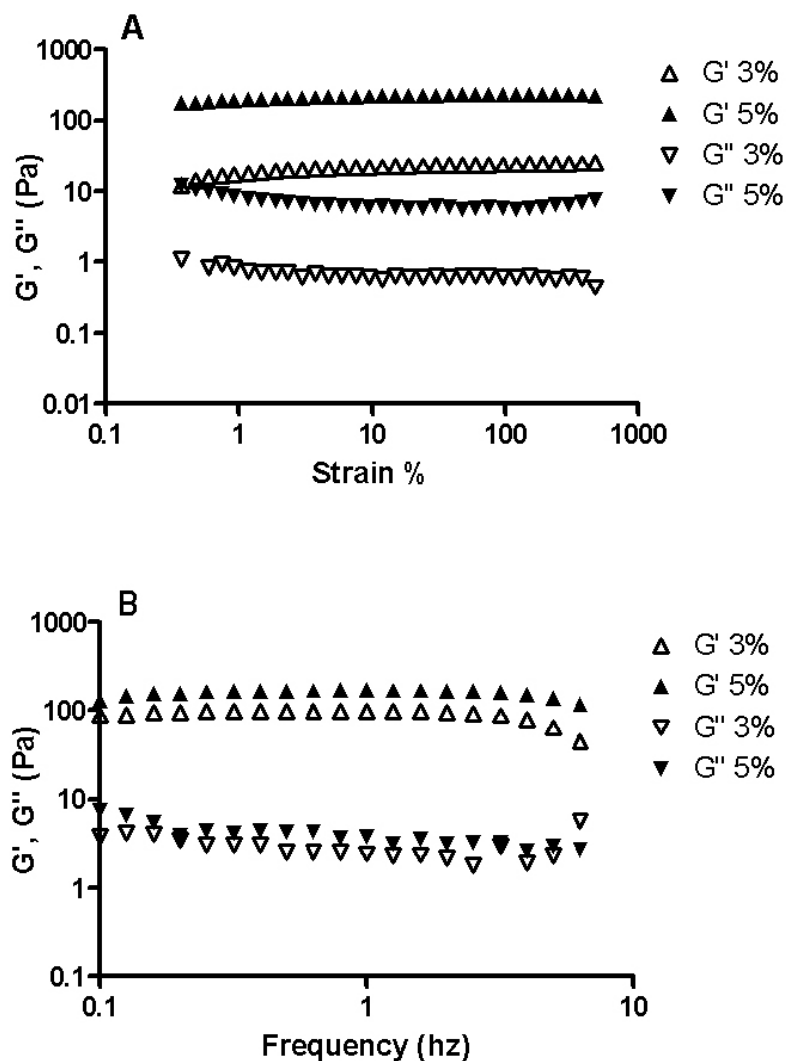


Figure 4.4. Influence of strain (A) and frequency (B) on G' and G'' of hydrogels. The rheological measurements were carried out on 3 and 5 % w/v hydrogels prepared using copolymer and crosslinker in 1:1 stoichiometry. The strain sweep test establishes the regime of linear viscoelasticity (LVE). The frequency sweep test shows that the hydrogels are elastic than viscous and that they have the ability to resist structural changes under strain.

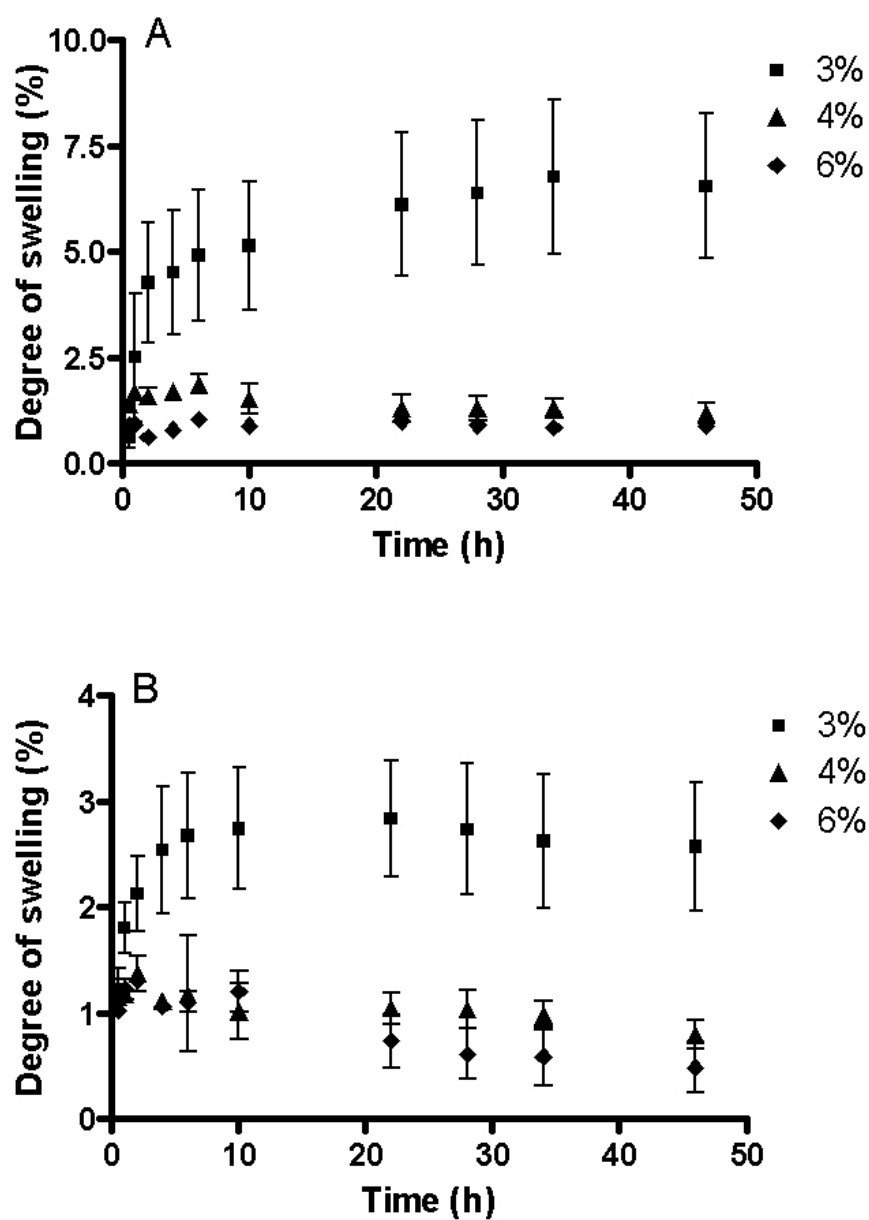


Figure 4.5. Swelling kinetics of the hydrogels as a function of time. 3, 4 and 6 % w/v hydrogels were prepared using 1:1 (A) and 1:2 (B) stoichiometries. All measurements were performed in triplicate and plotted as mean \pm SEM. The degree of hydrogel swelling decreases with increasing copolymer and crosslinker concentrations.

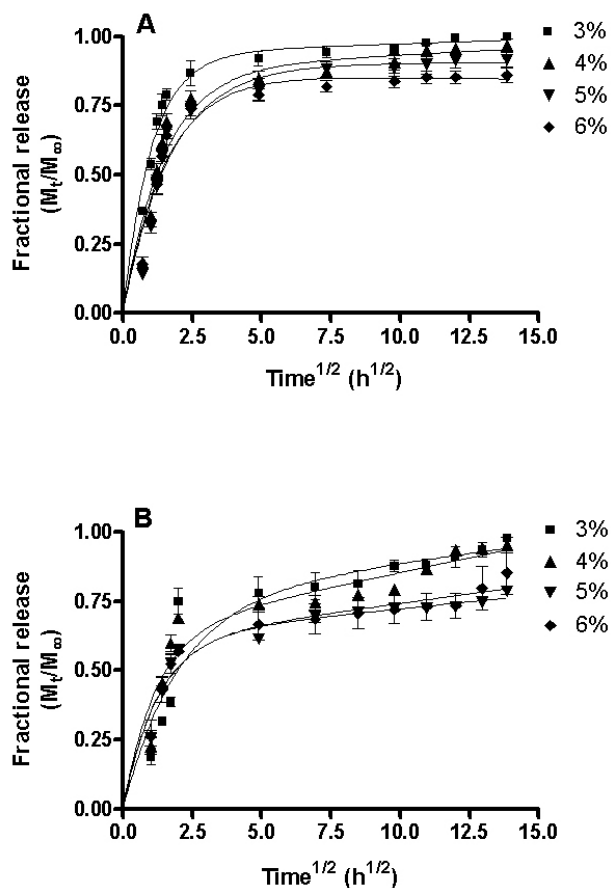


Figure 4.6. Fractional release of pilocarpine as a function of time for 3, 4, 5 and 6 % w/v hydrogels prepared using 1:1 (A) and 1:2 (B) stoichiometries. All measurements were performed in triplicate and plotted as mean \pm SEM. The release data were fitted using a two-phase exponential association equation in GraphPad Prism 4 software. The goodness of fit (R^2) for the different hydrogels varied from 0.76 to 0.93. The initial burst release of pilocarpine appears to correlate well with the swelling phase ($\sim 0-3$ h) as shown in Figure 4. 4. Once swelling terminates, a sustained release phase begins. The higher burst phase appears to also be affected by pore size with the largest pore size hydrogel (3 %) having the largest burst effect. The release mechanism is non-fickian or anomalous involving both diffusion and polymer relaxation ($0.5 < n < 1$). An increase in copolymer/crosslinker concentration results in a slower pilocarpine release

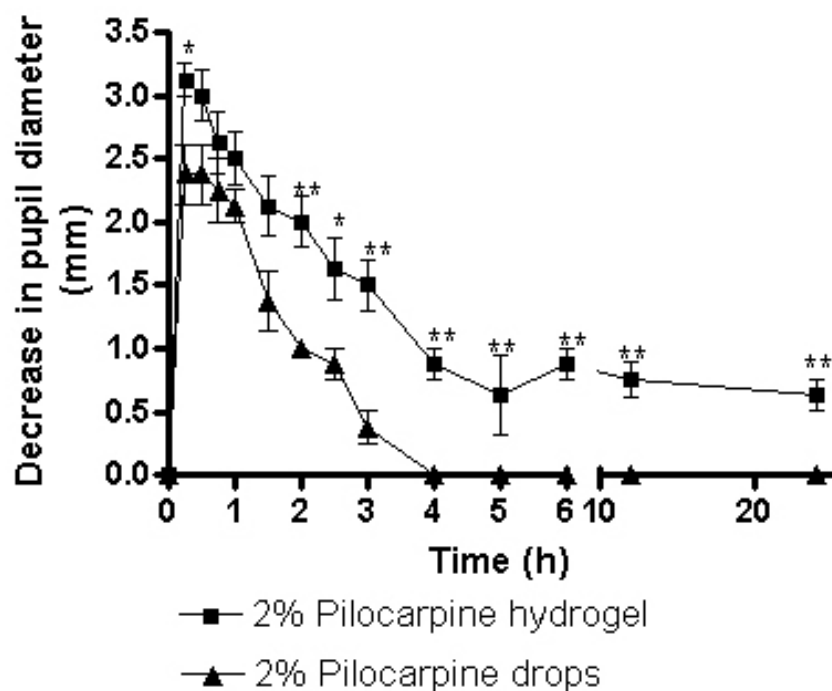


Figure 4.7. Decrease in pupil diameter vs. time for pilocarpine-loaded hydrogel (4 %, w/v, copolymer and crosslinker in 1:2 stoichiometries) and aqueous pilocarpine (2 %, w/v) solution in PBS. Mean \pm SEM of four determinations is reported. The statistically significant differences in pupil diameter changes between both the groups is denoted by * ($p < 0.05$) and ** ($p < 0.01$). The hydrogel shows sustained pharmacological response for a period of 24 h.

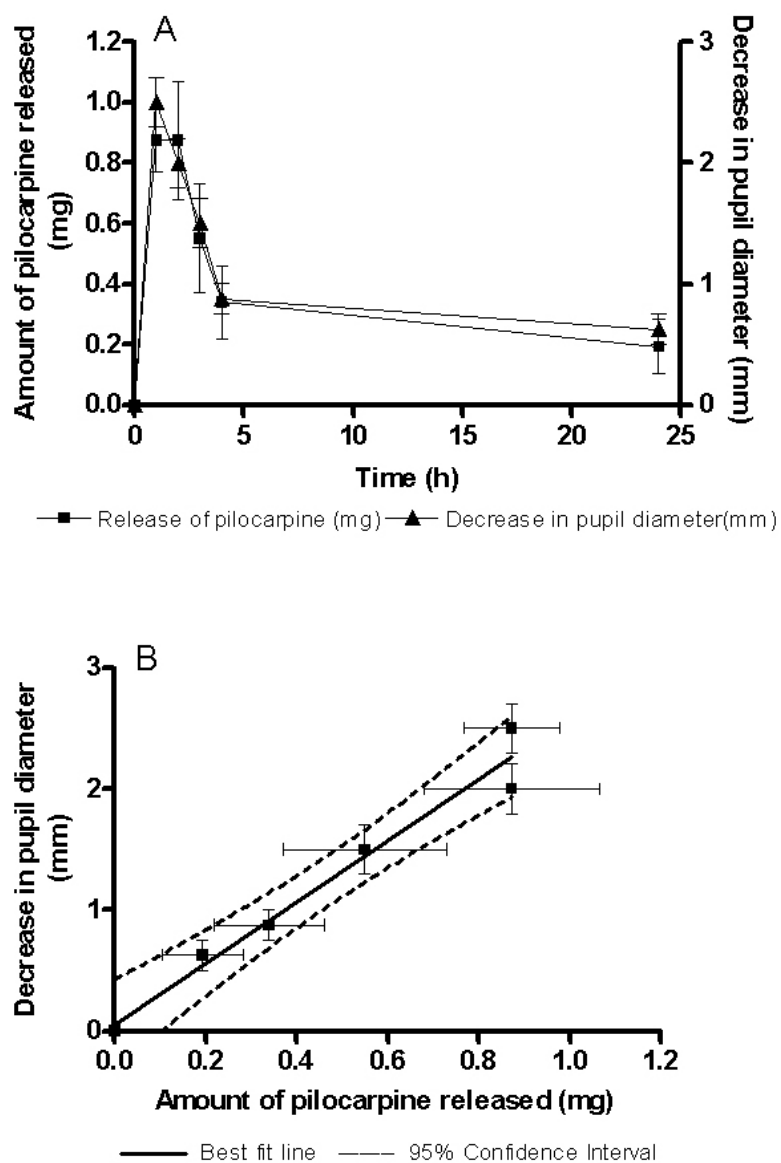


Figure 4.8. Correlation between in vitro pilocarpine release and pupillary constriction obtained in vivo. A linear correlation is evident with an R^2 of 0.97. As the amount of pilocarpine available for absorption decreases, a corresponding increase in pupil diameter is observed. Data are reported as mean \pm SEM. Solid line indicates the best fit line and dashed line indicates the 95 % confidence interval.

5 EVALUATION OF NITROGEN MUSTARD SKIN WOUND PROGRESSION AND BARRIER PROPERTY IN A MOUSE MODEL

5.1 Introduction

Sulfur Mustard (SM), a potent chemical warfare agent, is the most abundantly produced and stockpiled vesicant worldwide [1]. SM has cytotoxic, cytostatic and mutagenic effects caused by both the alkylation of DNA, RNA, proteins and phospholipids, and by inhibition of DNA replication [1, 54, 196]. SM is a threat to both civilians and military personnel due to lethal or incapacitating injuries to the eyes, lungs and skin. Skin is particularly susceptible to SM exposure due to its large surface area and rapidly proliferating keratinocytes of the basal layer [43, 197, 198]. The onset of symptoms depends on the vapor concentration and exposure time of SM, as well as temperature, moisture, and anatomical location. Higher doses of SM and moist thin epidermal layers are known to shorten the symptom-free latency period [49]. SM may affect both the epidermis and dermis of skin, but it generally manifests as edema, inflammation and cell death in the basal keratinocyte layer at the site of injury. Histopathologically this layer shows highest cell damage such as karyolysis and pyknosis [50, 51]. Blister formation occurs between the epidermis and dermis within several hours after SM exposure [52, 53]. The dermis is comparatively less affected, but over time shows signs of discrete necrosis, decreased number of fibroblasts and histiocytes. Biopsies at the exposed areas are characterized by a detachment of the epidermis, areas of necrosis, massive cellular infiltration, capillary engorgement and thrombosis [51]. Cell death, separation of cellular layers, and cellular infiltrate are the common histopathological changes that occur in the skin after SM exposure.

In the current study nitrogen mustard (mechlorethamine hydrochloride, bis (2-chloroethyl) methylamine, chloromethine, mustine, NM) was used as a surrogate to simulate SM injury in the skin since it is less regulated and eliminates the need for a specialized containment facility [196, 199-204]. Although considered less toxic than SM, NM is chemically closely related to it and has similar vesicant properties [196]. Through the alkylation properties of its chloroethyl groups, NM induces interstrand and intrastrand crosslinks in DNA leading to cell death [205-207]. NM has been widely used as a therapeutic agent for the treatment of Hodgkin's lymphoma [208-210], cutaneous T-cell lymphoma [211, 212] and mycosis fungoides [213-215]. However, NM is not selective towards neoplastic cells and is toxic to all rapidly dividing cells causing undesirable side effects including bone marrow depression, GIT disorders, mutagenesis, teratogenesis and even carcinogenesis [205, 206, 216].

SM and NM quantitatively differ in their cutaneous permeation rate and injury producing ability, both of which are greater for SM [217, 218]. However, cutaneous exposure to both SM and NM produces similar histopathological and immunohistochemical effects as a result of their direct effect on the basement membrane zone [218]. Due to its similarities with SM, NM was used as a model vesicant to simulate SM injuries in the skin. SKH-1 hairless mouse, which is widely used for dermal research [203, 219, 220] is used as an animal model to evaluate the histopathological and inflammatory affects of dermally applied NM.

To develop effective countermeasures for vesicant injured skin, it is important to study the effect of vesicants post exposure on wound progression and barrier properties of skin. The integrity of skin affects the permeation of topically applied drugs, which in turn affects pharmacological efficacy. Current literature does not provide any information regarding the dose and time dependent effects of NM on skin or the effect of vesicants on dermal permeability. Hence evaluation of the toxic effects and permeability of skin after NM exposure can provide valuable information on wound progression and its integrity.

In the current study, the progression of dermal wounds after cutaneous exposure to NM was evaluated qualitatively from the dose and time dependent effects of NM using histology of skin and quantitatively from the levels of inflammatory biomarkers in skin. The loss of skin integrity was correlated to the barrier function by measuring the permeation of various molecular markers at 0, 24, 72 and 168 h after NM exposure. Compounds varying in hydrophilicity and molecular weight/molecular radius were used as probes for measuring the effect of physicochemical properties of drugs on permeation through vesicant exposed skin. The purpose of this study is to develop a dermal wound model for evaluating vesicant wound progression and barrier properties of skin.

5.2 Materials and methods

5.2.1 Materials

Female SKH-1 hairless mice (6-10 weeks old) were purchased from Charles River Laboratories (Wilmington, MA). [3H] mannitol (99% pure, specific activity=20ci/mM) was purchased from American Radiolabeled Chemicals, Inc (St. Louis, MO). Rhodamine 123, nitrogen mustard (NM), acetone, Fluorescein isothiocyanate labeled dextran's

(FITC-dextran's) with molecular weight's of 4000 (FD-4), 10000 (FD-10), 20000 (FD-20) and 40000 (FD-20) were purchased from Sigma-Aldrich (St. Louis, MO). Acuderm Acu-Punch biopsy punches and 10% formalin were purchased from Fisher Scientific (Pittsburgh, PA). Trizol reagent were obtained from Invitrogen Corporation (Carlsbad, CA) and High Capacity cDNA Reverse Transcription Kit with RNase inhibitor was obtained from Applied Biosystems (Foster City, CA). Eppendorf Phase Lock Gel was obtained from Brinkmann Instruments (Westbury, NY). RNA Storage Solution was obtained from Ambion (Austin, TX). Primer and probe sets for IL-1 β , TNF- α and Glyceraldehyde-3-phosphate dehydrogenase (GAPDH) were designed by TaqMan Assay-By-Design service (Applied Biosystems, Foster City, CA). Molecular Dynamics Personal Densitometer and ImageQuant are from Amersham Bioscience (Piscataway, NJ). A Franz diffusion cell apparatus (PermeGear, Hellertown, PA) was used for drug permeation studies. The histology sections were observed using a light microscope (Leica DM-LB, magnification 10 x; Leica Microsystems Wetzlar GmbH, Wetzlar, Germany). Images were captured and acquired using ProgRes camera and ProgRes Capture Pro Software 2.6 respectively (Jenoptik Laser, Optik, Systeme GmbH, Jena, Germany). A Tecan GENios microplate reader (Tecan, Durham, NC) was used to measure fluorescence of FITC-dextrans and rhodamine 123. The radioactivity of 3[H] mannitol was measured using a Wallac 1409 Liquid Scintillation Counter (LSC) (Wallac Oy, Turku, Finland).

5.2.2 Dose and time dependent effect of NM on mice skin

A SKH-1 hairless mouse model was used to assess NM dermal wound progression *in vivo*. All animal studies were conducted in accordance with the protocol approved by

Laboratory Animal Services (LAS), Rutgers University. NM dissolved in acetone was applied topically to the dorsal skin of mice and left in the hood overnight to degas. A standard circular template (15 mm) was used to ensure uniform exposure area of NM on all mice. For the dose response study, topical wounds were created by application of 5, 25, 50, 75 and 100 μ moles NM. The mice were euthanized by CO₂ gas and punch biopsies were collected at 24 h after exposure to evaluate the dose dependent effects of NM on dermal wound formation. The dose of NM at which a lesion forms and mice survive for at least 168 h was chosen for time response, inflammatory biomarkers and permeation studies. For the time response study, topical wounds were created by application of 5 μ moles of NM (which was based on the results of the dose response study) and punch biopsies were collected from the wounded skin at 0, 24, 72 and 168 h. The skin samples were fixed in 10% formalin and histology evaluated by H&E staining. Both the dose and time response treatments included five mice in each group.

5.2.3 Measurement of inflammatory biomarkers

5.2.3.1 Measurement of edema

Punch biopsies from the dorsal wounded skin of mice were collected at 0, 24, 72 and 168 h. The weight of the tissue was measured and the results were reported as mean \pm SEM of five mice in each treatment group. One way analysis of variance (ANOVA) was used to determine the significance of NM exposure time on edema.

5.2.3.2 Measurement of mRNA levels

The punch biopsy samples from the wounded skin of mice collected at 0, 24, 72 and 168 h were snap frozen in liquid nitrogen and stored at -80°C until further analysis of RNA.

The results were reported as mean \pm SEM of five mice in each treatment group. One way ANOVA was used to determine the significance of NM exposure time on mRNA levels of the inflammatory biomarkers interleukin 1 β (IL-1 β) and tumor necrosis factor α (TNF- α).

5.2.3.2.1 RNA isolation and reverse transcription

The RNA isolation and reverse transcription were performed as previously described [221]. Briefly, total RNA was isolated from the tissue samples using TRIzol reagent, according to the manufacturer's instructions. Eppendorf phase lock gel, a product that eliminates interface-protein contamination during phenol extraction and was added during centrifugation. The RNA pellet was dissolved in RNA storage solution and RNA quantitated spectrophotometrically at 260 nm Total RNA (1 μ g) was reverse-transcribed into cDNA using a High Capacity cDNA Reverse Transcription Kit for reverse transcriptase-polymerase chain reaction (RT-PCR). A minus reverse transcriptase reaction was used as a control.

5.2.3.2.2 Real-time polymerase chain reaction

The mRNA levels of IL-1 β and TNF- α were measured from cDNA samples by TaqMan gene expression assay. To compensate for variations in input RNA amounts, and efficiency of reverse transcription, GAPDH an endogenous control gene was also quantified, and results were normalized to these values.

5.2.4 Evaluation of barrier property of skin by measurement of permeability of molecular markers through NM exposed skin

The damage caused by vesicant exposure on the integrity and barrier properties of skin was evaluated by measuring the variations in permeability of mice skin exposed to NM, at various time points following exposure. [3H] mannitol (molecular weight = 182.17) was used as a hydrophilic marker; FD-4, FD-10, FD-20 and FD-40 were used as molecular weight markers; Rhodamine 123 (molecular weight = 380.82) was used as a lipophilic marker. The permeability profiles were evaluated on mice skin collected at 0 (controls), 24, 72 and 168 h after exposure to NM.

5.3 Results and Discussion

5.3.1 Dose and time dependent effects of NM on mouse skin

Histology of NM exposed mouse skin indicated a dose and time dependent wound progression. Figures 5.1 and 5.2 are representative H & E stained histological sections of mouse skin that depict a dose and time dependent response to NM exposure, respectively. The histology of control skin shows an intact epidermis and dermis, healthy nuclei in the epidermis, fibroblasts in the dermis and a continuous skeletal muscle. Exposure to NM for 24 h resulted in the following histopathological effects at the entire dose range (5-100 μ moles): edema (increased size of the dermis), infiltration of inflammatory cells in the dermis, shrinkage/condensation of nuclei in the epidermis (pyknosis) and discontinuity of the skeletal muscle. However, separation of the epidermis from the dermis was found to be strictly dependent on the exposure dose of NM. At an exposure dose of 5 μ moles of NM, the epidermis remained attached to the dermis in most areas. Increasing doses of NM (25, 50 μ moles), resulted in larger areas of the epidermis separating from the dermis,

and complete detachment of the epidermis was observed at higher doses (75, 100 μ moles). All mice exposed to NM at doses greater than 5 μ moles survived for less than a week confirming that NM is extremely toxic when applied topically. Based on the results of the above study, a concentration of 5 μ moles of NM was chosen for further studies such as evaluation of time response, levels of inflammatory biomarkers and barrier properties of the skin after NM exposure.

Figure 5.2 shows the time dependent effects of NM exposure on mouse skin. NM induced wound progression was followed for upto 168 h after exposure. Histology of skin samples obtained 24 h after NM exposure, mainly showed edema, pyknotic nuclei in the epidermis, inflammatory infiltration and discontinuity of the skeletal muscle. In the skin samples obtained 72 h after NM exposure, edema, separation of the epidermis from the dermis, death of the epidermal cells (no nuclear staining) and discontinuity of the skeletal muscle was observed. At 168 h after NM exposure, reepithelization in the epidermis (a sign of wound healing) from the wound edges was observed along with necrosis in the dermis. Reepithelization was mainly characterized by epidermal hyperplasia (increased keratinocyte proliferation in the epidermis) and hyperkeratosis (thickening of the stratum corneum). It has been shown that reepithelization is essential for wound repair in order to restore the intact epidermal barrier and occurs by the movement of epithelial cells from the edge of the unwounded tissue across the site of injury [222-226]. The results of the above time response study indicate that the NM (5 μ moles) induced wound progresses from 0 - 72 h and wound healing initiates between 72 - 168 h in SKH-1 mice.

5.3.2 Measurement of inflammatory biomarkers

SM exposure on skin elicits an inflammatory response that results in increased edema and production of several inflammatory cytokines [12, 13, 43, 64, 227-237]. The release of cytokines can induce a strong chemotactic response that attracts neutrophils and macrophages. The number of infiltrating cells is dependent on the dose and time of SM exposure [69]. The time dependent effects of NM on mouse skin were quantitatively measured from the extent of edema and the mRNA levels of pro inflammatory cytokines IL-1 β and TNF- α .

5.3.2.1 Measurement of edema

The tissue weight of biopsy from skin exposed to NM was measured to determine the extent of edema. Edema is the most common inflammatory response caused by mustard exposure on mice skin [203]. Figure 5.3 indicates that dermal edema is dependent on the duration of NM exposure. A significant increase ($p < 0.05$) in tissue weight was observed at 24, 72 and 168 h after exposure to NM, demonstrating marked edema in a time dependent manner, with edema being highest at 24 h.

5.3.2.2 Measurement of mRNA levels

IL-1 β and TNF- α are pro inflammatory cytokines that are important indicators of inflammatory response in a tissue. Figure 5.4 shows that the mRNA levels of IL-1 β and TNF- α increased at 24, 72 and 168 h after NM exposure relative to control skin, with peak activity at 168 h. Only the mRNA levels of IL-1 β at 168 h after NM exposure were found to be significantly higher than the control ($p < 0.05$) These results indicate that

targeting the inflammatory pathway could be an effective treatment option for healing dermal mustard injuries.

5.3.3 *Permeation profiles of markers through NM exposed skin*

The permeability of molecular markers is an important prediction of the integrity of skin after vesicant exposure, which in turn correlates to its barrier property *in vivo*. It can also be used to provide comprehensive data on the permeation properties of molecules as a function of molecular weight and lipophilicity, in skin subjected to variable degrees of damage. This data can be very useful in predicting the permeability of new compounds based on their physiochemical properties in intact and damaged skin.

The permeation profiles of molecular markers through NM exposed skin were evaluated for 24 h using a Franz diffusion cell apparatus. Figures 5.5, 5.6 and 5.7 show the cumulative amount of molecular marker permeated (cpm/cm² or ng/cm²) as a function of time (h). Table 5.1 shows the permeability coefficients of these markers through skin exposed to NM, at various time points following exposure. Flux (J) was obtained from the slope of the linear portion of the permeation curves and permeability coefficients (P) were calculated from flux using the equations below:

$$J = \frac{dQ}{dt.A} \quad (1)$$

$$P = \frac{J}{C_o} \quad (2)$$

Where J indicates the steady state flux, dQ the amount of drug permeated, A the dermal area exposed, dt the time of permeation and C_0 represents the initial drug concentration in the donor compartment.

The stratum corneum is the main barrier to dermal permeability of most drugs, particularly hydrophilic drugs [90, 91, 238, 239]. The stratum corneum can be damaged in numerous ways and this can result in increased transdermal permeability of drugs. At 24 h after NM exposure, the stratum corneum is damaged but still intact. At 72 h after NM exposure, incomplete to complete loss of stratum corneum occurs. Hyperkeratosis of the stratum corneum is seen in skin collected 168 h after NM exposure. To correlate the extent of NM damage on skin and hence its barrier properties, permeability of different molecular markers varying in their physicochemical characteristics was evaluated

^3H mannitol is a hydrophilic low molecular weight marker and its permeation through mice skin exposed to NM for various time periods was found to increase compared to the control (Figure 5.5). The order of permeation of mannitol is 72 h > 168 h > 24 h > control (Table 5.1). The high permeability of mannitol at 72 h corresponds to the maximum damage at this time point, due to the absence of stratum corneum and separation of epidermis from the dermis. Wound reepithelization starts in between 72-168 h and the barrier property of skin improves resulting in decreased permeation at 168 h compared to 72 h. The barrier property of skin is decreased at 24 h after NM exposure due to wound formation and hence results in increased permeation at 24 h compared to the control.

The effect of different molecular weight FITC-dextran's on permeability through intact and NM damaged skin was studied. FITC-dextran's which are hydrophilic in nature showed increased permeation through skin exposed to NM at various time periods following exposure, irrespective of their molecular weight (Table 5.1). The order of permeation of FD-4, FD-10, FD-20 and FD-40 is 72 h > 168 h > 24 h > control. The change in permeation at the different time points following NM exposure is similar to mannitol and hence the same factors (state of stratum corneum) affecting mannitol's permeation could be also be influencing FITC-dextran's permeation. The permeability of FITC dextran's through control and NM exposed skin declined with increasing molecular weight (FD-4 > FD-10 > FD-20 > FD-40) showing that permeability through skin is molecular weight dependent. Lower molecular weight compounds have higher permeation through skin compared to similar compounds of higher molecular weight.

Rhodamine 123 is a lipophilic cationic fluorochrome. The permeability of rhodamine 123 through control skin is much higher than that of the other molecular markers evaluated in the current study. This is due to the fact that cationic lipophilic compounds have higher permeation rates through the negatively charged lipophilic stratum corneum barrier [240]. Even though the permeation of rhodamine 123 through NM exposed skin increased relative to the control, the order of increased permeation is contrary to other markers evaluated in the current study. The order of rhodamine 123 permeation through NM exposed skin is 24h > 168h > 72 h > control. The higher permeation of rhodamine 123 through skin exposed to NM for 24 and 168 h compared to 72 h is likely due to the still intact stratum corneum at 24 h and new stratum corneum that is being formed at 168 h.

Also, at 24 h, the solubility and partitioning of rhodamine 123 into the viable, hydrophilic, edematous epidermis and dermis of skin might have resulted in higher permeation rates.

The permeability studies show that the integrity of skin is at its lowest 72 h after NM exposure which corresponds to the maximum damage observed at 72 h in the time dependent effects study (Figure 5.2). All the molecular markers showed an increased permeation through NM exposed skin compared to the control which implies that the barrier property is compromised in vesicant exposed skin.

5.4 Conclusion

A SKH-1 mouse model was developed to study the dose and time dependent effects of NM on dermal wound progression in a qualitative manner. Edema and mRNA levels of IL-1 β and TNF- α were used to evaluate the quantitative inflammatory response of NM on mouse skin. These inflammatory biomarkers can be used in wound healing efficacy studies of new countermeasures for mustard injured skin. Systematic data on the permeability of skin at various time periods after NM exposure is useful in evaluating the integrity and hence the barrier property of skin after vesicant exposure. The permeability of molecular markers through intact and NM exposed skin gives us an idea of the effect of physicochemical characteristics of drugs on permeation. Such data can be used to build pharmacokinetic simulation models for obtaining quantitative estimates of transdermal drug delivery rates.

5.5 Tables

Table 5.1. Permeability coefficients of different molecular markers through skin exposed to NM for 0, 24, 72 and 168 h

Molecular marker	Permeability coefficient (cm.h ⁻¹)x10 ⁻⁶			
	Control (No NM exposure)	24 h after NM exposure	72 h after NM exposure	168 h after NM exposure
³ [H] mannitol	27.45 ± 2.465	96.36 ± 13.68	1091 ± 216	157.7 ± 18.6
Rhodamine 123	161.5 ± 75.58	889.7 ± 124.4	477.1 ± 14.14	692.2 ± 18.32
FD-4	15.23 ± 1.758	28.55 ± 9.384	1270 ± 43.21	1054 ± 42.03
FD-10	5.055 ± 0.5354	9.517 ± 1.399	278.7 ± 10.18	157.2 ± 9.850
FD-20	1.844 ± 0.1467	3.147 ± 0.342	147 ± 8.529	43.82 ± 2.343
FD-40	1.667 ± 0.5567	2.598 ± 0.3761	75 ± 28.72	16.61 ± 0.6648

5.6 Figures

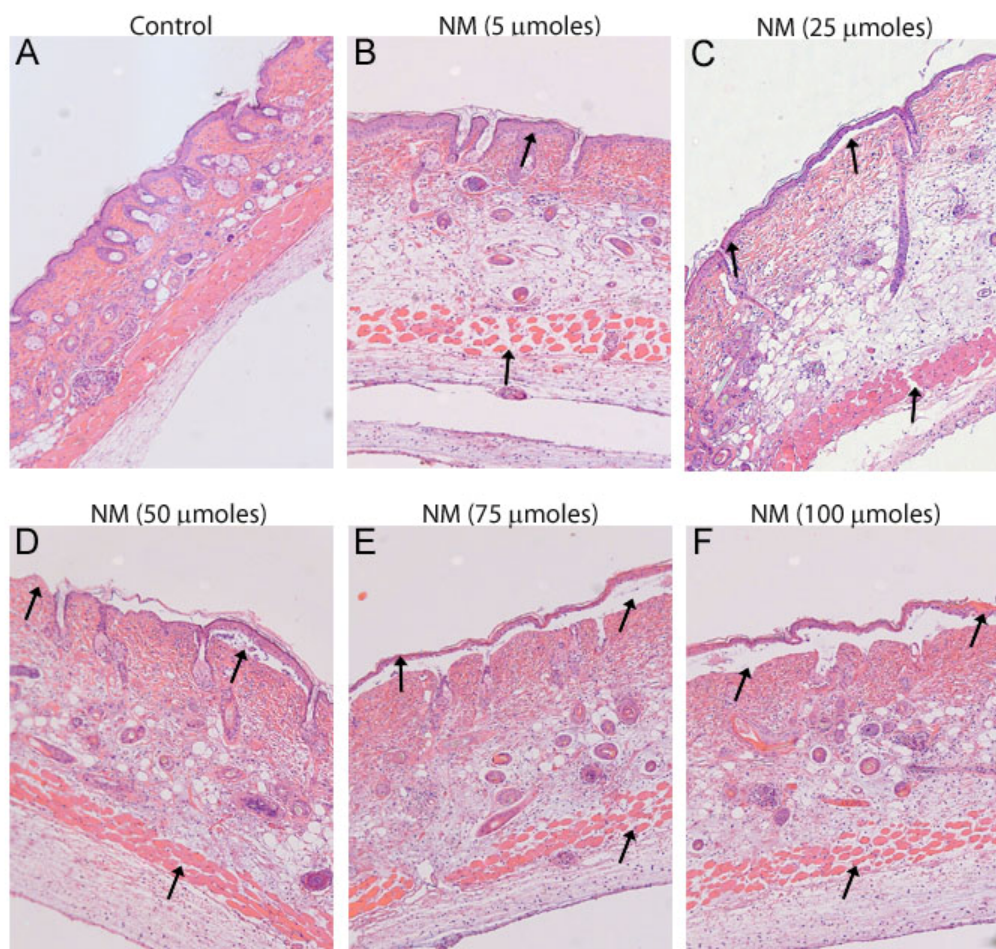


Figure 5.1. Dose dependent effects of NM exposure on mice skin visualized by H & E staining (10 x). The arrows in B denote pyknotic nuclei in epidermis and discontinuous skeletal muscle in the dermis. Arrows in C, D, E and F denote pyknotic nuclei in epidermis, separation of epidermis from dermis and discontinuous skeletal muscle in dermis. The separation of epidermis from the dermis progresses in a dose dependent manner from 5-100 μmoles.

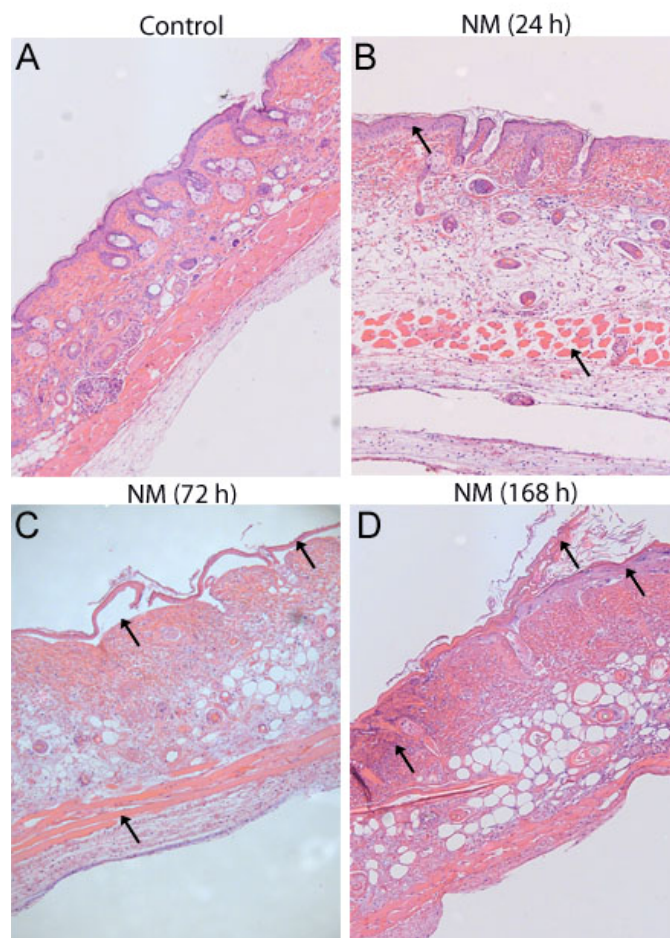


Figure 5.2. The histology of time dependent effects of NM exposure on mice skin at 10 x magnification visualized by H & E staining. The arrows in B denote pyknotic nuclei in epidermis and discontinuous skeletal muscle in the dermis. Arrows in C denote absence of nuclear staining in the epidermis, separation of epidermis from dermis and discontinuous skeletal muscle in dermis. Arrows in D denote dermal necrosis with, reepithelization from the wound edges characterized by epidermal hyperplasia and hyperkeratosis. These results show that wound progresses from 0 - 72 h and wound healing initiates between 72 - 168 h when SKH-1 mice are exposed to 5 μ moles of NM.

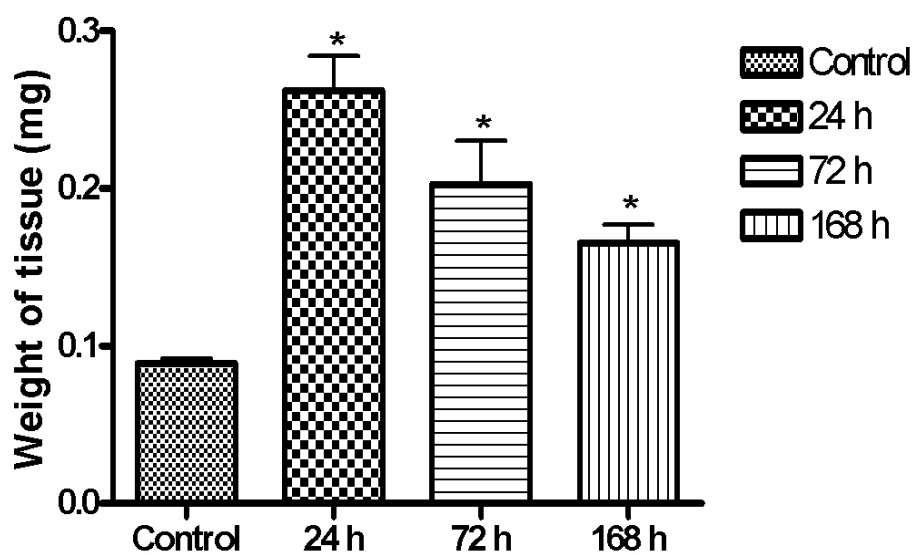


Figure 5.3. Time dependent inflammatory response of NM on mice skin measured by edema. A significant increase ($p < 0.05$) in tissue weight at 24, 72 and 168 h is seen demonstrating marked edema when skin is exposed to NM.

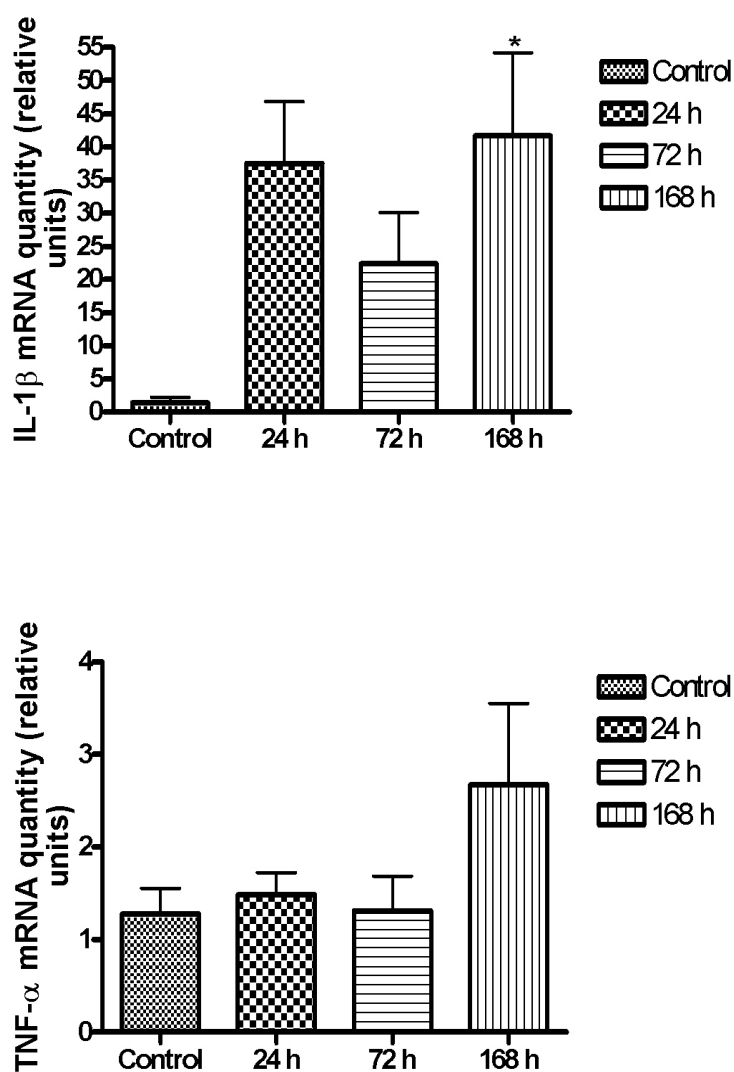


Figure 5.4. Time dependent effect of NM exposure on mice skin measured from the mRNA levels of IL-1 β and TNF- α .mRNA levels increased at 24, 72 and 168 h relative to control skin with peak activity at 168 h. Only the mRNA level of IL-1 β at 168 h post exposure was found to be significantly higher than the control (p<0.05).

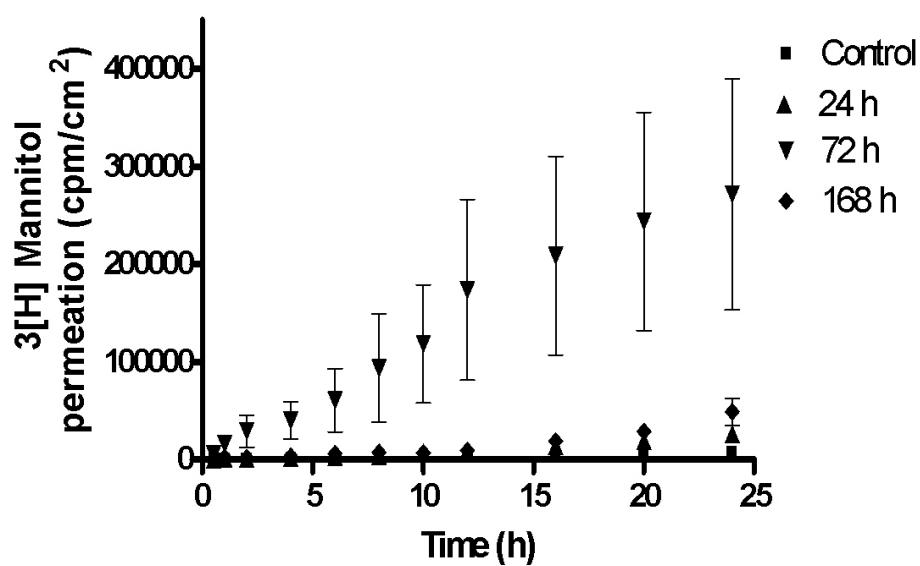


Figure 5.5. Permeation profile of ^3H mannitol (hydrophilic marker) through NM exposed mice skin. The order of permeation is $72\text{ h} > 168\text{ h} > 24\text{ h} > \text{control}$. The permeation of mannitol is significantly higher than the control at 24, 72 and 168 h ($p < 0.001$).

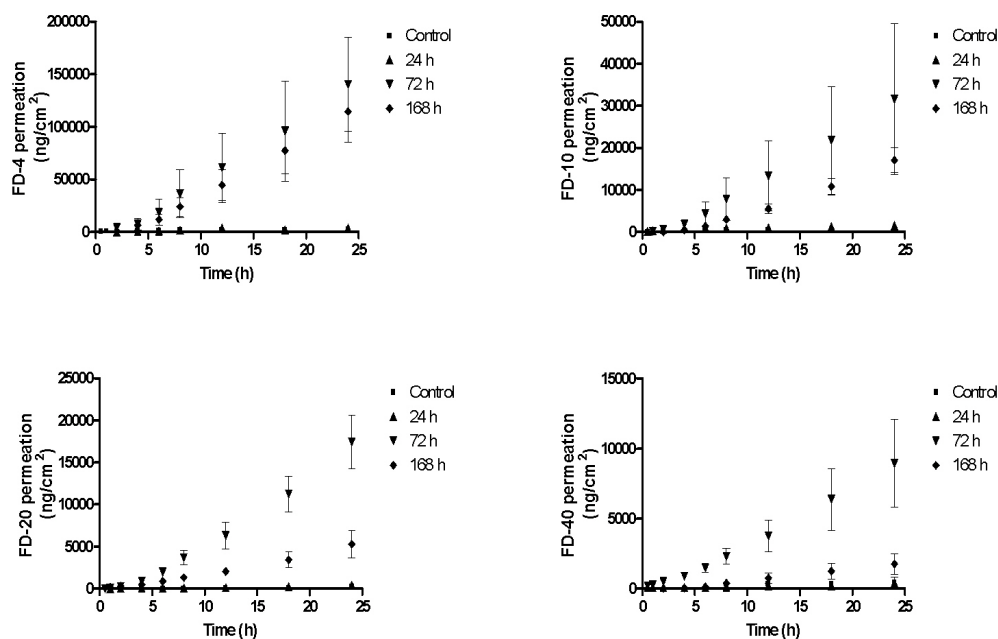


Figure 5.6. Permeation profile of FITC-dextran's (molecular weight markers) through NM exposed mice skin. The order of permeation is 72 h > 168 h > 24 h > control. The permeation of FD-4 is significantly higher than the control at 72 and 168 h ($p < 0.001$). The permeation of FD-10 is significantly higher than the control at 24 h ($p < 0.01$), 72 and 168 h ($p < 0.001$). The permeation of FD-20 is significantly higher than the control at 24 h ($p < 0.01$), 72 and 168 h ($p < 0.001$). The permeation of FD-40 is significantly higher than the control at 72 and 168 h ($p < 0.001$).

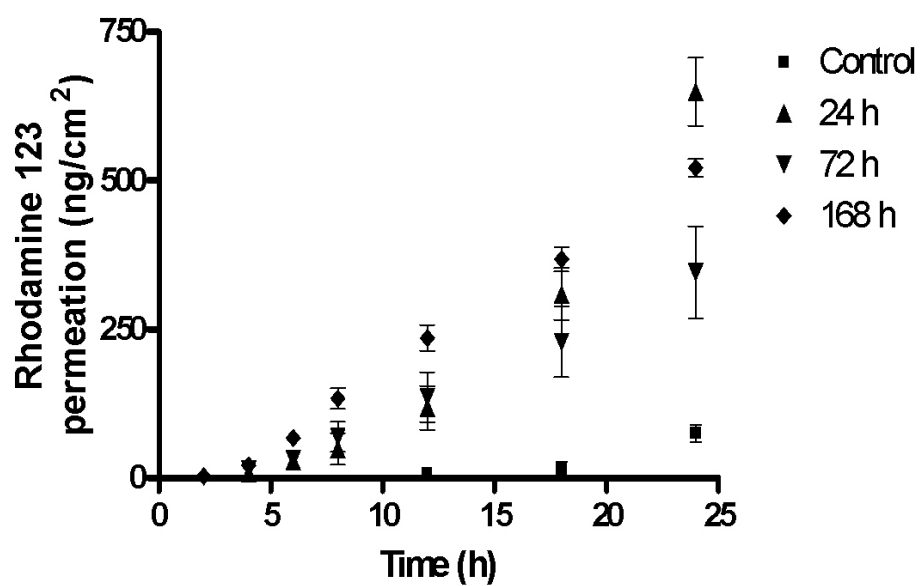


Figure 5.7. Permeation profile of rhodamine 123 (lipophilic marker) through NM exposed mice skin. The order of permeation is 24 h > 72 h > 168 h > control. The permeation of mannitol is significantly higher than the control at 24 h ($p < 0.001$), 72 h ($p < 0.01$) and 168 h ($p < 0.001$).

6 DOXYCYCLINE LOADED POLY(ETHYLENE GLYCOL) HYDROGELS FOR OCULAR WOUND HEALING APPLICATION

6.1 Introduction

Sulfur mustard (SM, 2,2-dichlorethyl sulfide) is a potent cytotoxic and mutagenic vesicant that was used as a chemical warfare agent for the first time during World War I and in over 10 subsequent conflicts [241, 242]. In the 1980's, SM was used in the Iran-Iraq war, affecting not only military personnel but also 100,000 civilians [243, 244]. Exposure to SM causes devastating injuries to the eyes, skin and respiratory system [3, 245], however the eyes are the most sensitive tissue to SM with a threshold of 12 mg.min/m^3 , compared to 200 mg.min/m^3 for the skin. Even low doses of SM induce incapacitation, visual impairment and panic [3]. Although the molecular mechanisms for SM-induced injury are unclear, it is known that the vesicant alkylates DNA, RNA and proteins and causes inflammation, tissue damage and cell death [3]. MMPs are a family of enzymes that enhance the action of many activating factors during inflammatory response and contribute to tissue degradation [5-7, 9, 10, 12, 13, 15, 16]. MMP-9 has been identified as a potential target of therapy for SM damage since it was found that its expression and activation quantitatively increases over time in response to SM exposure [12, 13]. The cornea is clinically impaired by SM exposure exhibiting chronic inflammation and increased MMP activity [246]. Decreased MMP-9 activity in humans has been found to correlate with accelerated wound healing [18, 19]. Hence, intervention targeting of both the inflammatory response and increased protease expression could provide a therapeutic approach for the treatment of SM-induced corneal wounds.

Doxycycline is a long acting semi-synthetic tetracycline, which is well recognized for its therapeutic efficacy in treating MMP mediated ocular surface diseases, such as rosacea, recurrent epithelial erosions and sterile corneal ulcerations.[247-249]. Doxycycline has been found to inhibit MMP-9 activity *in vivo* in the corneal epithelial cells of experimental dry eye [26] as well as *in vitro* in human corneal epithelial cells [22, 23]. Treatment with doxycycline has been shown to be beneficial in attenuating acute and delayed ocular injuries caused by SM exposure [27, 28]. The drug is an inexpensive, FDA approved antibiotic that likely promotes wound healing by reducing inflammation and protease activity.

The blood ocular barriers, which include the blood-aqueous and blood-retina barriers protect the eye, but prevent drug distribution to the anterior and posterior chambers, limiting ocular bioavailability [250, 251]. Drug diffusion into the eyes from the systemic circulation is slow and inefficient. Most drugs applied to the eye surface as solutions have ocular bioavailability in the range of about 10% with most of the drug being cleared by local systemic absorption [251, 252]. Solutions are in contact with the eye surface for a very short period of time as the tear film quickly washes them away. The contact time, local drug concentration and thereby duration of action can be prolonged by designing topical formulations with higher viscosities [253].

The ideal drug delivery system for corneal wound repair should be nontoxic, transparent, easy to administer, possess rheological properties to maintain its structural integrity, provide a microbial barrier, release the drug in a controlled and sustained manner and

decrease the time of wound healing. There are very few controlled drug delivery systems reported for corneal wound repair applications [170, 254-257]. Although doxycycline is commercially available in a wide variety of dosage formulations including tablets, capsules and suspensions, topical ocular doxycycline eye drop formulations are to this day compounded by a pharmacist. Since there are currently no ocular formulations commercially available for doxycycline, there is a critical need for a controlled release doxycycline delivery system that can be easily applied to the eye to promote wound healing. Earlier, we have shown that pilocarpine-loaded ocular hydrogels provide sustained drug release and increased pharmacological efficacy in comparison to pilocarpine drops [77]. As ocular drug delivery systems, hydrogels provide prolonged corneal contact time, reduced drug loss from the corneal surface, and convenient administration. PEG based hydrogels are used in the current study since PEG is FDA approved, non-toxic, water soluble, easily processable and highly stable to temperature and pH [33, 34, 171]. The hydrogels evaluated in the current study are formed *in situ*, in other words, they are liquids upon instillation and undergo a phase transition at physiological pH to form the hydrogel. This occurs by covalent intermolecular crosslinking of polymer chains through reversible thioester bonds resulting in biodegradable viscoelastic hydrogels. In this study, doxycycline loaded fast forming PEG hydrogels were designed for the treatment of simulated mustard injuries using surrogate vesicants and evaluated in a rabbit corneal organ culture model.

6.2 Materials and methods

6.2.1 Materials

The polymers 8-arm-PEG-SH (20 kDa, 83.8% total activity by NMR) and 8-arm-PEG-N-hydroxysuccinimide (PEG-NHS) (20 kDa, 95.1% total activity by NMR) were custom synthesized by NOF Corporation (White Plains, NY). Doxycycline hyclate, agar, ascorbic acid, RPMI 1640 vitamin solution, ciprofloxacin, haematoxylin dye, CEES and NM were obtained from Sigma-Aldrich (St. Louis, MO). CoorsTek spot plates, eosin, Pen-Fix, methanol, acetonitrile, oxalic acid and HPLC grade solvents were obtained from Fisher Scientific (Suwanee, GA). The optical transmission (OT) of the hydrogel was determined using a Milton Roy Spectronic Genesys 5 spectrophotometer (Thermo Fisher Scientific, Pittsburgh, PA). Rheological data were obtained on a SR-2000 rheometer from Rheometric Scientific Inc (Piscataway, NJ) and analyzed by RSI orchestrator software. A Franz diffusion cell apparatus (PermeGear, Hellertown, PA) was used for drug release and permeation studies. Polycarbonate membranes used for *in vitro* release studies were purchased from GE Osmonics Labstore (Minnetonka, MN). Waters HPLC system equipped with a UV detector and an Eclipse XDB-C₈ column (Agilent, Zorbax, 4.6 x 150 mm) was used to analyze doxycycline concentration. Rabbit eyes were obtained from Pel-Freeze Biologicals (Rogers, AR). Dulbecco's modified eagle's medium (DMEM), High glucose DMEM, MEM-non essential amino acid solution (MEM-NEAA), Alexa-Fluor 488-conjugated goat anti-mouse IgG antibodies, 4',6-diamidino-2-phenylindole (DAPI) and Prolong Gold were obtained from Invitrogen Corporation (Carlsbad, CA). The cryomolds and Tissue-Tek OCT was obtained from Sakura Finetek (Torrance, CA). Normal goat serum was obtained from Jackson ImmunoResearch Laboratories (West

Grove, PA). Mouse anti MMP-9 monoclonal antibody (catalog no MAB3309) were obtained from Millipore (Billerica, MA). A Microm HM505E cryostat was used for sectioning of cornea. The histology sections were observed using a light microscope (Leica DM-LB, magnification 40x; Leica Microsystems Wetzlar GmbH, Wetzlar, Germany). Images were captured and acquired using a ProgRes camera and ProgRes Capture Pro Software 2.6, respectively (Jenoptik Laser, Optik, Systeme GmbH, Jena, Germany).

6.2.2 Hydrogel formation

Hydrogels (5-22.5, w/v) were prepared by mixing the solutions of 8-arm-PEG-SH and 8-arm-PEG-NHS in PBS (pH 8) and leaving the mixture to stand at room temperature (RT) to form the hydrogel. Hydrogel was considered to be formed when the solution ceased to flow from the inverted tube [258]. For example, to prepare a 5% (1:1) hydrogel, aqueous solutions of PEG-SH and PEG-NHS were separately prepared by dissolving 5.0 mg of each polymer in 100 μ L of buffer. The two solutions (total volume = 200 μ L) were mixed in a glass vial and allowed to stand at RT. Hydrogels were formed in 90 seconds. Similar procedure was used to obtain 7.5, 10, 15, and 22.5% hydrogel with 1:1 and 1:2 stoichiometries. Hydrogels used for optical transmission, degree of swelling, drug loading and *in vitro* release studies were 200 μ L in volume, 9 mm in diameter, and 0.3 mm in thickness.

6.2.3 Optical Transmission (OT)

The hydrogels were screened for their potential application as drug delivery systems for corneal wound repair. Different hydrogel compositions [5% (1:1); 7.5% (1:1); 7.5% (1:2); 10% (1:1); 15% (1:1); 15% (1:2); and 22.5% (1:2)] were analyzed for their OT properties. The hydrogels (200 μ L) were placed in a quartz cuvette containing distilled water and transmission of light was measured at 480 nm [185]. A cuvette containing only distilled water was used as reference. All OT studies were done in triplicate and the mean \pm SEM reported. One way analysis of variance (ANOVA) was used to determine the effect of hydrogel composition on its optical transmission.

6.2.4 Rheology

The rheological measurements of 5% (1:1), 7.5% (1:1), 7.5% (1:2), 15% (1:1) and 15% (1:2) hydrogels were performed using a rheometer with cone plate geometry at 37 °C (plate diameter: 25 mm, gap: 3 mm, 2° angle) [143, 144]. The hydrogel samples were equilibrated on the plate for 5 min to reach the running temperature before each measurement. Rheological test parameters, storage/elasticity (G') and loss/viscosity (G'') moduli were obtained under dynamic conditions of non-destructive oscillatory tests. The dynamic strain sweep test was performed at a constant frequency of 1 Hz with percent strain ranging from 10^{-1} to 10^2 . The dynamic frequency sweep test was carried out at a constant strain of 1% (linear viscoelastic region) with frequency ranging from 10^{-1} to 10^1 Hz. All the rheological studies were done in triplicate and the mean \pm SEM reported. Two way ANOVA was used to determine the effect of hydrogel composition on its rheological properties.

6.2.5 Swelling studies

The degree of swelling for different hydrogels [5% (1:1); 7.5% (1:1); 7.5% (1:2); 10% (1:1); 15% (1:1); 15% (1:2); and 22.5% (1:2)] was measured. Hydrogels were placed in a vial and weighed (initial weight) prior to being immersed in PBS (pH 7.4) and placed in an incubator at 37 °C. The degree of swelling of the hydrogels was calculated by weighing the vials after removing the PBS at predetermined time intervals. The buffer was replaced after every measurement and the hydrogels were allowed to swell until equilibrium is reached. The degree of swelling for each hydrogel was determined by using the equation below:

$$\%Swelling = \frac{(W_s - W_o)}{W_o} \times 100 \quad (1)$$

Where W_s is the weight of the swollen hydrogel at time t and W_o is the initial weight. All measurements were made in triplicate for each hydrogel using separate samples and the mean \pm SEM reported. Two way ANOVA was used to determine the effect of hydrogel composition on its degree of swelling.

6.2.6 In vitro doxycycline loading and release

6.2.6.1 Drug loading efficiency

The 10% (1:1), 15% (1:1), 15% (1:2), and 22.5% (1:2) hydrogels loaded with 0.25% w/v of doxycycline were used for drug loading and release studies. The hydrogels were dissected into small pieces and suspended in 5 mL PBS (pH 7.4). The suspension was sonicated for 30 min to completely extract doxycycline from the hydrogel. The amount of doxycycline extracted was quantified by RP HPLC analysis at a wavelength of 350 nm. 0.01M oxalic acid, acetonitrile and methanol (70:18:12) were used as mobile phase at a

flow rate of 1 mL/min. After extraction, suspension containing the hydrogel was stored for several days at 4°C and then reanalyzed to ensure the complete extraction of doxycycline from the hydrogel. Doxycycline was stable under the storage conditions, as determined by HPLC analysis.

6.2.6.2 *In vitro* release

In vitro release from the hydrogels was studied on a Franz diffusion cell apparatus with a diameter of 5 mm and a diffusional area of 0.636 cm². A polycarbonate membrane (0.4 μ) was sandwiched between the lower cell reservoir and the glass cell-top containing the sample for doxycycline release studies. The receiving compartment (volume 5.1mL) was filled with PBS (pH 7.4). The system was maintained at 37°C using a circulating water bath and a jacket surrounding the cell. The receiving medium was continuously stirred (600 rpm) with a magnetic bar to avoid stagnant aqueous diffusion layer effects. 200 μL sample of each hydrogel formulation containing 0.25% w/v doxycycline was prepared and placed in the donor compartment, which was then sealed with parafilm and aluminum foil to prevent evaporation. Aliquots (200 μL) were collected from the receiver compartment at predetermined intervals and replaced with equal volume of PBS to maintain sink conditions throughout the study. The concentration of doxycycline in the release medium was determined using RP HPLC. The cumulative amount of doxycycline released from the hydrogel was determined using a calibration curve. All release experiments were done in quadruplicate and the results were reported as mean ± SEM. The release data were fitted using a two-phase exponential association equation in

GraphPad Prism 4 software. Two way ANOVA was used to determine the effect of hydrogel composition on the *in vitro* doxycycline release.

6.2.7 *Ex vivo* evaluation using Rabbit Cornea Organ Culture Model+

A rabbit cornea organ culture model system adapted from Foreman, et al [259] was used to evaluate healing after exposure to model vesicants CEES and NM, followed by subsequent treatment with doxycycline drops or doxycycline hydrogels. Rabbit eyes were stored in DMEM (with penicillin, streptomycin, amphotericin B and gentamicin) and transported to the laboratory on ice. Corneas with a surrounding 2 mm scleral rim were dissected from the eye and placed with the epithelial side facing down into spot plates containing a small amount of DMEM to prevent drying of the epithelium. The corneal endothelial concavity was then filled with DMEM containing 0.75% agar at 50°C and this mixture was allowed to set (usually within 1 min). Corneas were then inverted and transferred to 60 mm sterile tissue culture dishes and cultured at 37°C in a humidified 5% CO₂ incubator in the presence of medium (500 mL high glucose DMEM, 5 mg ciprofloxacin, 5 mL of 100x MEM- NEAA, 5 mL RPMI 1640 vitamin solution and 50 mg ascorbic acid). To moisten the epithelium, 500 µL of medium was added drop wise to the surface of the corneal epithelium every 8 h. The level of medium in dishes was allowed to rise only to the corneal-scleral rim. All agents were added drop wise to the central cornea. Either 200 nmoles CEES (dissolved first in absolute ethanol and then DMEM) or 100 nmoles NM (dissolved first in saline and then DMEM) were applied onto the cornea and allowed to remain there unwashed for 2 h. The 2 h time period approximately simulates the time that would pass before an exposure is recognized (based on the delayed times for tearing and pain) and medical help is secured.

6.2.7.1 Permeation of doxycycline through vesicant exposed rabbit's cornea

Permeability studies were performed in a Franz diffusion cell apparatus to evaluate the effect of vesicants on permeability barrier properties of cornea. Corneas in the organ culture were treated with either 100 nmoles CEES or 200 nmoles CEES or 100 nmoles NM and put into designated incubator at 37°C for 2 h. Corneas untreated with either of the above vesicants were used as controls. After 2 h, the corneas were placed horizontally on the receptor compartment with the endothelial surface facing the receiver compartment of the Franz diffusion cell set up. The donor half cell was carefully placed on top of the receptor half cell and clamped. 200 µL sample of 15% (1:2) hydrogel encapsulating 0.25% w/v doxycycline was placed in the donor compartment. Aliquots (200 µL) were collected from the receiver compartment at predetermined intervals and replaced with equal volume of PBS to maintain sink conditions through out the study. The concentration of doxycycline in the release medium was determined using a RP HPLC as described above. The cumulative amount of doxycycline permeated through the corneas was determined using a calibration curve. All permeation experiments were done in triplicate and the results reported as mean \pm SEM. Two way ANOVA was used to determine the statistical significance of permeation between different treatment groups.

6.2.7.2 Wound healing efficacy of doxycycline loaded hydrogels on corneas exposed to CEES and NM

The corneas in organ culture were exposed to either 200 nmoles CEES or 100 nmoles NM and incubated for 2 h at 37°C. Medium was replaced with fresh medium after 2 h and then each cornea was treated with doxycycline. Doxycycline solution (2M in 50 µl) was added drop wise to the central cornea 3 times over the subsequent 24 h, whereas 15%

(1:2) doxycycline hydrogel (6M in 50 μ l) was applied once. After 24 h, the corneas were put in cryomolds containing Tissue-Tek O.C.T. compound with the epithelial side facing down and placed on ice for 15 min before snap freezing them in liquid nitrogen. Corneas were stored at -80°C until sectioned for histology and immunofluorescence (IF) analysis. The 10 μ m corneal sections were stained using a modified Hematoxylin & Eosin (H & E) staining method. The corneal sections were fixed in a Pen-Fix solution for 60 s, stained with H & E, dehydrated through graded alcohols, immersed in xylene and covered with a cover slip. Digital images were captured with a light microscope at 40x magnification.

6.2.7.3 Detection of MMP-9 in vesicant exposed and treated corneas by immunofluorescence

The sectioned corneas (10 μ m) were fixed in 100% methanol for 10 min at -20°C. After rinsing with PBS nonspecific binding was blocked with 5% normal goat serum for 1 h. The blocking agent was removed and the sections were incubated with primary mouse anti human MMP-9 monoclonal antibodies (1:400) overnight at 4°C. Sections were blotted and washed four times with PBS/Tween and incubated for 1 h at RT in dark with Alexa-Fluor 488-conjugated goat anti-mouse IgG secondary antibodies (1:1000). The sections were washed with PBS/Tween, counterstained with DAPI for 5 min, mounted with Prolong gold and cover slipped. Negative controls replaced primary antibodies with PBS. Digital epifluorescent images were captured from a light microscope at 494 nm excitation and 517 nm emission and acquired at 10x magnification.

6.3 Results and Discussion

6.3.1 Mechanism of hydrogel formation

Hydrogels were formed by the intermolecular crosslinking of polymer chains, resulting from the reaction of eight-arm PEG polymers containing the thiol groups (8-arm-PEG-SH) with another eight-arm polymer containing the N-hydroxysuccinimidyl ester groups (8-arm-PEG-NHS) at RT in aqueous buffer (PBS, pH 8) (Scheme 6.1). The thiol groups are known to react with active esters under neutral to slightly alkaline pH to give thioester bonds (Scheme 6.2). The thioester bonds are hydrolytically labile and therefore impart *in vivo* biodegradability to the hydrogel network under physiological conditions [260].

Hydrogels of different compositions (5-22.5% w/v) were formed by varying the concentration and ratios of the two polymers (Table 6.1). Hydrogels were not formed when polymer concentrations were less than 5%, possibly due to insufficient intermolecular crosslinking. The 5% (1:1), 7.5% (1:1), 7.5% (1:2), 10% (1:1), 15% (1:1), 15% (1:2), 22.5% (1:2) hydrogels were formed in 90, 85, 75, 65, 55, 45 and 30 s, respectively. Thus, an increase in polymer concentration results in faster hydrogel formation due to more efficient crosslinking reaction. The faster hydrogel formation with 1:2 stoichiometries is due to the fact that the NHS ester has a half life of ~ 1 h at room temperature at pH ~ 8 [261]. Consequently, when the NHS ester is present only in equimolar concentrations, there is a possibility of incomplete reaction. The presence of NHS ester in excess (1:2) excludes this possibility and also explains the reason behind faster hydrogel formation using 1:2 stoichiometries.

6.3.2 OT

Formulations developed for the eye should ideally be transparent and therefore OT measurements were carried out at 480 nm using a UV-Vis spectrophotometer. Hydrogels with OT $\geq 90\%$ were classified as transparent, those in the 10-90% range were classified as translucent, and those $\leq 10\%$ as opaque [185]. The % OT of various hydrogels is shown in Figure 6.1 and as can be seen from the figure, all hydrogels used in this study are transparent. It was also observed that a change in hydrogel composition produces a statistically significant effect ($p < 0.05$) on their optical transmission properties. An increase in the concentration of 8-arm-PEG-SH and/or 8-arm-PEG-NHS resulted into a slight decrease in the transparency of the hydrogels. The transparent characteristic of these hydrogels could be beneficial for their use as ocular drug delivery systems.

6.3.3 Rheology

The retention behavior and physical integrity of hydrogels can be assessed *in vivo* by measuring their mechanical strength and viscoelastic properties [143, 144]. Hydrogels with good mechanical strength are expected to maintain their integrity and help prevent physical drug loss from blinking *in vivo* [147]. The viscoelastic properties of the hydrogels were evaluated by strain sweep test (Figure 6.2) and frequency sweep test (Figure 6.3). The strain sweep test allows the determination of linear viscoelasticity (LVE) range and the subsequent choice of strain value to be used in the frequency sweep test. The frequency sweep test provides a ‘fingerprint’ of the viscoelastic system under non destructive conditions [145, 146]. Both the strain sweep test and frequency sweep test are used to obtain the rheological parameters G' (storage/elastic modulus), G''

(loss/viscous modulus) and loss tangent/phase angle ($\tan \delta = G''/G'$). G' represents the elastic storage of energy and is a measure of how well-structured a hydrogel is. G'' represents the viscous energy dissipation and changes depending on the viscosity of the hydrogel. The strain sweep test results suggest that G' dominates in both the formulations and this is supported by the results obtained from the frequency sweep test. Since G' was one order higher than G'' , the hydrogels are more elastic than viscous in the investigated frequency range. Figure's 6.2 and 6.3 also show that G' is independent of frequency and strain whereas G'' is weakly dependent on both. The hydrogels crosslinked in a 1:2 ratio have slightly higher G' and G'' than hydrogels crosslinked in a 1:1 ratio. This can be attributed to the formation of denser and stronger crosslinking networks in 1:2 hydrogels.

A change in hydrogel composition resulted in a statistically significant effect ($p < 0.001$) on the mechanical strength of the hydrogels. The hydrogels containing higher concentrations of polymers [15% (1:1) and (1:2)] showed a higher and constant G' under increasing frequency, suggesting that the hydrogels have the ability to resist structural changes under strain. The small $\tan \delta$ values indicate that G' is the dominant feature in all the hydrogels and that variations in hydrogel composition do not result in extreme variations in rheological parameters. The rheological data show that the hydrogels have good viscoelastic properties, which might help prolong their ocular residence time and prevent structural breakage. An increased contact time in turn may lead to an increased duration of pharmacological response.

6.3.4 Swelling studies

Hydrogels are swelling controlled systems and the degree of swelling is a measure of the crosslinking density of hydrogels, which is also important for regulating their pore size. The equilibrium degree of swelling of a hydrogel directly influences the rate of water sorption, the permeability to drugs and the mechanical strength of the hydrogel. Therefore, the effect of concentration of the polymers on the degree of swelling was determined. Figure 6.4 shows the degree of swelling expressed as percent swelling plotted against time for 5% (1:1), 7.5% (1:1), 7.5% (1:2), 10% (1:1), 15% (1:1), 15% (1:2) and 22.5% (1:2) hydrogels. The hydrogels in this study showed a relatively lower degree of swelling (<7%) when compared to other hydrophilic hydrogels reported in the literature [123, 124]. The hydrogels crosslinked in a 1:1 ratio initially swelled rapidly, and then gradually reached equilibrium. Furthermore, the hydrogels crosslinked in a 1:2 ratio showed a much lower degree of swelling (<3%) than hydrogels crosslinked in a 1:1 ratio (<7%). A change in hydrogel composition resulted in a statistically significant effect ($p < 0.001$) on the degree of swelling. Hence, a smaller pore size of the hydrogels obtained from increasing the polymer concentration or crosslinking ratio results in a lower degree of hydrogel swelling [193, 194].

6.3.5 *In vitro* doxycycline loading and release

Doxycycline loading efficiency results show that 22.5% (1:2), 15% (1:2), 15% (1:1) and 10% (1:1) hydrogels resulted in doxycycline loading efficiencies of 44.7, 47.5, 51.4 and 48.2%, respectively. Higher drug loading efficiency was observed when equivalent ratios of the polymers were used.

The doxycycline release profiles from different hydrogels were studied *in vitro* using a Franz diffusion cell apparatus. A plot of cumulative amount of doxycycline released ($\mu\text{g}/\text{cm}^2$) as a function of time (h) (Figure 6.5) demonstrates that doxycycline entrapped in the hydrogel shows sustained drug release for about 7 days (168 h) with 80 to 100% of doxycycline being released from different formulations. From Figure 6.5, it appears that as the total concentration of the polymers increased in the hydrogels, the release of doxycycline was sustained. Also, as the crosslinking density increases from 1:1 to 1:2 in the hydrogels, a slower sustained doxycycline release was observed. A statistically significant ($p < 0.001$) decrease in drug release was observed as the polymer concentration and crosslinking density increased in the hydrogels. The formation of a well-defined crosslinked network contributes to the decreased pore size and slower drug release from the hydrogels. The release data were fitted using two-phase exponential association equation in GraphPad Prism 4 software. The goodness of fit for the different hydrogels varied from 0.87 to 0.99.

The relative influence of diffusion and polymer relaxation on the mechanism of doxycycline release was determined by fitting the experimental data (first 60% of the total amount released) to the Ritger-Peppas equation [140].

$$\frac{M_t}{M_\infty} = kt^n \quad (2)$$

In Equation 2, M_t/M_∞ is the fractional release of the drug, k is the proportionality constant, n is the diffusional exponent and t is the time. The diffusion exponent was calculated from the slope of the natural logarithmic values (\ln) of the fractional release as a function of time (Table 6.2). The release mechanism for all of the hydrogels was found

to be Non-Fickian or Anomalous suggesting that the rates of diffusion and polymer relaxation are comparable ($0.5 < n < 1$). Doxycycline release was dependent on water migration into the hydrogel and drug diffusion through continuously swelling hydrogels.

Table 6.2 shows the flux and diffusion exponent (n) values for various hydrogel formulations. Flux was calculated from the slope of the linear portion of the cumulative amount of doxycycline released ($\mu\text{g}/\text{cm}^2$) as a function of time (h) plot. The order of flux and diffusional exponent for the hydrogels is 10% (1:1) > 15% (1:1) > 15% (1:2) > 22.5% (1:2). The flux values decreased with increasing polymer concentration and crosslinking density. This can be attributed to the smaller pore size of the hydrogels resulting in a lower degree of swelling and slower drug release. The *in vitro* release studies show that by changing the concentration of the polymers and crosslinking density, drug release from hydrogels can be tailored.

6.3.6 *Ex vivo* evaluation using Cornea Organ Culture Model

6.3.6.1 *Permeability studies*

Permeability studies were performed to evaluate the barrier function (transcorneal drug permeability) of vesicant-exposed corneas. The corneal epithelium is generally the rate limiting barrier to ocular penetration of topically applied drugs [73, 74]. The barrier is primarily due to the presence of annular tight junctions (zonula occludens), which completely surround and effectively seal the corneal epithelial cells, thus providing a diffusional barrier to drug absorption into the anterior chamber of the eye [72]. The permeability properties of vesicant-exposed corneas were expected to increase by disrupting the zonula occludens. Since the absorption-controlling biological membrane

(i.e., cornea) would no longer be functional, the hydrogel delivery system would have to provide the rate controlling properties.

OT, rheology, degree of swelling and *in vitro* drug release properties of the hydrogel were considered for selection of the appropriate composition of hydrogel to be applied on the cornea. The 15% (1:2) hydrogel showed high OT (>97%), high mechanical strength ($G' > 10000$ Pa), low degree of swelling (<2%), slow sustained drug release (89% doxycycline released in 168 h) and therefore it was chosen for further studies including evaluation of corneal permeation and wound healing efficacy. Even though the 22.5% (1:2) hydrogel showed desirable physicochemical properties (OT>96%, <2% degree of swelling and 80% doxycycline released in 168 h), the 15% (1:2) hydrogel was preferred since it satisfied the requirements for an ideal ocular drug delivery system at lower polymer concentrations.

The permeation profiles of doxycycline through CEES and NM-exposed corneas were evaluated for 24 h using a Franz diffusion cell apparatus. Figure 6.6 shows a plot of the cumulative amount of doxycycline permeated ($\mu\text{g}/\text{cm}^2$) as a function of time (h). Table 6.3 shows the lag times and permeability coefficients of doxycycline permeation through CEES and NM-exposed cornea. The lag time for doxycycline permeation was determined by extrapolating the linear portion of the permeation curve to x-axis. Flux (J) was obtained from the slope of the linear portion of the permeation curve and permeability coefficient (P) was calculated from flux using the equations below.

$$J = \frac{dQ}{dt.A} \quad (3)$$

$$P = \frac{J}{C_o} \quad (4)$$

Where J indicates the steady state flux, dQ the amount of drug permeated, A the corneal area exposed, dt the time of permeation and C_0 represents the initial drug concentration in the donor compartment.

The permeability of doxycycline through CEES and NM-exposed corneas was significantly higher than untreated corneas ($p < 0.0001$) by 2.5 to 3.3 fold. The cumulative amount of doxycycline permeated through vesicant-exposed corneas is almost equal to the cumulative amount released in 24 h, which verifies that corneal epithelium no longer acts as a barrier for permeation of drugs after exposure.

The two major factors that determine ocular drug absorption to the anterior ocular tissues via transcorneal absorption are ocular contact time of the delivery system and drug permeability in the cornea [262]. The contact time of most conventional ocular solutions ranges between 5-25 minutes due to eye blinking and tear drainage that promote rapid clearance and reduced bioavailability, resulting in a short duration of pharmacological response in the eye [76, 78-80]. In our previous report [77] we showed that hydrogel drug delivery system can improve pharmacological efficacy by increasing the ocular residence time. Since the corneal epithelial barrier is compromised when exposed to vesicants, the current hydrogel system can be expected to promote wound healing not only by prolonging ocular contact time but also by providing a continuous drug release at the injury in a sustained manner.

6.3.6.2 *Wound healing efficacy of doxycycline loaded hydrogels on corneas exposed to CEES and NM.*

CEES (half mustard, 2-chloroethyl ethyl sulfide) and NM (nitrogen mustard, mechlorethamine hydrochloride) are structural analogs of SM and have been used widely as surrogates to simulate SM injury in the eyes, lung and skin without the need for a specialized containment facility [196, 199-204]. Four corneas were evaluated for wound healing efficacy in each treatment group and representative H & E stained histological sections are shown in Figure 6.7. The doxycycline solution was applied drop wise three times over the 24 h time period (every 8 h). The doxycycline 15% (1:2) hydrogel was applied as a solution that gelled in a few seconds after instillation onto the cornea. The hydrogel formed a thin transparent film, and likely because of its high water content, the hydrogel was retained in place for the entire duration of the study (24 h). This adherence is analogous to a contact lens where the attraction between the lens polymer and the tear film on the cornea holds the lens in place [263, 264].

The histology of the control cornea showed an epithelium with normal thickness and an intact stroma with corneal keratocytes separated by extracellular matrix. The controls treated with hydrogel (not shown) and doxycycline hydrogel were very similar to the controls demonstrating that the hydrogel did not cause damage to the cornea. The CEES-exposed corneas exhibited a loss of distinctness of the epithelial-stromal border with frequent dipping into the stroma (also known as pitting). This visible damage, seen in foci throughout the cornea at the epithelial-stromal junction was expected, since this is the known target area of vesicants. In addition, the cells of the anterior stroma were swollen. CEES-exposed corneas treated with doxycycline in solution have an epithelial-stromal

border that appears more normal when compared to those without treatment. The epithelial cell layer demonstrated less pitting, looking more like control tissues. CEES-exposed corneas treated with doxycycline hydrogel were similar to those treated with doxycycline solution, and thus were also much more normal in appearance than CEES-exposed corneas. The flattening of the epithelial-stromal border suggests that these corneas are perhaps more like controls than the CEES-exposed corneas treated with doxycycline solution. CEES causes mild damage, and therefore the difference in corneal wound healing efficacy between doxycycline solution and the doxycycline hydrogel would be expected to be minimal. The most significant differences that were seen indicated that the hydrogel ameliorated pitting.

Severe damage to the epithelium with NM causes epithelial cell sloughing, epithelial cell dissociation and pitting. The epithelium is detached from the stroma and the epithelial cells are separated, apparently having lost their cell to cell junctions. Where the epithelium is still attached, the basal cell nuclei appear to be more distant from the stroma than in controls. When treated with doxycycline in solution for 24 h after NM exposure, the epithelial-stromal border is somewhat improved. However there are still many areas where the epithelium is detached from the stroma and in areas where the epithelium and stroma are still attached, the basal cell nuclei were more distant from the stroma than in controls. For NM-exposed samples treated with doxycycline hydrogel, the epithelium remains attached to the basement membrane in most areas and shows a significant improvement in the appearance of the epithelial-stromal border. Doxycycline in solution probably did not show superior efficacy because drop wise application on a curved

surface would favor a low retention time and only a small percentage of the doxycycline would be expected to remain in the wound area. The PEG doxycycline hydrogel on the other hand showed a great improvement over the NM-exposed corneas. In a sense, it acted as a bandage, improving the doxycycline-cornea contact time and preventing epithelial sloughing. The higher wound healing efficacy of doxycycline loaded hydrogels compared to doxycycline in solution most likely is due to the increased contact time and sustained doxycycline release.

6.3.6.3 Detection of MMP-9 in vesicant exposed and treated corneas by immunofluorescence

MMP-9 is a corneal epithelial product upregulated by wounding [246] and is specifically localized at the edge of the migrating epithelial sheet. MMP-9 spreads distally throughout the wound site, in a timely manner correlating with remodeling at the basement membrane zone. Very low amounts are seen in unwounded corneas [9, 265]. The IF staining of corneas exposed to CEES and NM, and subsequently treated with doxycycline either in solution or hydrogel for 24 h are shown in Figure 6.8. In the controls, a very small amount of MMP-9 staining (green) is seen under the basal epithelial cells in the basement membrane zone. The staining at the apical epithelial cells is typical of the corneal epithelium's auto-fluorescence. Others have verified that staining in the basal epithelial cells in the basement membrane is real MMP-9 IF [9, 265]. Nuclei were stained blue.

For CEES exposed corneas, there is a moderate increase in MMP-9 staining observed in the basement membrane zone, apical cells and a small amount throughout the epithelium.

For CEES-exposed corneas subsequently treated with doxycycline in solution, there is a slight, if any, decrease in staining. However, applying a doxycycline hydrogel after CEES exposure reduces immunoreactivity in the basement membrane zone and returning the sub epithelial expression to its original low MMP-9 levels.

For NM-exposed cornea, a drastic increase in MMP-9 staining was observed at the basement membrane zone, reflecting the greater wounding by NM. The corneas exposed to NM, then treated with doxycycline in solution showed a less intense level of fluorescence. However, in this treatment group, there remained many areas where the epithelial cells were totally detached from the stroma. In this case there were few epithelial cells to secrete MMP-9 and thus there was a lower intensity of fluorescence in those areas. For NM-exposed samples treated with doxycycline hydrogel, the fluorescence was significantly less intense than NM exposure without treatment. Most areas show the epithelium to be in contact with the stroma. Hence intervention of MMP-9 activity with doxycycline hydrogels should be pursued as a potential treatment option for healing of mustard injuries in the eye.

6.4 Conclusions

Mustard injuries to the cornea have been shown to upregulate MMP-9. Thus agents that inhibit MMPs such as doxycycline are being evaluated as potential therapeutics. In the current study, the results suggest that doxycycline delivered by the hydrogel will be more effective for treatment of mustard injuries than doxycycline applied in solution. The *in situ* PEG hydrogels prepared and evaluated in the current study are biodegradable and optically transparent. They show resistance to external forces and provide sustained

doxycycline release for up to 7 days. These hydrogel formulations can be administered as a solution which rapidly forms a hydrogel capable of withstanding shear forces in the eye. As expected, the permeability studies show that the barrier property of the cornea is compromised when exposed to vesicants, further allowing drug access to the cornea. The *ex vivo* histology and immunofluorescence results show that the hydrogel formulation provides a superior wound healing response compared to a similar dose of drug in solution. This is likely due to prolonged corneal contact time over the curve of the corneal surface. Overall, the results support the rationale behind using PEG-based hydrogels as ocular drug delivery systems.

6.5 Tables

Table 6.1. Composition of 0.25% w/v doxycycline PEG hydrogel formulations evaluated in the current study.

Polymer ratios	Gelation time (s)	Hydrogel composition		
		8-arm-PEG-SH (% w/v)	8-arm-PEG-NHS (% w/v)	Total weight of polymers (% w/v)
(1:1)	90	5	5	5
(1:1)	85	7.5	7.5	7.5
(1:2)	75	5	10	7.5
(1:1)	65	10	10	10
(1:1)	55	15	15	15
(1:2)	45	10	20	15
(1:2)	30	15	30	22.5

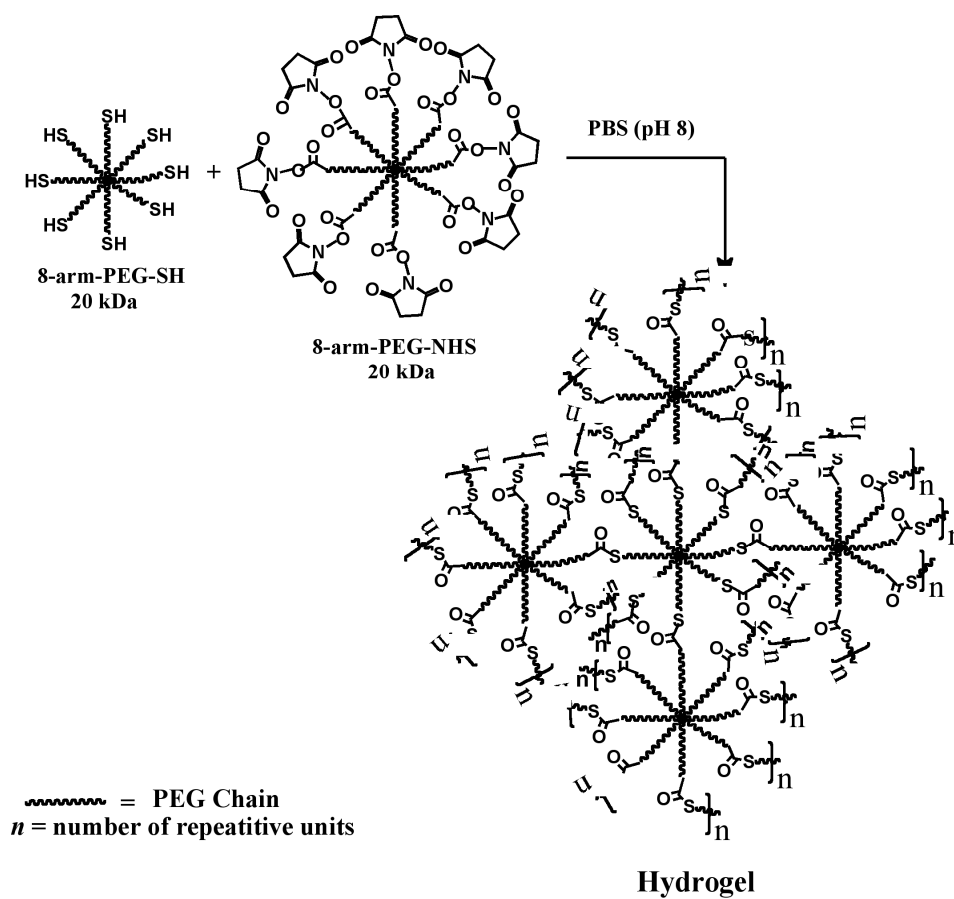
Table 6.2. Estimation of flux and diffusion exponent (n) for various hydrogel formulations.

%Hydrogels (PEG-SH:PEG-NHS)	Flux (J) ($\mu\text{g}/\text{cm}^2 \text{sec}^{-1}$) $\times 10^{-6}$	Diffusion exponent (n)
20 % w/v (1:1)	4.34	0.95
30 % w/v (1:1)	3.94	0.92
30 % w/v (1:2)	3.85	0.81
45 % w/v (1:2)	3.22	0.74

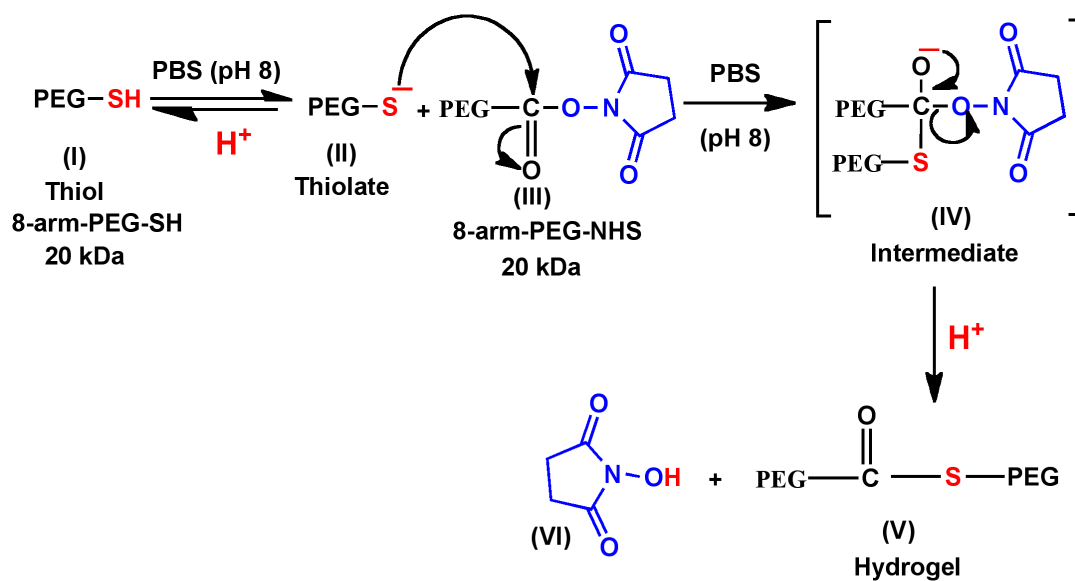
Table 6.3. Estimation of lag time and permeation coefficient of doxycycline through vesicant-exposed corneas

Cornea exposed to vesicants	Permeation coefficient (P) (cm h ⁻¹) x 10 ⁻⁴	Lag time (h)
Unexposed (Control)	15.11 ± 0.8217	3.339
CEES (100 nmoles)	36.76 ± 1.744	2.496
CEES (200 nmoles)	50.46 ± 1.838	2.665
NM (100 nmoles)	41.15 ± 1.849	2.925

6.6 Figures



Scheme 6.1. Hydrogel formation by intermolecular crosslinking of PEG polymers containing mutually reactive thiol (8-arm-PEG-SH) and N-hydroxysuccinimidyl ester (8-arm-PEG-NHS) groups at room temperature in buffer (pH 8). The hydrogel networks are produced by the formation of thioester bonds.



Scheme 6.2. Mechanism of formation of thioester bonds by reaction of thiol group with N-hydroxysuccinimidyl ester. The 8-arm-PEG-SH (I) exists as a thiolate (II) in PBS (pH 8), which acts as a nucleophile and attacks the carbonyl carbon of 8-arm-PEG-NHS (III) to form the intermediate (IV) leading to the formation of thioester bonds accompanied by the cleavage of N-hydroxysuccinimide.

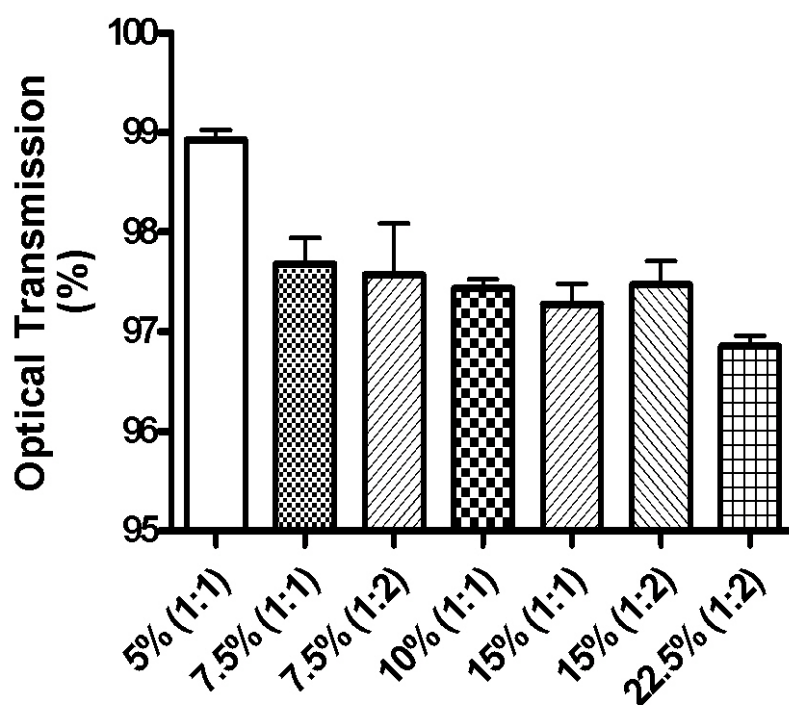


Figure 6.1. Optical transmission of 5% (1:1), 7.5% (1:1), 7.5% (1:2), 10% (1:1), 15% (1:2), 15% (1:1), and 22.5% (1:2) hydrogels. All the hydrogels were found to be transparent. A change in hydrogel composition resulted in a statistically significant effect ($p < 0.05$) on their optical transmission properties. A slight decrease in transparency of the hydrogels was observed with an increase in the polymer concentration and their crosslinking ratios.

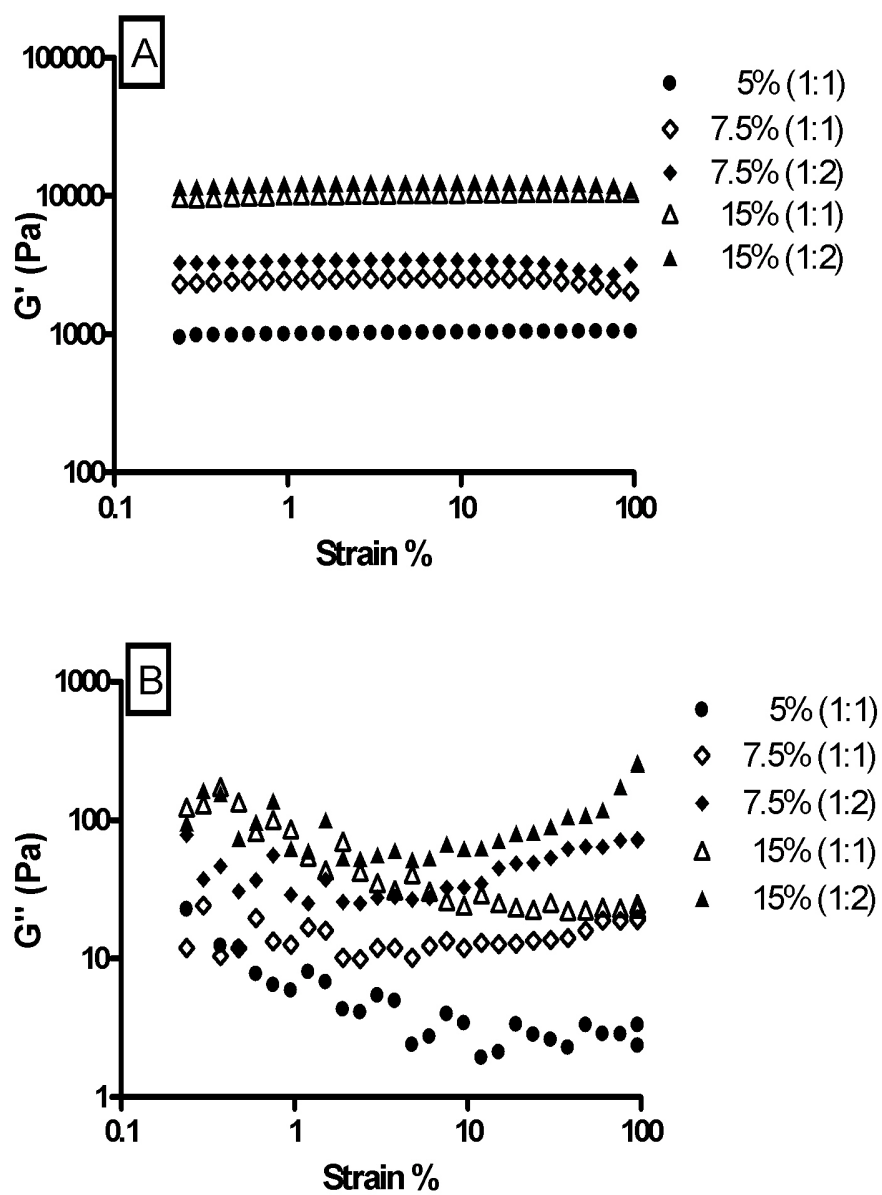


Figure 6.2. Influence of strain on G' (A) and G'' (B) of 5% (1:1), 7.5% (1:1), 7.5% (1:2), 15% (1:1), and 15% (1:2) hydrogels. The strain sweep test establishes the range of linear viscoelasticity (LVE) for the hydrogels.

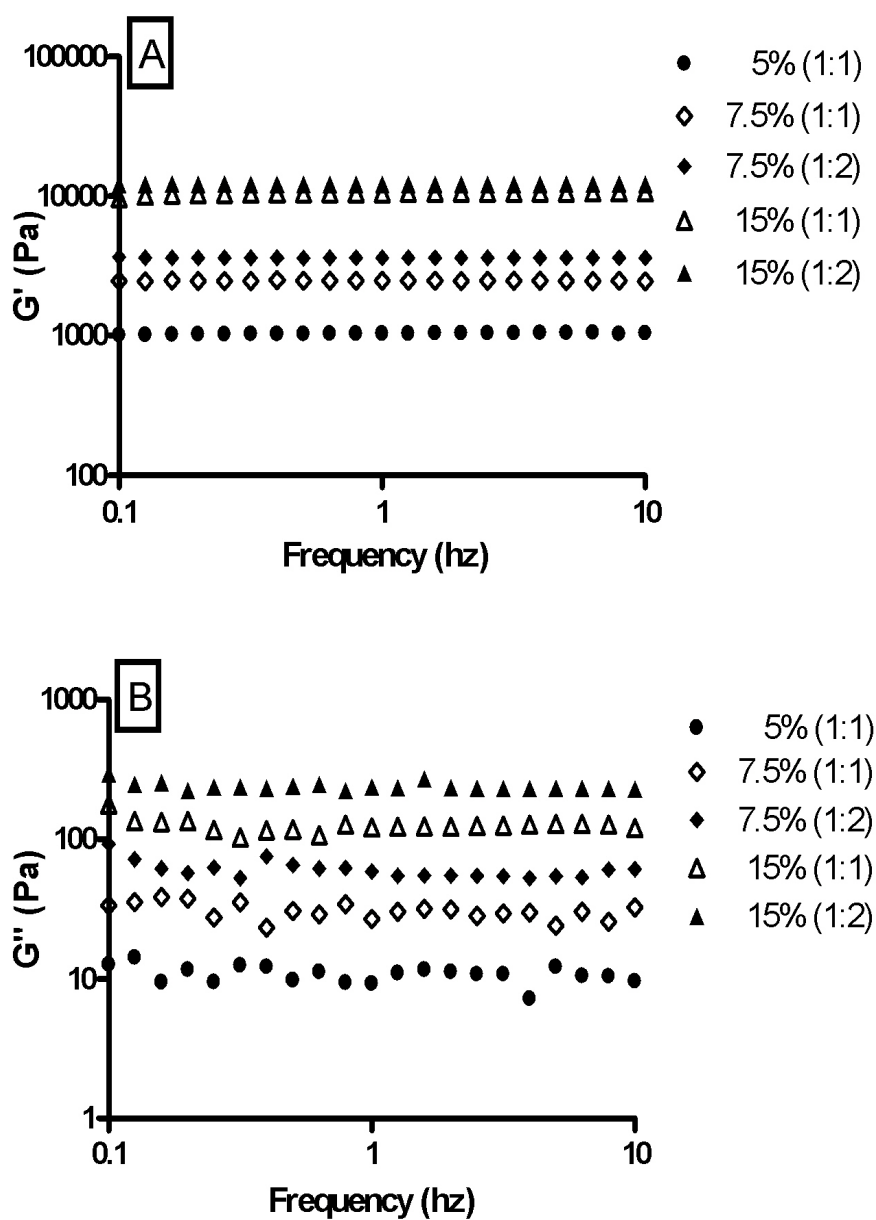


Figure 6.3. Influence of frequency on G' (A) and G'' (B) of 5% (1:1), 7.5% (1:1), 7.5% (1:2), 15% (1:1), and 15% (1:2) hydrogels. The frequency sweep test shows that the hydrogels are more elastic than viscous and that they have the ability to resist structural changes under strain. A change in hydrogel composition resulted in a statistically significant effect ($p < 0.001$) on the viscoelasticity of the hydrogels.

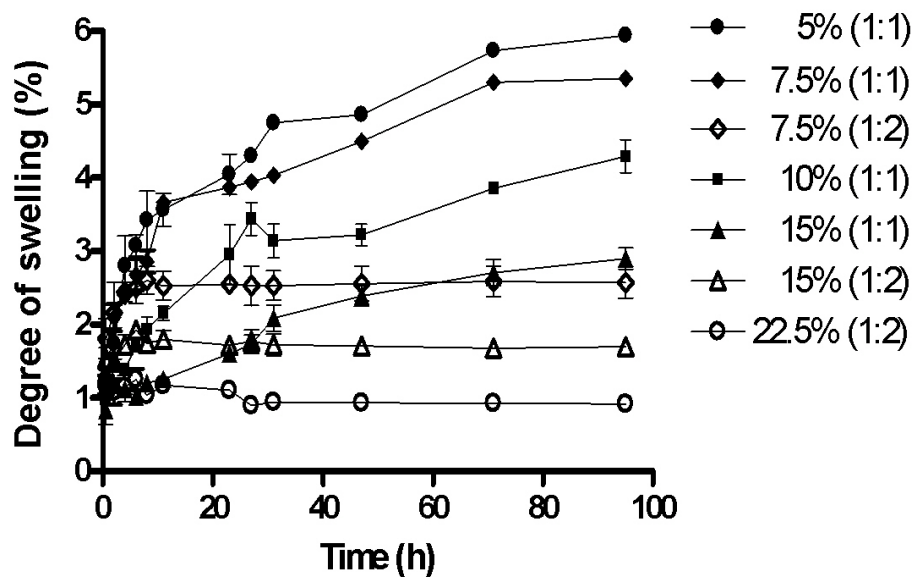


Figure 6.4. Effect of polymer concentration and crosslinking density on the swelling kinetics of 5% (1:1), 7.5% (1:1), 7.5% (1:2), 10% (1:1), 15% (1:1), 15% (1:2), and 22.5% (1:2) hydrogels. The higher the concentration of polymers and crosslinking density, the lower is the degree of swelling.

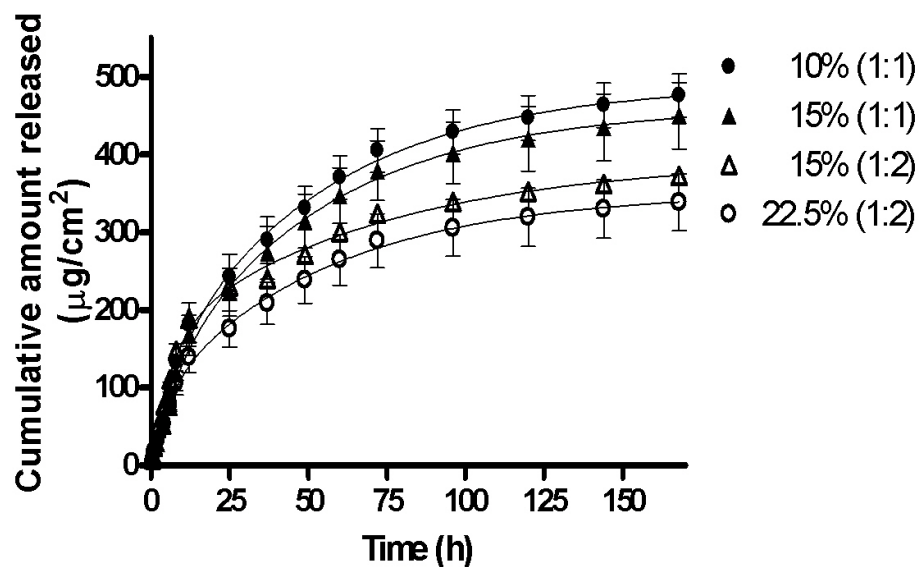


Figure 6.5. Cumulative amount of doxycycline released as a function of time for hydrogels: 10% (1:1), 15% (1:2), 15% (1:1), and 22.5% (1:2). The release data were fitted using a two-phase exponential association equation in GraphPad Prism 4 software. The goodness of fit varied from 0.87 to 0.99. The release mechanism is non-Fickian or anomalous involving both diffusion and polymer relaxation ($0.5 < n < 1$).

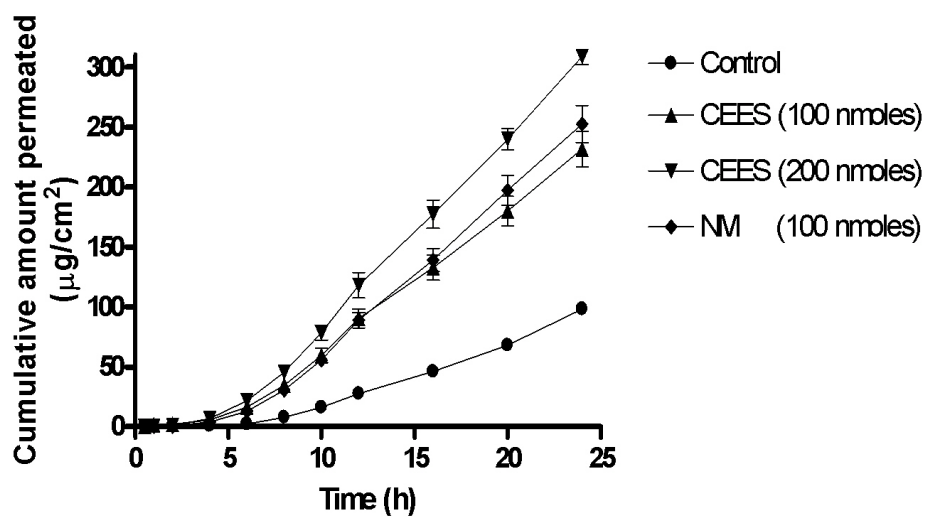


Figure 6.6. Cumulative amount of doxycycline permeated as a function of time through cornea exposed to different concentrations of CEES and NM. The permeability of doxycycline through CEES and NM-exposed corneas was significantly higher than the controls ($p < 0.0001$) by 2.5 to 3.3 fold.

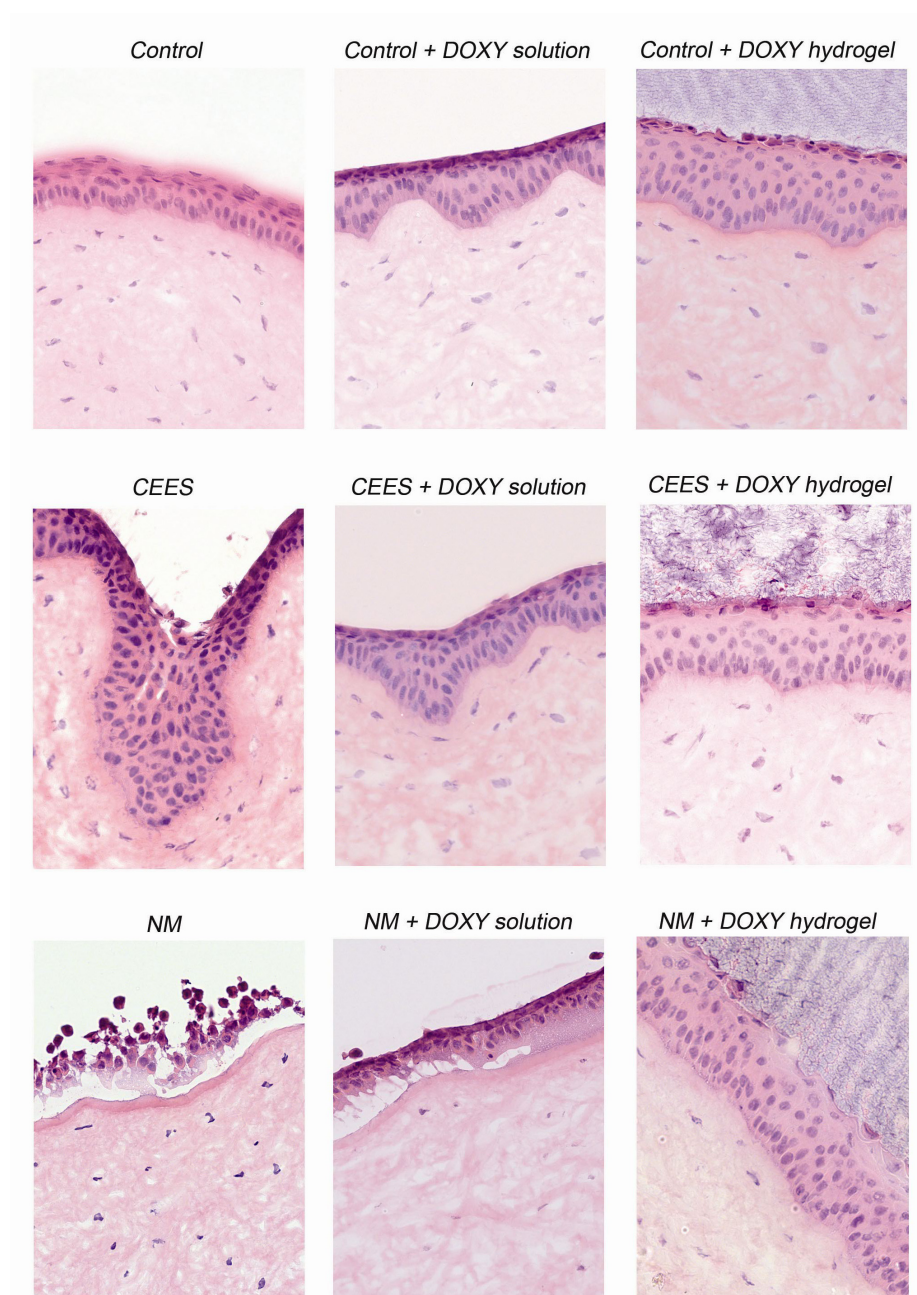


Figure 6.7. H & E staining to visualize the histology of CEES and NM-exposed corneas treated for 24 h with doxycycline in solution or in a hydrogel. The damaged area is where the epithelium meets the stroma. The wound healing efficacy of doxycycline solution was close to the doxycycline hydrogel for CEES exposed corneas, as the extent of damage was comparatively mild. However, a superior wound healing efficacy was observed with hydrogels over solutions when harshly damaged NM-exposed corneas were treated with doxycycline.

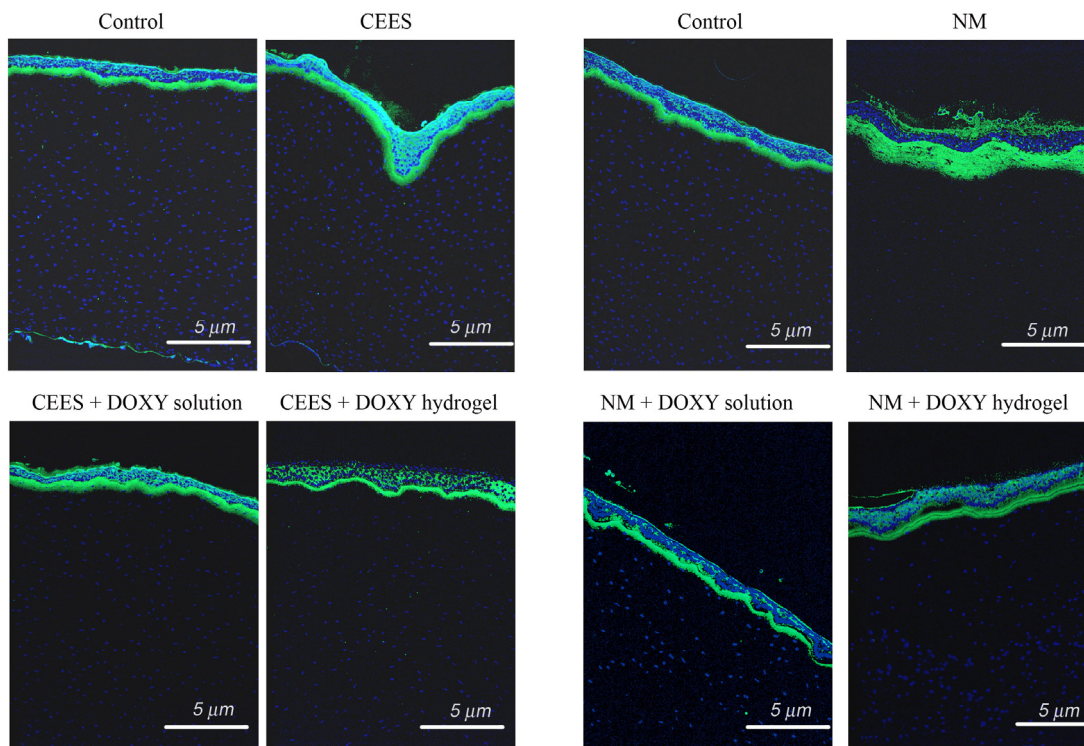


Figure 6.8. Immunofluorescent staining of corneas exposed to CEES and NM and subsequently treated with doxycycline either in solution or hydrogel. The intensity of MMP-9 staining, increased from exposure to CEES and NM, was significantly decreased by doxycycline both in solution and hydrogel. However, the doxycycline hydrogel also improved the attachment between the epithelium and stroma after NM exposure. This demonstrated that the doxycycline hydrogel formulation was more effective than doxycycline in solution.

7 DOXYCYCLINE HYDROGELS WITH REVERSIBLE CROSSLINKS FOR DERMAL WOUND HEALING APPLICATION

7.1 Introduction

Sulfur Mustard (1, 5-dichloro-3-thiapentane; SM) is a blistering/vesicating agent that was used widely for chemical warfare in the past century. Injuries produced by SM are more pronounced in the eye, lung and skin [1]. SM rapidly penetrates the skin causing edema, erythema blisters, lesions, ulceration and necrosis. The clinical signs of injury are delayed 2-24 h after exposure depending on temperature, moisture, anatomical location of the site of exposure and also on the absorbed dose [3, 43]. Although the molecular mechanisms of SM induced injury are unclear, SM can alkylate DNA, RNA, proteins and phospholipids causing inflammation, tissue damage and cell death [1, 3, 54, 196]. In recent years, the targeting of civilian populations by groups willing to employ chemical warfare agents has intensified the need to develop countermeasures. The most devastating aspect of SM exposure is that wound healing occurs over a prolonged time period as compared to other blister-forming injuries resulting from, for example ultraviolet (UV) exposure [43]. SM exposure on skin elicits an inflammatory response that results in increased production of several inflammatory cytokines like interleukins (IL-8, IL-6, IL-1 α , IL-1 β), tumor necrosis factor α (TNF- α), nuclear transcription factor kappa B (NF- κ B), along with induction of matrix metalloproteinase-9 (MMP-9) [12, 13, 43, 64, 227-237].

Doxycycline is a Food and Drug Administration (FDA) approved antibiotic that could potentially promote dermal wound healing by reducing inflammation and protease activity at the wound site. It is a tetracycline analog with anti-inflammatory properties that also acts by inhibiting MMP-9 independent of its antimicrobial properties. Since drugs delivered orally have limited bioavailability in the skin and can often result in systemic toxicity, therapy involving local drug administration is preferred to limit systemic toxicity while increasing drug concentration at the site of injury [100, 101].

Traditionally, the dermal wound healing agents included liquid and semi-solid formulations have short residence time on the wound site, especially where there is a measurable degree of exuding wound fluid [94]. Conventional dry dressings like cotton, wool, gauze, lint and bandages shed fibers into the wound, adhere to the wound base and do not provide a moist wound environment [266]. Recently developed wound dressings represent an improvement over traditional wound healing agents that essentially retain and create a moist environment around the wound to facilitate wound healing. Modern dressings are classified according to the materials from which they are produced, including hydrocolloids, alginates and hydrogels, and generally occur in the form of gels, thin films and foam sheets [94]. The hydrocolloid dressings are not suitable for infected wounds which require a certain amount of oxygen to heal rapidly [95, 97]. Alginate dressings require moisture to function effectively and cannot be used for dry wounds, as well as wounds covered with hard necrotic tissue as they could dehydrate the wound and delay healing [94, 266, 267]. Foam dressings are not suitable for dry epithelializing

wounds or dry scars as they rely on exudates to achieve an optimum wound healing environment [98].

Hydrogels have been vastly researched for dermal wound healing application in the past decade. Hydrogels are a crosslinked network of hydrophilic polymers that have the ability to absorb large amount of water and swell, while maintaining their three-dimensional structure. The advantages of hydrogels compared to other wound dressings are fluid absorption, hydration of the wound bed, and cooling of the wound surface, which may relieve the symptoms of SM exposure such as erythema, burning, itching, pain and cutaneous lesions [165, 166, 268-270]. Hydrogels are permeable to water vapor and oxygen, but do not leak liquid water [148]. Depending on the state of hydration of the tissue, hydrogels can absorb or donate water to the wound environment [149]. Hydrogels leave no residue, are malleable and improve reepithelization of wounds. The maintenance of moist wound bed has been widely accepted as the most ideal environment for effective wound healing [155]. Many clinical studies attest to the benefits of moist wound healing [162] and demonstrate that hydrogel dressings led to quicker healing, reduced pain and cost savings when compared to saline dressings [163].

The current chapter focuses on developing topical doxycycline hydrogel formulations for the treatment of mustard injured skin. In the current study Nitrogen Mustard (mechlorethamine hydrochloride; NM) was used as a surrogate to simulate SM injury in the skin without the need for a specialized containment facility [196, 199-204]. Poly(ethylene glycol) (PEG) based hydrogels are used since PEG is FDA approved, non-

toxic, water soluble and highly stable to pH and non immunogenic [77]. The hydrogels evaluated in the current study are formed *in situ* by covalent inter and intramolecular crosslinking of polymer chains through reversible disulfide bonds. Fast forming doxycycline hydrogels are designed and developed for the treatment of simulated mustard injuries using surrogate vesicants and evaluated for their wound healing efficacy in an SKH-1 hairless mouse model.

7.2 Materials and methods

7.2.1 Materials

The polymer 8-arm-PEG-SH was custom synthesized by NOF Corporation (White Plains, NY). Doxycycline hyclate, Poly Vinyl Pyrrolidone (PVP) and PEG 600 were purchased from Sigma-Aldrich (St. Louis, MO). Methanol, acetonitrile, oxalic acid and HPLC grade solvents were obtained from Thermo Fisher Scientific (Pittsburgh, PA). Rheological evaluations were performed on a SR-2000 rheometer from Rheometric Scientific Inc (Piscataway, NJ) equipped with RSI orchestrator software. Drug release and permeation studies were performed using Franz diffusion cell apparatus from Permgear, Hellertown, PA. Doxycycline was quantified using Waters HPLC system equipped with a UV detector and an Eclipse XDB-C₈ column (Agilent, Zorbax, 4.6 x 150 mm) was used to analyze doxycycline concentration. Human cadaver skin was obtained from New York Firefighter's skin bank (New York, NY). Tape stripping was done by Scotch magic tape from 3M (St. Paul, MN). A Discovery C18 column (Sigma-Aldrich, St. Louis, MO; 125 x 4 mm; 5 μ m) was used for Liquid Chromatography and Mass Spectroscopy (LC-MS) analysis of doxycycline. LC pump Spectra System P4000, auto

sampler Spectra System AS300 and LCQ Deca Mass spectrometer and Xcalibur software were purchased from Thermo Finnigan (Thermo Fisher Scientific, Pittsburgh, PA). Differential Scanning Calorimetry (DSC) was performed on Q10 differential scanning calorimeter and analyzed using Universal Analysis software (TA instruments, New Castle, DE).

7.2.2 Synthesis and characterization of 8-arm-PEG-S-thiopyridyl

To a stirred solution of 8-arm-PEG-SH (1 g) in acetic acid/methanol (5 mL, 1:20) 2-aldrithiol (0.210 g) was added and the reaction mixture was stirred for 12 h at room temperature (RT) to obtain 8-arm-PEG-S-TP (thiopyridyl terminated 8-arm-PEG). After completion of the reaction, the solvent was removed under reduced pressure to get crude 8-arm-PEG-S-TP. The crude 8-arm-PEG-S-TP was purified by size exclusion column chromatography using Sephadex G-25 and water as eluent. The fractions collected were lyophilized to get pure compound (Yield: 71 % (0.74 g)), which was characterized by ^1H -NMR, DSC and XPS.

NMR: The ^1H NMR spectrum was recorded in CDCl_3 on a Varian NMR 500 MHz spectrometer facilitated with AutoX probe and VnmrJ software.

8-arm-PEG-S-TP, ^1H -NMR: (CDCl_3 , 500MHz) δ 3.01 (t, 16H, $J = 2, 4$ Hz, $\text{CH}_2\text{-S-}$) 3.55-3.75 (brm, $-\text{CH}_2\text{-CH}_2\text{O-PEG}$ chain), 7.15 (t, 8H, $J = 2, 4$ Hz, TP-H), 7.78 (t, 8H, $J = 2, 4$ Hz, TP-H) 7.81 (d, 8H, $J = 4$ Hz, TP-H), 8.46 (d, 8H, $J = 2$ Hz, TP-H).

XPS: X ray photoelectron spectroscopy (XPS) was performed using XSAM 800 KRATOS apparatus with a 127 mm radius concentric hemispherical analyzer (CHA). An

Al K α radiation with photon energy of 1486.6 eV is used as X-ray source; photoelectrons are detected by the CHA operated in the fixed retarding ratio mode FRR5 (survey scans), and in the fixed analyzer transmission mode FAT80 (detail scans) with pass energies of 80 eV. One scan is conducted to record the survey spectra, and few scans to record the detail spectra. The XPS quantification method, based on the comparison of relative intensities of photoelectron peaks, allows the calculation of the atomic fraction for each component, assuming their total intensities to be 100% and using the corresponding sensitivity factors. The measurements were performed under UHV conditions with a residual pressure of about 10^{-9} Torr.

DSC: Thermograms for 8-arm-PEG-SH and 8-arm-PEG-S-TP were recorded using nitrogen as purge gas (flow rate of 50 mL/min). Indium was used to calibrate the enthalpy and temperature values. The thermograms were recorded on crimped sealed aluminum pans for samples weighing 4 – 6 mg. The heat cool heat cycles were used to record the thermograms. The samples were equilibrated at -10°C, ramped at 5°C/min to 200°C, quench cooled to -10°C and equilibrated before the second heat cycle at 5°C/min to 200°C.

7.2.3 Hydrogel formation

Hydrogels were prepared by crosslinking of the 8-arm-PEG-SH (20 kDa) branched thiol terminated PEG polymer. 8-arm-PEG-SH was crosslinked using either hydrogen peroxide (H₂O₂ hydrogel) or 8-arm-PEG-S-TP (S-TP hydrogel) in the stoichiometric ratio of 1:1 in phosphate buffer (PB, pH 8) at RT. The hydrogel compositions were varied using different concentrations of polymers as shown in Table 1. Hydrogel formation was

determined by the “inverted tube method” and hydrogels were considered to have formed once the solution ceased to flow from the inverted tube [258]. Hydrogel disks (200 μ L in volume, 9 mm in diameter, and 0.3 mm in thickness) were used for evaluating the degree of swelling, drug loading efficiency and *in vitro* release studies.

7.2.4 Determination of physicochemical properties of the hydrogel

7.2.4.1 Swelling studies

The degree of swelling was evaluated for 4 and 8 % H₂O₂ hydrogels and 5 and 8 % S-TP hydrogels. Hydrogels were placed in a vial and weighed prior to being suspended in 5 mL phosphate buffer saline (PBS, pH 7.4) and placed in an incubator at 37 °C. The degree of swelling of the hydrogels was calculated by weighing the vials after removing the entire PBS at predetermined time intervals. The same amount of buffer was replaced after each measurement and the hydrogels were allowed to swell until equilibrium was reached. The degree of swelling for each hydrogel was determined by using the equation below:

$$\%Swelling = \frac{(W_s - W_o)}{W_o} \times 100 \quad (1)$$

Where W_s is the weight of the swollen hydrogel at time t and W_o is the initial weight. All measurements were made in triplicate for each hydrogel using separate samples and the mean \pm SEM of the values was reported. Two way analysis of variance (ANOVA) was used to determine the effect of hydrogel composition on its degree of swelling.

7.2.4.2 Effect of formulation additives

Glycerin, PVP and PEG 600 were used as additives in the hydrogel formulation. The hydrogels comprising these additives are referred hereafter as hydrogels with additives. The optimal concentration of additives was determined by measuring the degree of dehydration and retention time of hydrogel formulation on mice skin. Rheometry and DSC were used to evaluate the effect of additives on the mechanical strength and crosslinking properties of the hydrogels, respectively. The retention time (24 h) of hydrogels on SKH-1 mouse skin was investigated by visual examination.

7.2.4.2.1 Rheology

The rheological measurements of 4 and 8 % H₂O₂ hydrogels and 5 and 8 % S-TP hydrogels in the presence and absence of formulation additives were performed using a rheometer with cone plate geometry at 37 °C (plate diameter: 25 mm, gap: 3 mm, 2° angle) [143, 144]. The hydrogel samples were equilibrated on the plate for 5 min to reach the running temperature before each measurement. Rheological test parameters, storage/elasticity (G') and loss (G'') moduli were obtained under dynamic conditions of non-destructive oscillatory tests. The strain sweep test was performed at a constant frequency of 1 Hz with percent strain ranging from 10^{-1} to 10^1 . The frequency sweep test was carried out at a constant strain of 1 % (linear viscoelastic region) with frequency ranging from 10^{-1} to 10^1 Hz. All the rheological studies were done in triplicate and the mean \pm SEM reported. Two way ANOVA was used to determine the effect of hydrogel composition and formulation additives on its rheological properties.

7.2.4.2.2 DSC

Thermograms for the 4 and 8 % H₂O₂ hydrogels and 5 and 8 % S-TP hydrogels with and without formulation additives were recorded using DSC as described above in section 7.2.2.

7.2.5 *Reversible nature of hydrogels*

The time for reduction of disulfide bonds in presence of reducing agent was evaluated using different concentrations of glutathione (GSH) in PBS pH 7.4.

7.2.6 *In vitro release studies*

7.2.6.1 *Drug loading efficiency*

4 and 8 % H₂O₂ hydrogels and 5 and 8 % S-TP hydrogels were used for drug loading and release studies. The hydrogel discs containing 0.25 % w/v of doxycycline were dissected into small pieces and suspended into 5 mL PBS (pH 7.4). The suspension was sonicated for 30 min to completely extract doxycycline from the hydrogel. The amount of doxycycline extracted was quantified by reverse phase (RP) HPLC analysis at a wavelength of 350 nm. 0.01M oxalic acid, acetonitrile and methanol (70:18:12) were used as mobile phase at a flow rate of 1 mL/min. The retention time for doxycycline was 6 min. After extraction, the suspension containing the hydrogel was stored for several days at 4°C and then reanalyzed to ensure the complete extraction of doxycycline from the hydrogel. Doxycycline was stable under the storage conditions used, as determined by HPLC analysis.

7.2.6.2 *In vitro doxycycline release*

In vitro release studies were performed as previously described [271] using a Franz diffusion cell apparatus with a diameter of 5 mm and a diffusional area of 0.636 cm². A polycarbonate membrane (0.45 μ) was sandwiched between the lower cell reservoir and the glass cell-top containing the sample for doxycycline release studies. The receiving compartment (volume 5.1 mL) was filled with PBS (pH 7.4). The system was maintained at 37 °C by using a circulating water bath and a jacket surrounding the cell. The receiving medium was continuously stirred (600 rpm) with a magnetic bar to avoid stagnant aqueous diffusion layer effects. 200 μ L of each hydrogel formulation containing 0.25 % w/v doxycycline was prepared and placed in the donor compartment, which was then sealed with parafilm and aluminum foil to prevent evaporation. Aliquots (200 μ L) were collected from the receiver compartment at predetermined intervals and replaced with equal volume of PBS to maintain sink conditions throughout the study. The concentration of doxycycline in the release medium was determined using a RP HPLC as described above. The cumulative amount of doxycycline released from the hydrogel was determined using a calibration curve. All experiments were done in triplicate and the results are reported as mean \pm SEM. The release data were fitted using two-phase exponential association equation in GraphPad Prism 4 software. Two way ANOVA was used to determine the effect of hydrogel composition on the *in vitro* doxycycline release.

7.2.7 *In vivo* studies

7.2.7.1 *Formation of wounds*

SKH-1 hairless mice were used for permeability and wound healing efficacy studies. All animal studies were conducted in accordance with the protocol approved by Laboratory

Animal Services (LAS), Rutgers University. Dermal wounds were created by topical application of 5 μ moles of NM dissolved in acetone to the dorsal skin of mice. A standard circular template (15 mm) was used to ensure uniform exposure area on all mice. The mice were left in the hood overnight to degas after NM exposure. The mice were euthanized by CO₂ gas at predetermined time intervals for collection of wounded skin or punch biopsies to be used in permeability or wound healing efficacy studies respectively.

7.2.7.2 Permeation of doxycycline through NM-exposed skin

Doxycycline permeability on mice skin exposed to NM for 0 (control), 24, 72 and 168 h. was studied using a similar procedure to the *in vitro* release studies using a Franz diffusion cell set up. Mice skin was placed in PBS (pH 7.4) for 1 h prior to being sandwiched between the lower cell reservoir and the glass cell-top. Sample of doxycycline (200 μ L) in PBS (pH 7.4) was placed in the donor compartment. Aliquots (200 μ L) were collected from the receiver compartment at predetermined intervals and replaced with equal volume of PBS to maintain sink conditions through out the study. The concentration of doxycycline in the release medium was determined using a RP HPLC as described above. The cumulative amount of doxycycline permeated through skin was determined using a calibration curve. All permeation experiments were done in triplicate and the results reported as mean \pm SEM. Student's t-test was used to determine the effect of barrier properties of NM exposed skin on the permeation of doxycycline.

7.2.7.3 In vivo wound healing efficacy of doxycycline hydrogels

7.2.7.3.1 Application of doxycycline hydrogels

150 μ l of 8 % 8-arm-PEG-SH in PB (pH 8.0) containing 0.25 % w/v doxycycline and 5.4 μ l of H_2O_2 were applied simultaneously on wounded area of mouse to result in 8 % H_2O_2 hydrogels. 80 μ l of 8 % 8-arm-PEG-SH in PB (pH 8.0) containing 0.25 % w/v doxycycline and 80 μ l of 8 % 8-arm-PEG-S-TP in PB (pH 8.0) were applied simultaneously on wounded area of mouse to result in 8 % S-TP hydrogels. Both the H_2O_2 and S-TP hydrogels were applied using a double barrel syringe and contain the formulation additives 5 % v/v glycerin, 4 % w/v PVP and 5 % v/v PEG 600.

7.2.7.3.2 Wound healing efficacy

Five treatment groups (n=5 per group) were evaluated to measure the wound healing efficacy of doxycycline loaded H_2O_2 / S-TP hydrogels on NM wounds. Two hours after exposure to NM, the wounded site was either left untreated (control) or treated with placebo H_2O_2 /S-TP hydrogels or doxycycline (0.25 % w/v) loaded H_2O_2 /S-TP hydrogels. Skin biopsies from the wounded site were collected at 0 (control), 24, 72, 168 and 240 h after exposure to NM. For histology analysis, the skin biopsies were fixed in 10 % formalin overnight before sectioning and analyzing by hematoxylin and eosin (H & E) staining. Digital images were captured with a light microscope at 40 x magnification.

7.3 Results and Discussion

7.3.1 Synthesis of 8-arm-PEG-S-TP

8-arm-PEG-S-TP was prepared by reaction of 8-arm-PEG-SH and 2-aldrithiol in acetic acid/methanol. The formation of 8-arm-PEG-S-TP was confirmed by 1H NMR. The signals corresponding to the aromatic proton of thiopyridyl groups appear at 7.15, 7.78,

7.81 and 8.46 ppm as seen from the proton spectrum of 8-arm-PEG-S-TP. The peaks for the PEG chain in 8-arm-PEG-S-TP appear at 3.55-3.75 (-CH₂-CH₂O-) and 3.01 (-CH₂-S-) ppm. The results were further affirmed by DSC analysis of the 8-arm-PEG-SH and 8-arm-PEG-S-TP. Figure 7.1 shows the melting temperatures for 8-arm-PEG-SH and 8-arm-PEG-S-TP at 53.3°C and 45.81°C. The shift of -7.56°C in the melting of 8-arm-PEG-SH when converted to 8-arm-PEG-S-TP confirms the substitution of the TP groups on PEG. These observations were consistent with those reported in the past [272, 273]. Furthermore, XPS analysis was conducted to confirm the number of thiol and nitrogen species present on 8-arm-PEG-S-TP. The atoms have valence and core electrons, and for each atom the core level binding provides a unique signature of that element. The binding energy 399 corresponds to nitrogen 1s/2 and 164 corresponds to sulfur 2p/1 (Figure 7.2). These studies confirmed that the ratio between sulfur and nitrogen atoms was 2:1, indicative of two sulfur and one nitrogen atom species present in the star shaped 8-arm-PEG-S-TP (Figure 7.2).

7.3.2 Hydrogel formation

Hydrogels with different compositions were investigated for their controlled drug delivery application on skin. 8-arm-PEG-SH was crosslinked in presence of either H₂O₂ (H₂O₂ hydrogel) or 8-arm-PEG-S-TP (S-TP hydrogel) resulting in the formation of a hydrogel network through disulfide bridges (Scheme 7.1 and Scheme 7.2). The hydrogel network in H₂O₂ hydrogels could result from inter or intramolecular disulfide bridges in 8-arm-PEG-SH formed due to the oxidation of thiol groups, while the hydrogel network resulting from the crosslinking of 8-arm-PEG-SH by 8-arm-PEG-S-TP is exclusively through the formation of intermolecular disulfide bridges. 4 and 8 % H₂O₂ hydrogels and

5 and 8 % S-TP hydrogels each containing 1:1 stoichiometric ratios of these components to 8-arm-PEG-SH were evaluated in the current study (Table 7.1). The gelation times for 4 and 8 % H_2O_2 hydrogels are 75 and 55 s, respectively. The faster formation of hydrogels with the increased concentration of polymers might be due to formation of rapid and intense crosslinking networks, reducing the time for gelation. The 5 and 8 % S-TP hydrogels formed in less than 10 s indicating that total polymer concentration has little effect on the gelation time of S-TP hydrogels.

7.3.3 Reversible nature of hydrogels

Hydrogels with reversible crosslinks were developed for topical wound healing of vesicant injuries. Disulfide exchange reaction involves the transfer of existing disulfide bond to free thiol containing moieties that are present in the reducing agent. In the current study, the reduction of disulfide bonds in hydrogels was investigated using GSH as reducing agent. GSH acts as a thiolate moiety at basic and mild acidic conditions and it gets oxidized in the process while cleaving the existing disulfide bonds. Exchange reactions do not change the total number of disulfide bonds but rather shuffle the species forming them. The possible products in the presence of excess GSH are 8-arm-PEG-SH, 8-arm-PEG-S-S-G, G-S-S-G and 8-arm-PEG-SH which may have few arms bearing either 'SH' or 'S-S-G' termini as shown in Scheme 7.3. GSH solutions (1, 3 and 5 % w/v) in PBS (pH 7.4) were used to study the reversibility of disulfide bridges in hydrogels. It was observed that, 5 % GSH solution cleaved the disulfide bonds in 10 - 15 min as compared to the 1 and 3 % GSH solutions which required 30 - 40 min and 15 - 20 min, respectively. These results demonstrate that crosslinks in the H_2O_2 and S-TP

hydrogels can be reversed facilitating easy removal of hydrogels from the damaged tissue without the necessity of peeling them off.

7.3.4 Degree of swelling

The swelling behavior of hydrogel influences its surface and mechanical properties as well as the drug release kinetics. Hydrogels are swelling controlled systems and the degree of swelling is a measure of its crosslinking density which is important for regulating its pore size. Figure 7.3 shows the degree of swelling expressed as percent swelling plotted against time for 4 and 8 % H_2O_2 hydrogels and 5 and 8 % S-TP hydrogels. Both the H_2O_2 and S-TP hydrogels swelled initially and then gradually reached equilibrium. Compared to hydrophilic hydrogels reported in the literature, a relatively lower degree of swelling (< 1 % for H_2O_2 hydrogels and < 1.5 % for S-TP hydrogels) was observed in this case [123, 124]. Furthermore, the degree of swelling decreased with an increase in polymer concentrations. The decrease in hydrogel swelling with increasing polymer concentrations is due to the smaller pore size and higher crosslinking densities [193, 194].

7.3.5 Effect of formulation additives

The hydrogels in the current study were developed for topical application on skin without the presence of adhesive backing materials. Formulation additives like glycerin, PVP and PEG 600 were used in the hydrogels to decrease the brittleness caused by water evaporation/dehydration and to increase their adhesiveness on skin. Glycerin is a well known humectant and plasticizer and was used to prevent dehydration of the hydrogels [274]. PEG 600 was used as a plasticizer and humectant [275]. PVP was used to increase

adhesiveness of hydrogel on skin and to impart viscosity and film forming ability [276]. The optimal concentration of the additives to prevent brittleness and increase retention time on mouse skin for upto 24 h was found to be 5 % glycerin, 4 % PVP and 5 % PEG 600.

7.3.6 Rheology

The mechanical strength and viscoelastic properties of the hydrogels were investigated using rheological measurements [143, 144] to assess their physical integrity *in vivo*. Viscoelastic properties were investigated because hydrogels with good mechanical strength are expected to maintain their integrity and help prevent physical drug loss from disintegration of the hydrogel [147]. The rheological studies were performed on 4 and 8 % H₂O₂ hydrogels (Figure 7.4) and 5 and 8 % S-TP hydrogels (Figure 7.5), with and without formulation additives. The strain sweep test was performed on all the hydrogels in order to establish the range of linear viscoelasticity (LVE) and to determine if the elasticity of the formulations differed, as expressed by the storage/elastic modulus (G'). The strain sweep test results (Figures 7.4A and 7.5A) suggest that G' dominates in all the hydrogels, both with and without formulation additives and this is supported by the results obtained from the frequency sweep test (Figures 7.4B and 7.5B). G' for all the hydrogels is one order higher magnitude than G'' (loss modulus), suggesting that the hydrogels are more elastic than viscous in the investigated frequency range.

Figure's 7.4A and 7.4B show that G' is independent of frequency and strain for all the H₂O₂ hydrogels with and without additives. However, G'' is independent of frequency and strain only in the H₂O₂ hydrogels without additives but is weakly dependent on

frequency and strain in the H₂O₂ hydrogels with additives. The G' and G'' values are almost similar for the hydrogels with and without additives suggesting that formulation additives have minimal influence on the rheological properties and hence the physical strength of H₂O₂ hydrogels.

Figures 7.5A and 7.5B show that G' is independent of frequency and strain for all the S-TP hydrogels with and without additives. G'' is also found to be independent of frequency and strain in all the S-TP hydrogels with an exception of the 8 % S-TP hydrogel without additives which was found to be dependent on frequency. The total polymer concentration in the hydrogels was found to influence both G' and G'' values for all the hydrogels with and without additives.

The loss tangent values ($\tan\delta = G''/G'$) indicate that the storage modulus is the dominant feature in all the hydrogels, as a small $\tan\delta$ indicates an elastic material. The rheological data show that both the H₂O₂ and S-TP hydrogels have good mechanical properties as evident by higher G' values, which might help prolong their contact time on the skin and prevent structural breakage.

7.3.7 DSC

The difference in crystallization behavior of polymer networks from that of linear polymers is well known [273]. The crosslinking of polymer chains result in a reduction of crystallinity. Figure 7.6 shows the influence of polymer concentration and presence of additives on melting temperatures of 4 and 8 % H₂O₂ hydrogels. The H₂O₂ hydrogels with additives show lower crystallization temperature when compared to hydrogels

without additives. Also, the crystallization temperatures slightly decreased with an increased concentration of polymers indicating higher crosslinking densities. Similar results were observed in case of the 5 and 8 % S-TP hydrogels, where a significant lowering in crystallization temperature of 8 % hydrogel was observed as compared to the 5 % hydrogel (Figure 7.7). In case of S-TP hydrogels, the crosslinks are highly defined as they result from intermolecular network formed between polymers 8-arm-PEG-SH and 8-arm-PEG-S-TP. Since PEG chains are bound, there is reduced mobility and a highly ordered crystalline structure is not achieved, as reflected by the lower melting temperature for S-TP hydrogels as compared to the H₂O₂ hydrogels. The main reason for the observed behavior is the restricted diffusion and orientation of the molten polymer chains as a result of crosslinking, and further, the crosslinks get excluded from the crystalline phase [273, 277]. The addition of formulation additives further enhances this phenomenon of restriction in movement of PEG chains to orient in crystalline phase causing a further lowering in melting temperature (Figures 7.6 and 7.7).

7.3.8 In vitro doxycycline loading and release

Doxycycline loading efficiency results show that 4 and 8 % H₂O₂ hydrogels entrapped 44.38 and 36.42 % w/w of loaded doxycycline. The 5 and 8 % S-TP hydrogels showed 46.17 and 43.94 % w/w doxycycline loading. The S-TP hydrogels appear to have higher drug loading efficiencies than the H₂O₂ hydrogels. The intramolecular crosslinks (H₂O₂ hydrogels) result in a hydrogel with collapsed structure as compared to hydrogels having intermolecular crosslinks (S-TP hydrogels) where the polymer branches (or arms) are stretched to form crosslinks with other polymer molecule. This could attribute for the difference in pore size and hence the drug loading efficiencies of the two hydrogels.

The doxycycline release profiles from the four different hydrogels were studied *in vitro* using a Franz diffusion cell apparatus. A plot of cumulative amount of doxycycline released ($\mu\text{g}/\text{cm}^2$) as a function of time (h) (Figure 7.8) demonstrates that doxycycline entrapped in both the H_2O_2 and S-TP hydrogels showed sustained drug release for about 10 days (240 h) with 73 to 84 % of doxycycline being released from different formulations. A slower drug release is observed for H_2O_2 hydrogels compared to S-TP hydrogels. The swelling data shows that the volume of hydrodynamic water associated with 4 % H_2O_2 hydrogels is lower as compared to the 5 % S-TP hydrogels which correlates with the collapsed structure of H_2O_2 hydrogels arising from intramolecular crosslinking. Also a slower doxycycline release was observed for hydrogels with higher concentrations of polymers which might be due to the formation of a tighter hydrogel network and decreased pore size. The release data were fitted using two-phase exponential association equation in GraphPad Prism 4 software and the goodness of fit for the different hydrogels varied from 0.83 to 0.96.

The relative influence of diffusion and polymer relaxation on the mechanism of doxycycline release was determined by fitting the experimental data (first 60 % of the total amount released) to the Ritger-Peppas equation [140].

$$\frac{M_t}{M_\infty} = kt^n \quad (2)$$

In Equation 2, M_t/M_∞ is the fractional release of the drug, ' k ' is the proportionality constant, ' n ' is the diffusion exponent and ' t ' is the time. The diffusion exponent ' n ' was

calculated from the slope of the natural logarithmic values (\ln) of the fractional release as a function of time (Table 7.2). The release mechanism for both the H_2O_2 hydrogels was found to be Non-Fickian or anomalous involving both diffusion and polymer relaxation ($0.5 < n < 1$). The release mechanism for both the S-TP hydrogels was found to be Super Case II transport which is due to the relaxation of the polymer as the hydrogel swells [278-280]. This correlates well with the swelling data, where the 5 % S-TP hydrogel with higher polymer content shows higher swelling as compared to the 4 % H_2O_2 hydrogel. For the drug to diffuse through the hydrogel, the polymeric chains must first relax to allow the diffusion process. The hydrogels described in the present study are based on PEG, which is a highly hydrophilic polymer with low glass transition temperature (T_g) [281]. The T_g of PEG hydrogels was found to be 27-28°C (data not shown). As compared to the glassy polymeric materials which exhibit a moving boundary of water phase in hydrogel layers, the diffusion of water is rapid in PEG hydrogels thereby attaining a rapid equilibrium [282]. This contributes for the observed Super Case II transport, as the hydrogel exhibits the ability to imbibe water and swell, and the whole polymer system is relaxed. Typically in glassy polymers the Super Case II transport occurs due to a plasticization process in the hydrogel layer which arises from a reduction of the attractive forces among polymeric chains that increase the mobility of macromolecules [283]. Thus diffusion rate increases with an increase in chain mobility and relaxation rate of the polymeric chains [284]. Both the non-Fickian and Super Case II transport mechanisms of drug diffusion are time dependent (t^{n-1}) [285]. Doxycycline release from both the H_2O_2 and S-TP hydrogels was dependent on two simultaneous processes- migration of water into the hydrogel and drug diffusion through continuously swelling hydrogels.

Table 7.2 shows the flux (J) and diffusion exponent (n) for various hydrogel formulations. Flux was calculated from the slope of the linear portion of the cumulative amount of doxycycline released ($\mu\text{g}/\text{cm}^2$) as a function of time. The flux and diffusion exponents decreased with an increase in polymer concentrations for both the H_2O_2 and S-TP hydrogels. This indicates a decrease in swelling and pore size of the hydrogels due to the formation of a tighter hydrogel. The *in vitro* release studies show that by changing the polymers and their concentrations, drug release from hydrogels can be tailored.

7.3.9 Doxycycline permeation in NM exposed skin

Permeability studies were performed to evaluate the barrier function (transdermal drug permeability) of vesicant-exposed skin. The stratum corneum is generally the rate limiting barrier to dermal penetration of topically applied drugs [90, 91, 238, 239]. The permeability property of vesicant-exposed skin is expected to increase by loss of stratum corneum and separation of the epidermis and dermis after vesicant exposure [43]. Since the biological membrane (i.e., stratum corneum) controlling drug influx would be less or no longer functional, the hydrogel delivery system would have to provide the rate controlling properties.

The permeation of doxycycline through skin exposed to NM for 0 (control), 24, 72 and 168 h was evaluated using a Franz diffusion cell apparatus. Figure 7.9 shows the plot of cumulative amount of doxycycline permeated ($\mu\text{g}/\text{cm}^2$) as a function of time. Table 7.3 shows the lag times and permeability coefficients of doxycycline permeation through NM-exposed skin. The lag time for doxycycline permeation was determined by

extrapolating the linear portion of the permeation curve to x-axis. Flux (J) was obtained from the slope of the linear portion of the permeation curve and permeability coefficient (P) was calculated from flux using the equations below.

$$J = \frac{dQ}{dt.A} \quad (3)$$

$$P = \frac{J}{C_o} \quad (4)$$

Where 'J' indicates the steady state flux, 'dQ' the amount of drug permeated, 'A' the dermal area exposed, 'dt' the time of permeation and 'C₀' represents the initial drug concentration in the donor compartment.

The permeability of doxycycline through NM-exposed skin for variable time points was found to increase significantly ($p < 0.01$) compared to the control. The order of permeation of doxycycline through NM-exposed skin is 72 h > 168 h > 24 h > control (Table 7.3) suggesting that stratum corneum no more acts as a barrier for permeation of drugs after vesicant exposure. The order of permeation of doxycycline suggests that highest damage after NM exposure is evident at 72 h and the barrier property of skin seems to improve in between 72 and 168 h, which is in accordance with the results published by others [203]. The two major factors that determine transdermal drug absorption are transdermal drug permeability and contact time of the delivery system on skin. Since the barrier property of skin is compromised when exposed to vesicants, the current hydrogel system can be expected to promote wound healing not only by prolonging the contact time but also by providing a continuous drug release at the injury site in a sustained manner.

7.3.10 In vivo wound healing efficacy of doxycycline hydrogels

For wound healing efficacy five mice were evaluated in each treatment group at 24, 72, 168 and 240 h after NM exposure and representative H & E stained histological sections are shown in Figures 7.10, 7.11, 7.12 and 7.13, respectively. The treatments were initiated 2 h after NM exposure and this time period approximately simulates the time that would pass before an exposure is recognized (based on the delayed times for symptoms) and medical help is secured. Two hours after exposure to NM, the wounded site was either left untreated (control) or treated with placebo H₂O₂/S-TP hydrogels or doxycycline (0.25 % w/v) loaded H₂O₂/S-TP hydrogels. The hydrogels described in the present study are *in situ* forming which when applied as a solution on mouse skin gelled in a few seconds. A thin film of hydrogel was formed, and because of the presence of formulation additives, the hydrogel was retained in place for upto 24 h. The hydrogel dressing was changed every 24 h by washing with a solution of 5 % GSH in PBS and the reversible nature of the hydrogel helped in its dissolution and easy removal without peeling off from wounded skin.

Figure 7.10 shows the histology of mice skin exposed to NM and subsequently treated with H₂O₂/S-TP placebo or doxycycline hydrogels for 24 h. The histology of control skin shows an intact epidermis and dermis, healthy nuclei in the epidermis and fibroblasts in dermis. The common histological features observed in all treatment groups 24 h after NM exposure, were edema (abundance of clear areas in the dermis), shrinkage/condensation of nuclei in the epidermis (pyknosis) and infiltration of inflammatory cells (blue colored) in the dermis. However, the untreated NM-exposed skin also shows signs of epidermal

separation from the dermis and higher infiltration of inflammatory cells compared to the placebo or doxycycline hydrogel treated groups. The placebo or doxycycline hydrogel treated groups do not show any signs of epidermal separation from the dermis. Hence the hydrogel acted as a bandage and prevented the separation of epidermis and dermis. Not much difference in histology was seen between the H₂O₂/S-TP placebo or doxycycline hydrogels.

Figure 7.11 shows the histology of mice skin exposed to NM and subsequently treated with H₂O₂/S-TP placebo or doxycycline hydrogels for 72 h. Edema, complete separation of epidermis from the dermis, death of epidermal cells (absence of nuclear staining) and infiltration of inflammatory cells in the dermis were seen in untreated skin at 72 h after NM exposure. The histology of skin treated with both the H₂O₂ and S-TP placebo hydrogels showed edema, pyknotic nuclei in the epidermis and areas where epidermis and dermis are slightly separated. The histology of skin treated with both the H₂O₂ and S-TP doxycycline hydrogels showed pyknotic nuclei in the epidermis but no separation of epidermis and dermis. The placebo and doxycycline hydrogels showed a significant improvement over untreated NM-exposed skin. H₂O₂/S-TP doxycycline hydrogels prevented the separation of epidermis from the dermis and hence represent an improvement over the H₂O₂/S-TP placebo hydrogels.

Figure 7.12 shows the histology of mice skin exposed to NM and subsequently treated with H₂O₂/S-TP placebo or doxycycline hydrogels for 168 h. The histology of untreated NM-exposed skin showed necrosis all over the dermis and no nuclear staining in the

epidermis implying that the tissue is dying. Only sections from two mice showed signs of reepithelization (sign of wound healing) from the wound edges in the epidermis (data not shown). The histology of skin treated with both the H₂O₂ and S-TP placebo hydrogels showed absence of nuclear staining in the epidermis and fibroblasts in the dermis. The histology of skin treated with both the H₂O₂ and S-TP doxycycline hydrogels showed reepithelization characterized by epidermal hyperplasia (increased keratinocyte proliferation) and hyperkeratosis (thickening of the stratum corneum). Reepithelization is essential for wound repair to restore the intact epidermal barrier and it occurs by the movement of epithelial cells from the edge of the unwounded tissue across the site of injury [222-226]. The H₂O₂/S-TP doxycycline hydrogels showed a significant improvement in NM-exposed wounds compared to the untreated and H₂O₂/S-TP placebo hydrogel treated groups.

Figure 7.13 shows the histology of mice skin exposed to NM and subsequently treated with H₂O₂/S-TP placebo or doxycycline hydrogels for 240 h. 100 % mice untreated after NM exposure died in between 168 and 240 h. Hence no representative histological sections are shown for this group. 80 and 100 % mice treated with H₂O₂/S-TP placebo and doxycycline hydrogels survived for 240 h after NM exposure implying that hydrogels in general have a beneficial effect and doxycycline hydrogels are better than the placebo hydrogels. The histology of S-TP placebo hydrogel treated NM-exposed group looked like a dying tissue. The histology of H₂O₂ placebo hydrogel treated NM-exposed group showed hyperplasia and hyperkeratosis, signs of wound healing. The histology of H₂O₂/S-TP doxycycline hydrogel treated NM-exposed groups showed a second

occurrence of reepithelization (first occurrence seen in sections 168 h after NM exposure). The reason for this could possibly be the retention of NM in skin which is being released at later times resulting in reoccurrence of reepithelization. This is similar to SM, which forms a reservoir in skin from which there is continual uptake of SM in the blood during the first few days after the application [43, 286].

H₂O₂/S-TP doxycycline hydrogels showed improved wound healing efficacy compared to untreated and H₂O₂/S-TP placebo hydrogel treated groups after NM exposure, evidenced by the survival rate and signs of wound healing. Among the two placebo hydrogels, H₂O₂ hydrogel showed a beneficial effect at 240 h. H₂O₂ is well known to oxidize mustard [287] and hence the H₂O₂ hydrogel might also be acting as a decontaminant to oxidize NM depot in skin resulting in a dermal wound healing effect. The increased pharmacological efficacy of doxycycline hydrogels could be due to increased doxycycline permeation in NM-exposed skin and continuous influx of doxycycline from the hydrogels. Hence doxycycline hydrogels should be pursued as a potential treatment option for healing of dermal mustard injuries.

7.4 Conclusions

The *in situ* gelling PEG hydrogels investigated in the current study can be applied topically as a solution on skin which forms a hydrogel by disulfide bonds. These hydrogels can be easily removed by spraying a reducing agent which reverses the disulfide crosslinks resulting in gel to sol conversion. Formulation additives decrease the dehydration of hydrogel and increase adhesiveness on skin for upto 24 h. The hydrogels

have a low degree of swelling, good mechanical strength and provide sustained doxycycline release for upto 10 days. The permeability studies show that the barrier property of skin is compromised when exposed to vesicants, allowing increased transdermal drug influx. The *in vivo* wound healing efficacy results show that doxycycline hydrogels provide a superior wound healing response on NM-exposed skin compared to untreated skin and skin treated with placebo hydrogels. Overall, the doxycycline loaded PEG-based hydrogels are promising for dermal wound healing application of mustard injuries.

7.5 Tables

Table 7.1. Composition of PEG hydrogel formulations evaluated in the current study

Ratio of components in the hydrogel (w/w)	Hydrogels	Hydrogel Composition				
		Gelation time (s)	8-arm-PEG-SH (% w/v)	H ₂ O ₂ volume (μl)	8-arm-PEG-S-TP (% w/v)	Total wt of polymers (% w/v)
(1:1)	4 % H ₂ O ₂	75	4	1.9	-----	4
(1:1)	8 % H ₂ O ₂	55	8	5.4	-----	8
(1:1)	5 % S-TP	< 10	5	-----	5	5
(1:1)	8 % S-TP	< 10	8	-----	8	8

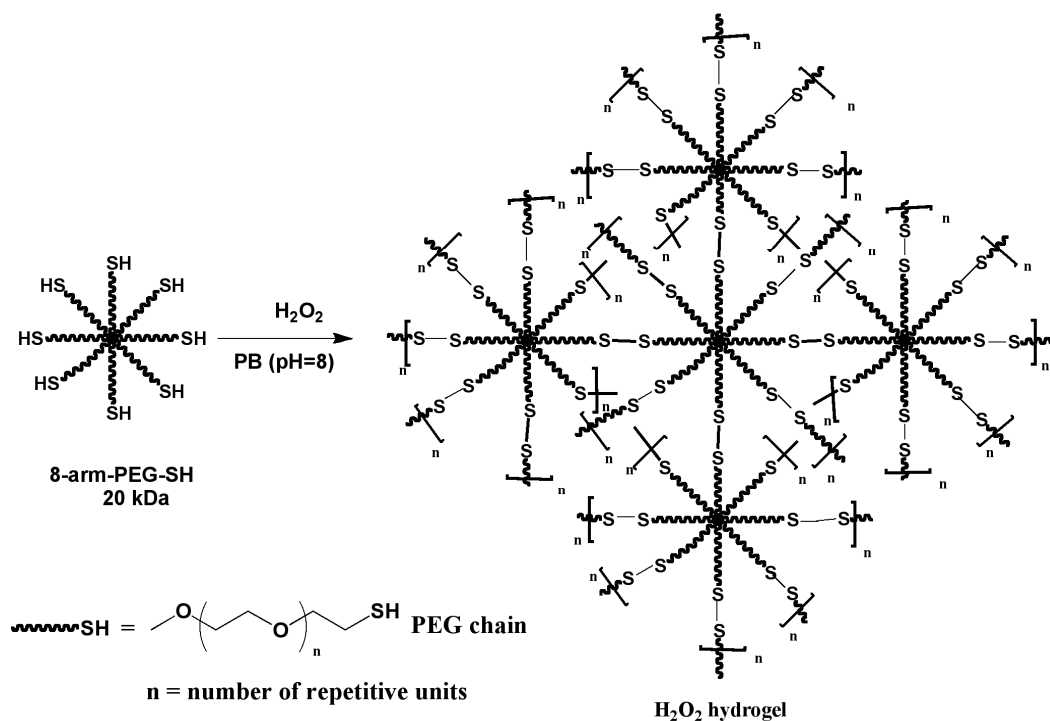
Table 7.2. Estimation of flux and diffusion exponents (n) for various hydrogel formulations.

% w/v Hydrogels	Flux (J) (mg cm ⁻² s ⁻¹) x 10 ⁻⁶	Diffusion exponent (<i>n</i>)
4 % H ₂ O ₂	4.91	0.65
8 % H ₂ O ₂	3.83	0.59
5 % S-TP	5.45	2.04
8 % S-TP	4.43	1.6

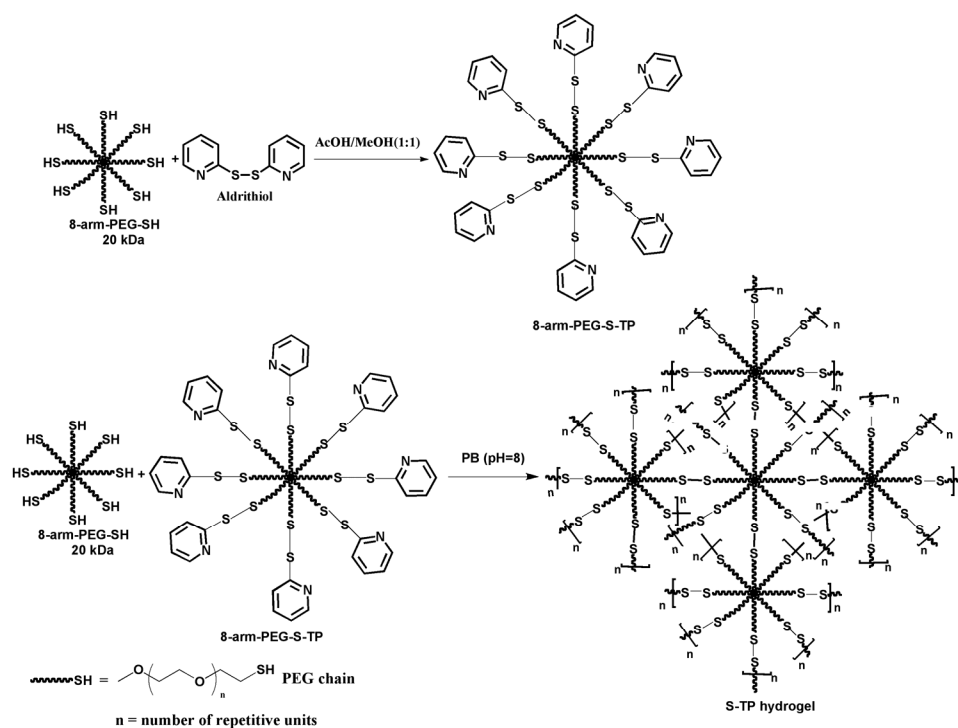
Table 7.3. Estimation of lag time and permeability coefficients for doxycycline through NM-exposed skin.

NM exposure time (h)	Lag time (h)	Permeability Coefficient (P) (cm. h ⁻¹) x 10 ⁻⁶
0 (Control)	6.998	0.5717 ± 0.06638
24	1.792	17.95 ± 5.868
72	1.620	661.9 ± 28.41
168	1.608	78.86 ± 6.827

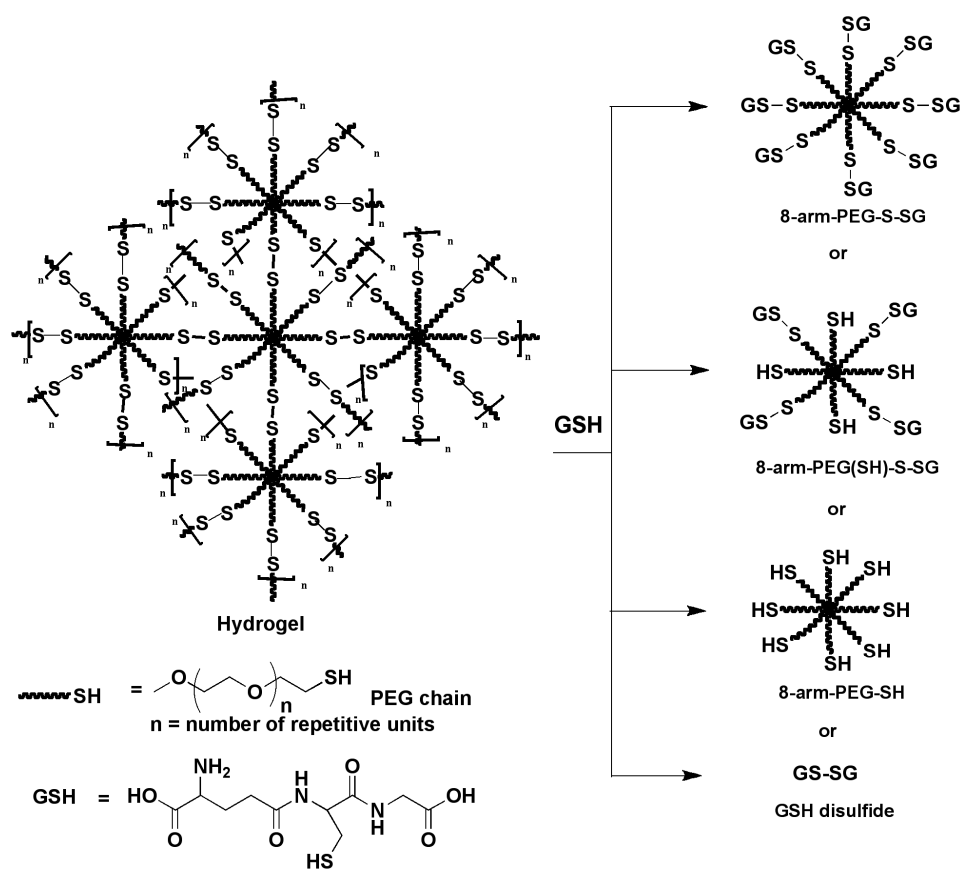
7.6 Figures



Scheme 7.1. Schematic representation of 8-arm-PEG-SH crosslinked by H_2O_2 in PB (pH 8) resulting in the formation of H_2O_2 hydrogels by disulfide bridges. The formation of disulfide bridges within the molecule results in intramolecular crosslinks and the formation of disulfide bridges between molecules results in intermolecular crosslinks.



Scheme 7.2. Schematic representation of thiopyridyl terminations appended on the 8-arm-PEG-SH to form 8-arm-PEG-S-TP. Thiopyridine is good leaving group and 8-arm-PEG-S-TP forms disulfide bridges with 8-arm-PEG-SH in PB (pH 8) resulting in S-TP hydrogels.



Scheme 7.3. Schematic representation of the reversible nature of hydrogels. The GSH acts as a thiolate moiety and attacks the disulfide bonds resulting in the breakdown on the hydrogel network (gel to sol transition). The possible products are 8-arm-PEG-SH, 8-arm-PEG-(SH)-S-SG, 8-arm-PEG-S-SG and GS-SG.

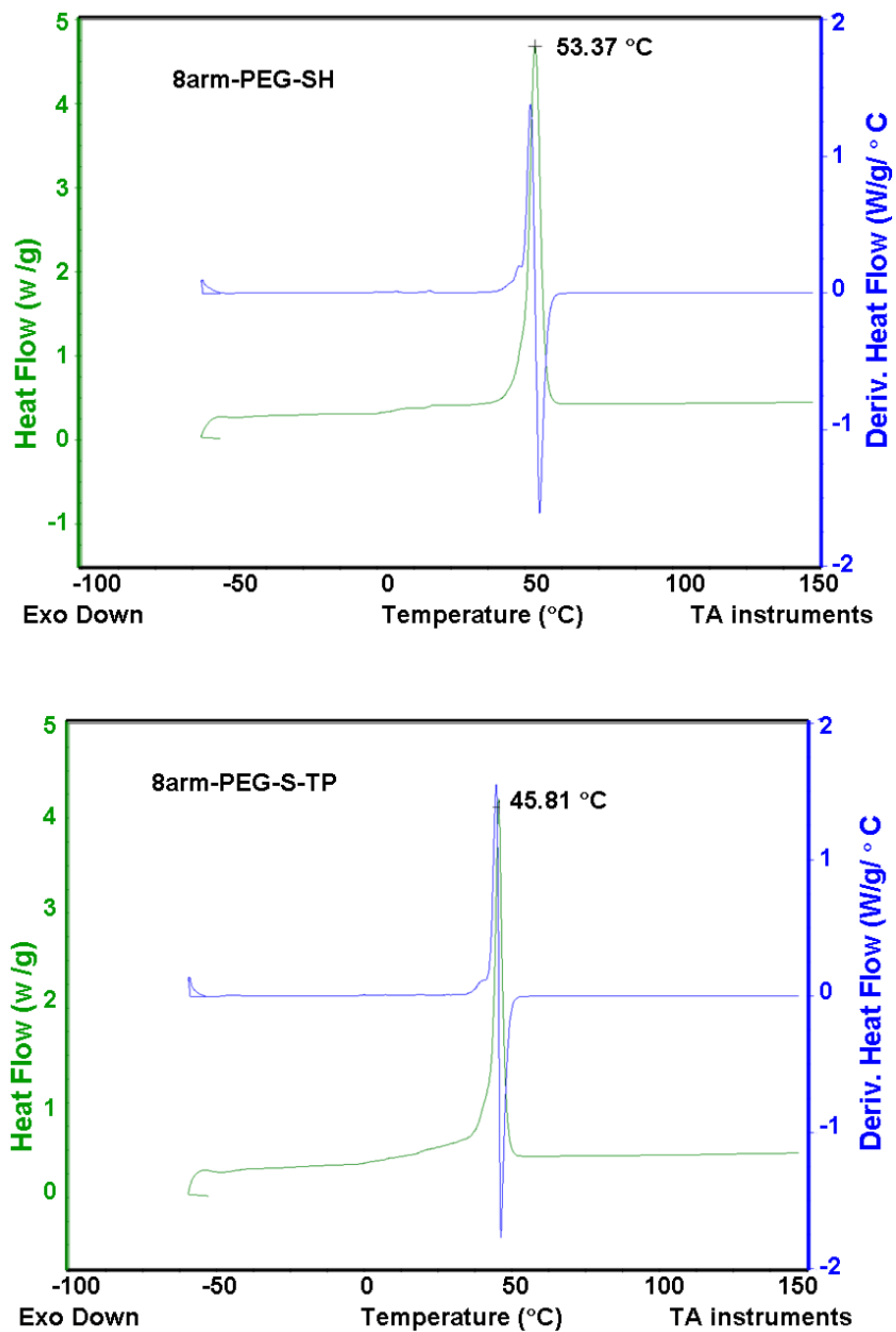


Figure 7.1. The DSC thermograms show the melting of 8-arm-PEG-SH and 8-arm-PEG-S-TP at 53.37°C and 45.81°C respectively, indicative of conversion of thiols to thiopyridine

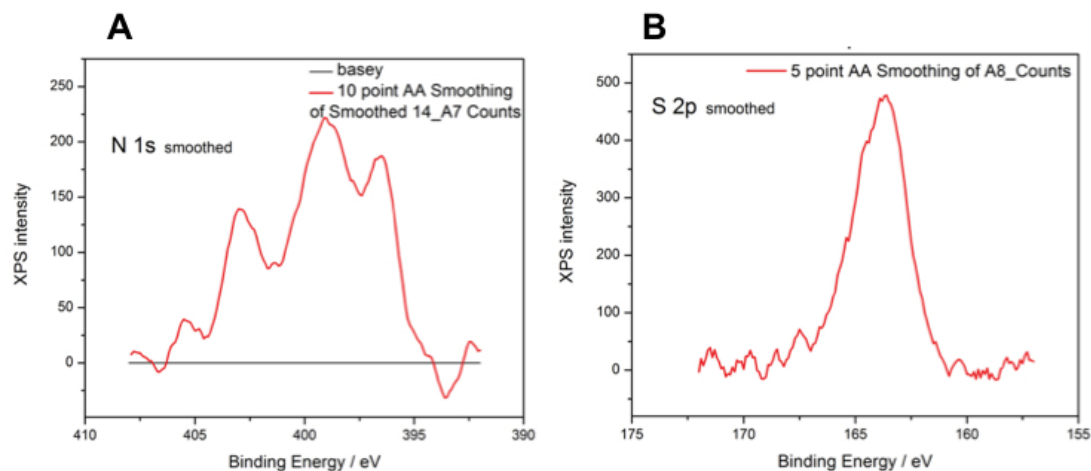


Figure 7.2. The XPS analysis shows the diffractograms for nitrogen and sulfur atoms and the ratio between sulfur and nitrogen was found to be 2.

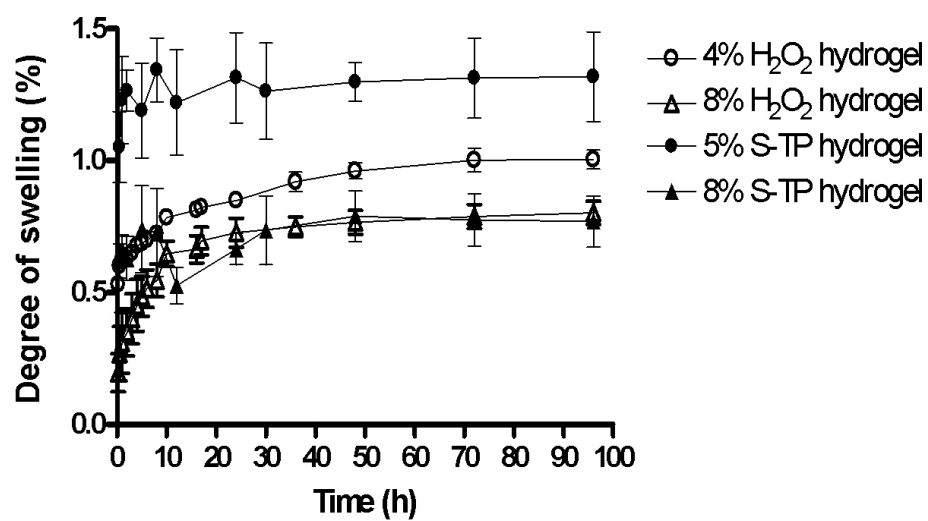


Figure 7.3. Effect of the concentration of polymers on swelling kinetics of 4, 8 % H₂O₂ hydrogels and 5, 8 % S-TP hydrogels. As the concentration of polymers is increased, the degree of swelling is lowered.

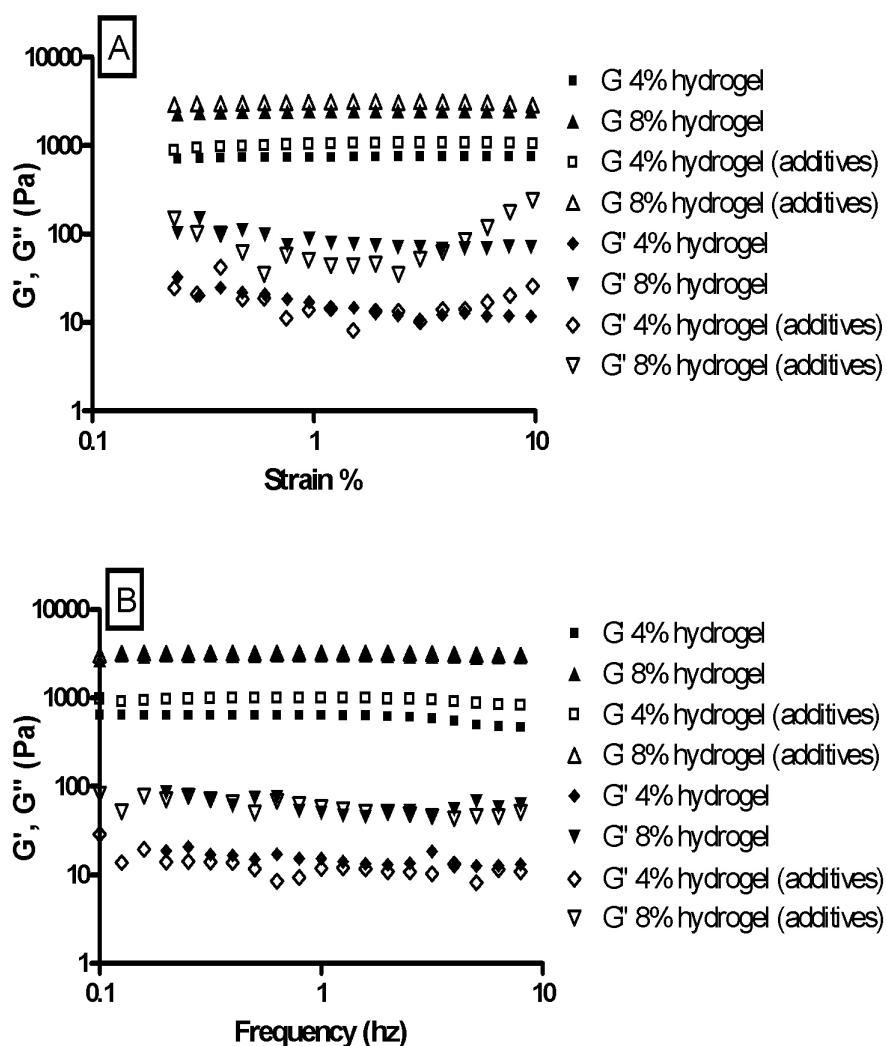


Figure 7. 4. Influence of strain (A) and frequency (B) on G' and G'' of 4 and 8 % H_2O_2 hydrogels with and without formulation additives. The strain sweep test establishes the regime of linear viscoelasticity (LVE). The frequency sweep test shows that the hydrogels are elastic than viscous and that they have the ability to resist structural changes under strain.

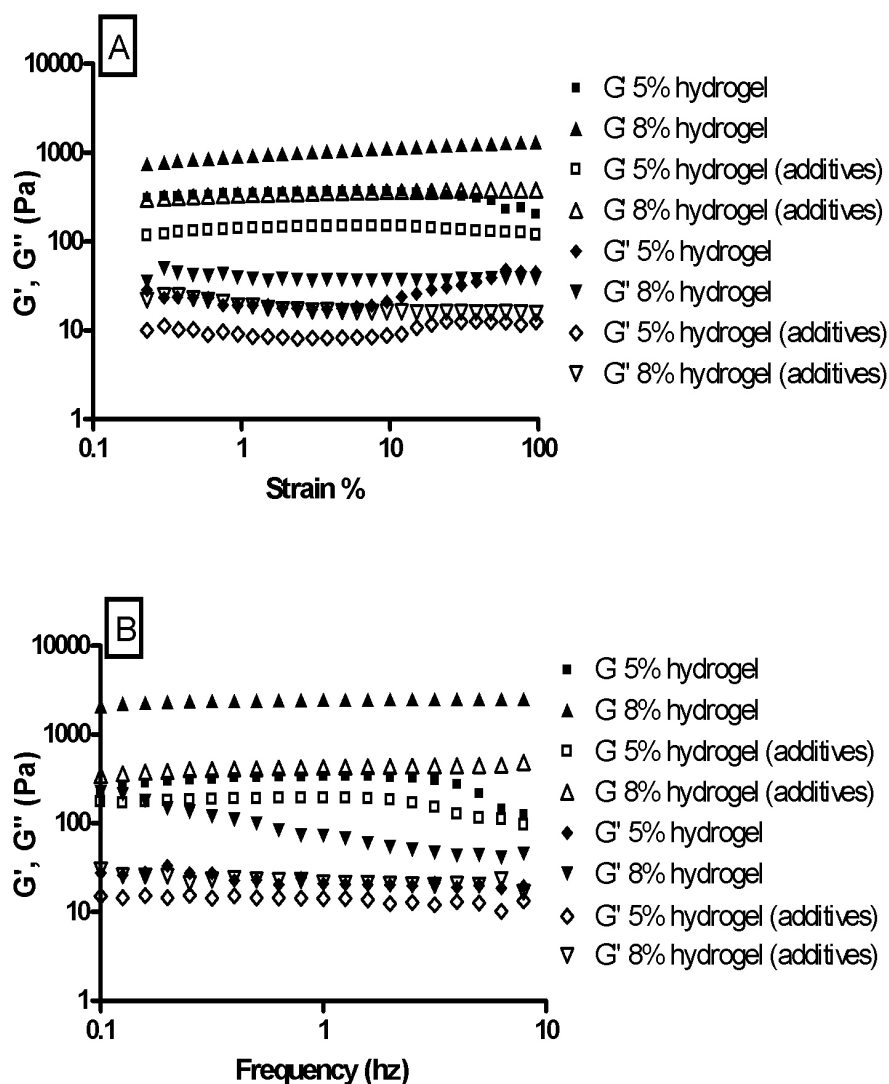


Figure 7. 5. Influence of strain (A) and frequency (B) on G' and G'' of 5 and 8 % S-TP hydrogels with and without formulation additives. The strain sweep test establishes the regime of linear viscoelasticity (LVE). The frequency sweep test shows that the hydrogels are elastic than viscous and that they have the ability to resist structural changes under strain.

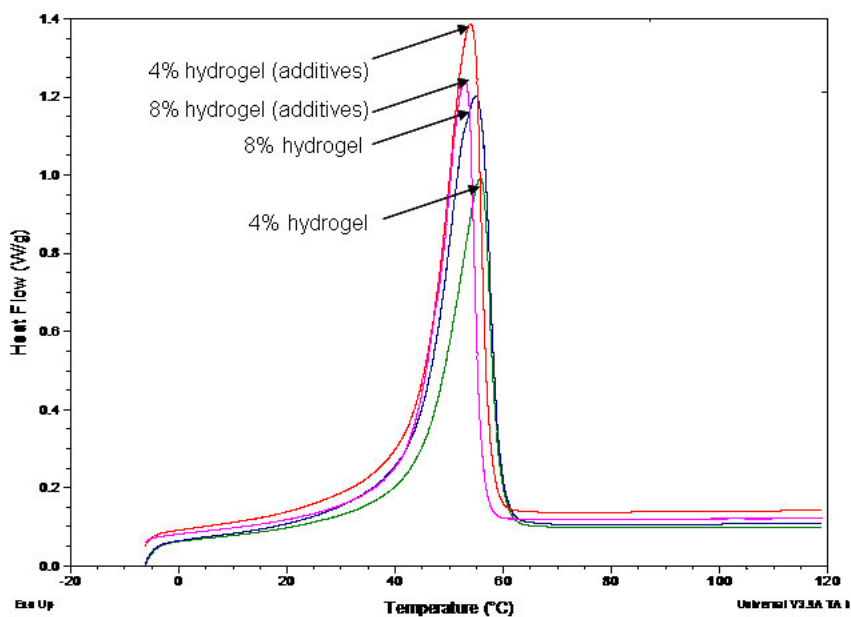


Figure 7.6. The DSC thermograms for the 4 and 8 % H_2O_2 hydrogels with and without formulation additives. With an increase in polymer concentration of the hydrogels, the melting of the PEG shifts to lower temperatures. The presence of formulation additives further restricts the motion of PEG chains lowering the melting temperature

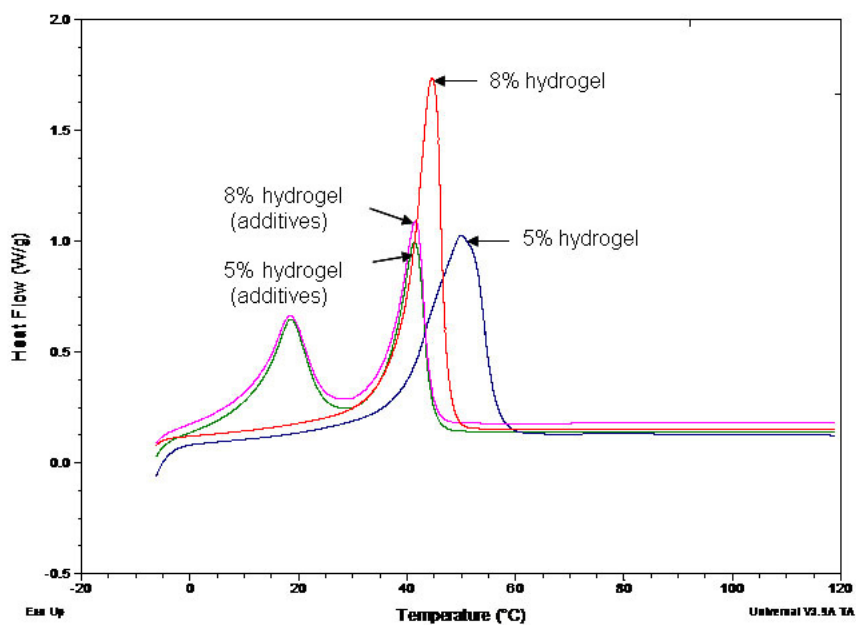


Figure 7.7. The DSC thermograms for the 5 and 8 % S-TP hydrogels with and without formulation additives. With an increase in polymer concentration of the hydrogels, the melting of the PEG shifts to lower temperatures. The presence of formulation additives further restricts the motion of PEG chains lowering the melting temperature.

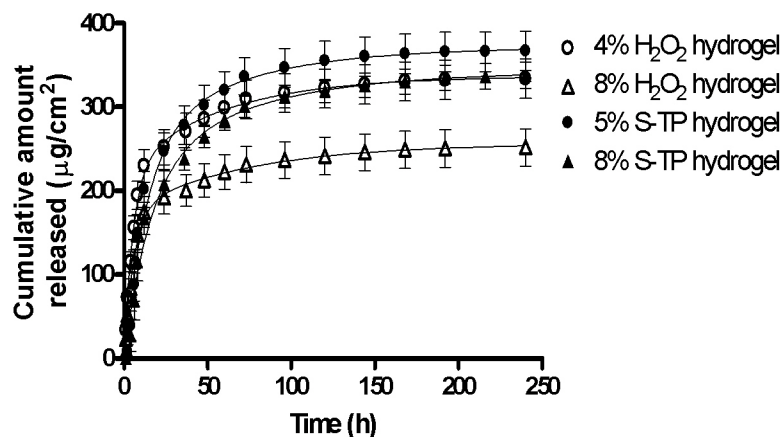


Figure 7.8. Cumulative amount of doxycycline released as a function of time for 4 and 8 % H₂O₂ hydrogels and 5 and 8 % S-TP hydrogels. The release data were fitted using two-phase exponential association equation in GraphPad Prism 4 software. The goodness of fit for the different hydrogels varied from 0.83 to 0.96. The release mechanism for the H₂O₂ hydrogels is non-fickian or anomalous involving both diffusion and polymer relaxation ($0.5 < n < 1$). The release mechanism for the S-TP hydrogels is super case II transport involving relaxation of the polymer as the hydrogel swells ($n > 1$).

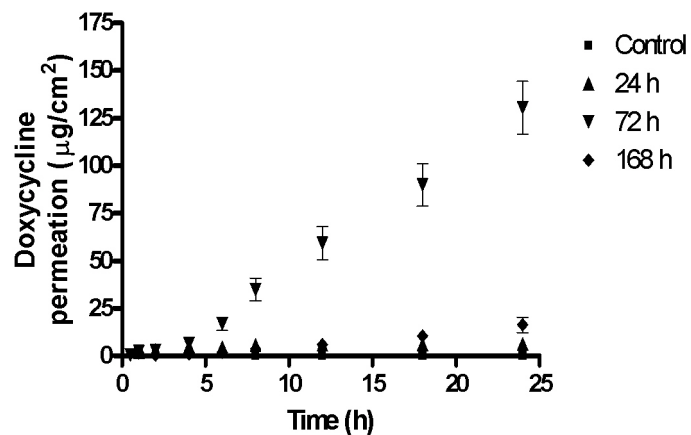


Figure 7. 9. Cumulative amount of doxycycline permeated as a function of time through NM-exposed skin.

The permeability of doxycycline through NM-exposed skin for variable time periods was found to increase significantly ($p < 0.01$) compared to the control. The order of permeation of doxycycline is 72 h > 168 h > 24 h > control.

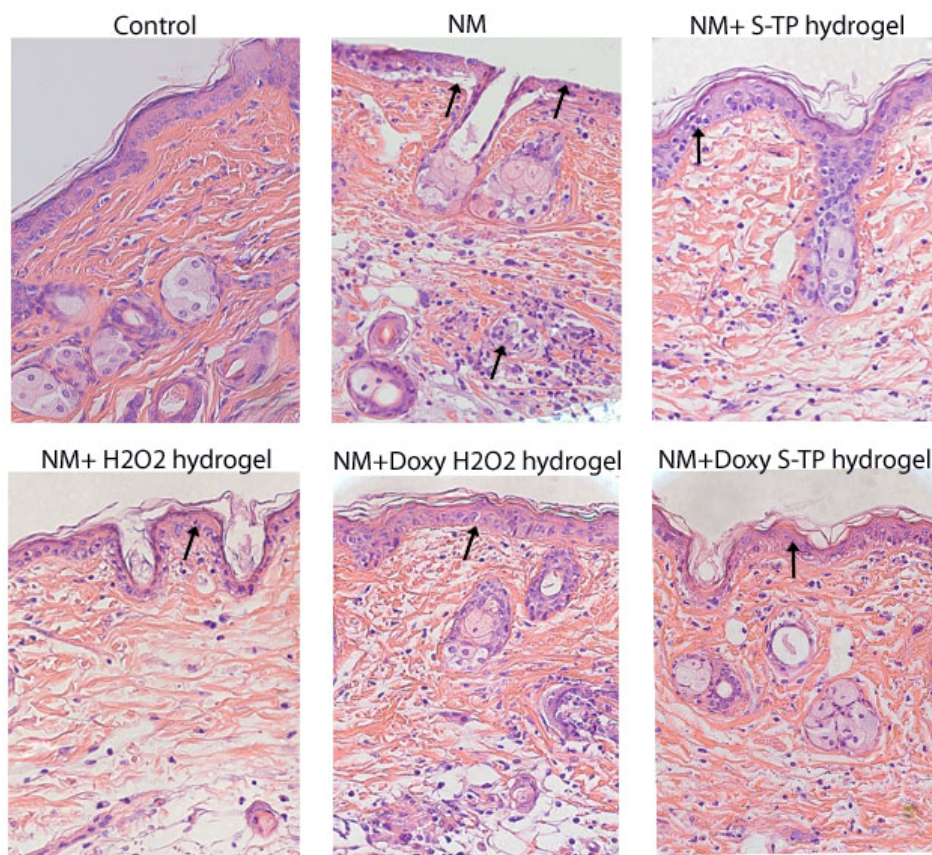


Figure. 7.10. Histology of mice skin exposed to NM and subsequently treated with H₂O₂/S-TP placebo or doxycycline hydrogels at 24 h. Unlike the untreated NM-exposed skin, the placebo and doxycycline hydrogel treatment groups do not show any signs of epidermal separation from the dermis. The hydrogels acted as a bandage and prevented the separation of epidermis and dermis.

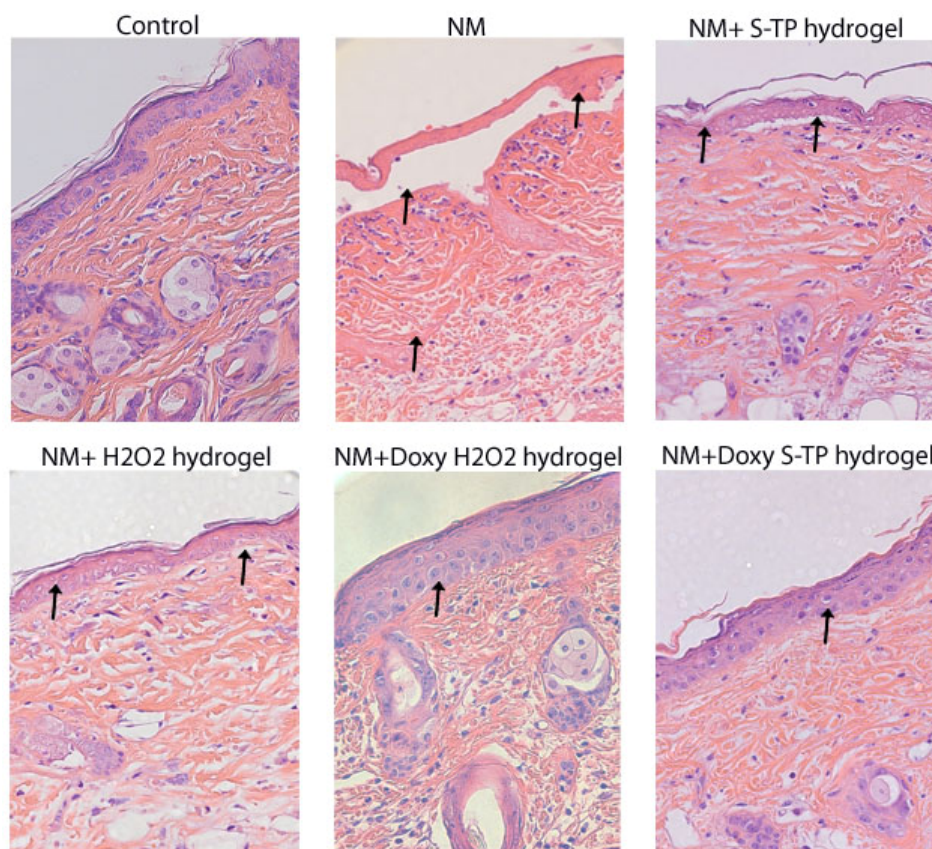


Figure 7.11. Histology of mice skin exposed to NM and subsequently treated with H₂O₂/S-TP placebo or doxycycline hydrogels at 72 h. The placebo and doxycycline hydrogels showed a significant improvement over untreated NM-exposed skin. Doxycycline hydrogels prevented the separation of epidermis from the dermis and hence represent an improvement over the placebo hydrogels.

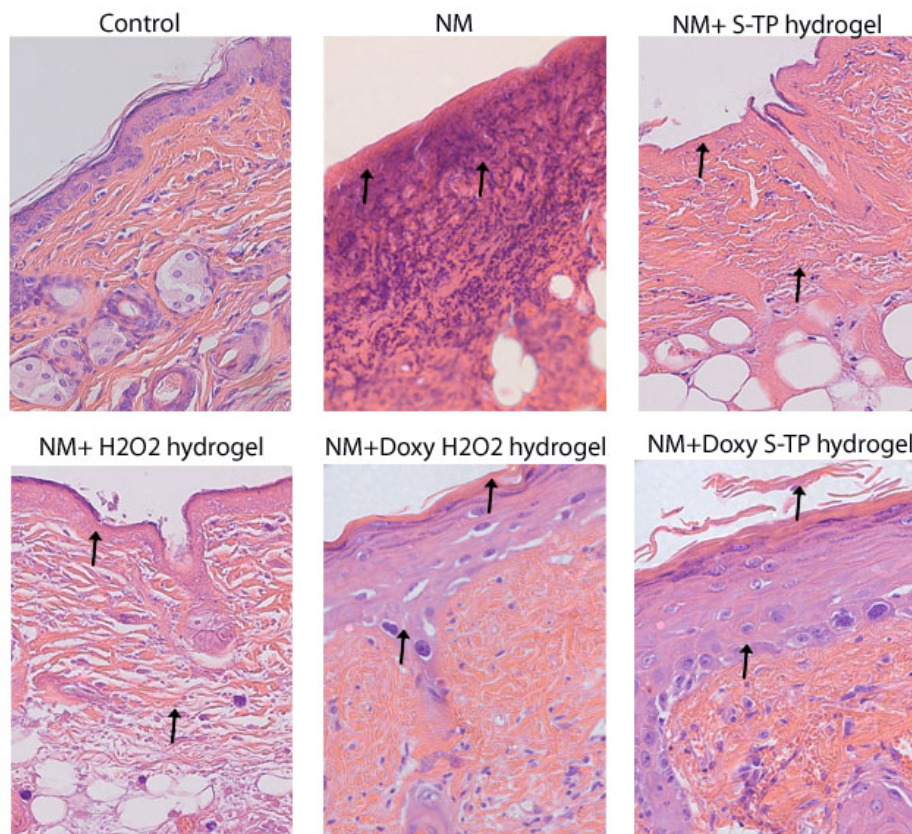


Figure 7.12. Histology of mice skin exposed to NM and subsequently treated with H₂O₂/S-TP placebo or doxycycline hydrogels at 168 h. The histology of both the H₂O₂ and S-TP doxycycline hydrogels showed reepithelization characterized by epidermal hyperplasia and hyperkeratosis, the first signs of wound healing. The doxycycline hydrogels showed a significant improvement in NM-exposed wounds compared to the untreated and placebo hydrogel treated groups.

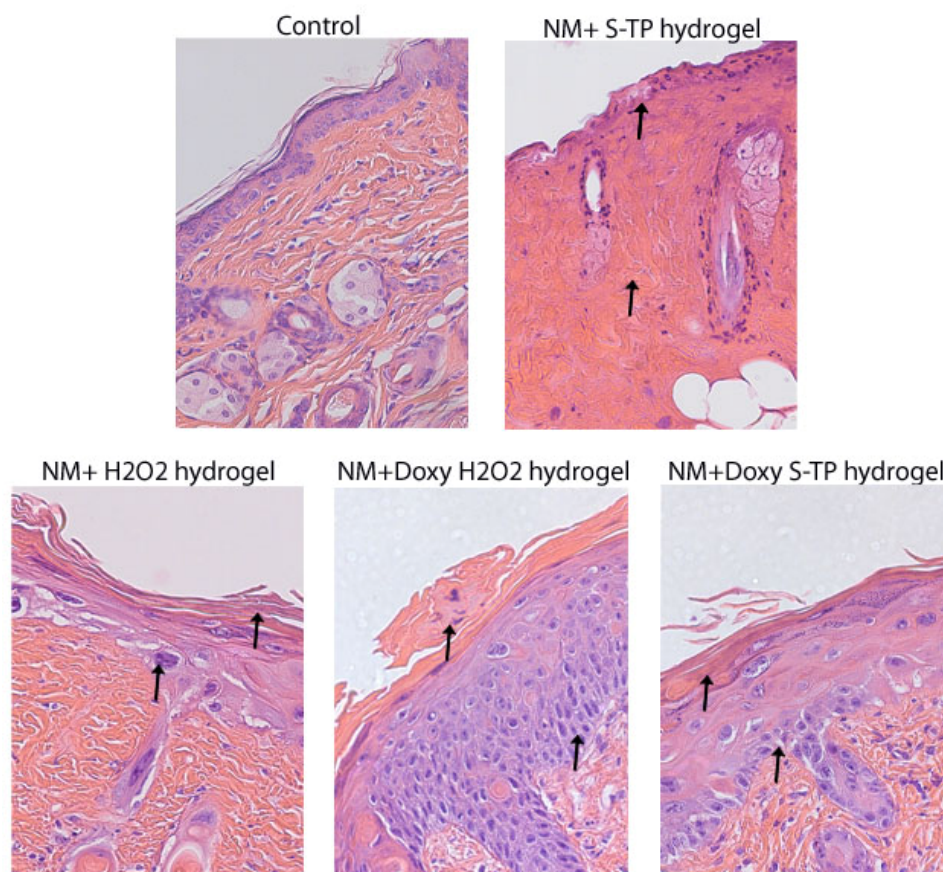


Figure 7.13. Histology of mice skin exposed to NM and subsequently treated with H_2O_2 /S-TP placebo or doxycycline hydrogels at 240 h. The doxycycline hydrogels showed improved wound healing efficacy compared to untreated and H_2O_2 /S-TP placebo hydrogel treated groups after NM exposure, evidenced by the 100 % survival and reepithelization in H_2O_2 /S-TP doxycycline hydrogels.

8 SUMMARY AND CONCLUSIONS

Sulfur mustard is a potent blistering and chemical warfare agent that mainly affects the eyes, lungs and skin. Currently there are no effective drugs or delivery systems to treat SM injuries. Doxycycline, acts by inhibiting inflammatory cytokines and MMP-9. In order to limit systemic toxicity that may be caused by oral drug delivery systems and to increase the local drug concentration at the site of injury, sustained release drug delivery systems are required. This dissertation project involves the design, development and evaluation of *in situ* forming hydrogels for topical administration to the eyes and skin for treatment of SM injuries. The hydrogels evaluated for ocular application are optically transparent, show resistance to external forces, retained on the cornea for the entire duration of the study (24 h), and provide sustained drug release for over a week. The doxycycline-loaded hydrogels showed superior wound healing efficacy compared to similar dose of the drug in solution, which might be due the prolonged contact time and sustained drug release at the injury site.

A dermal wound model was developed using NM to simulate SM injuries in SKH-1 mice. The pathological effects caused by NM on skin progress in a dose and time dependent manner. The permeability of NM-exposed skin (5 μ moles) increases significantly to different molecular markers at 24, 72, and 168 h compared to the control, suggesting that stratum corneum does not act as a barrier for transdermal drug absorption after vesicant exposure. Reversible hydrogels with formulation additives were designed for topical application to the skin. The hydrogels have the mechanical strength and

viscoelastic properties to help maintain their physical integrity *in vivo* and prevent drug loss from breakage. The hydrogels showed sustained doxycycline release for over 10 days. Wound healing efficacy studies show that doxycycline hydrogel treated groups showed significant improvement in wound healing compared to untreated or placebo hydrogel treated groups. Sustained doxycycline delivery was achieved over prolonged periods using novel *in situ* forming PEG hydrogels which showed superior ocular and dermal wound healing efficacies. In summary, sustained release hydrogel drug delivery systems are developed for topical application to the eyes and skin.

9 REFERENCES

- [1] K. Kehe, F. Balszuweit, J. Emmeler, H. Kreppel, M. Jochum, H. Thiermann, Sulfur mustard research-strategies for the development of improved medical therapy. *Eplasty* 8 (2008) e32.
- [2] Y. Solberg, M. Alcalay, M. Belkin, Ocular injury by mustard gas. *Surv Ophthalmol* 41(6) (1997) 461-466.
- [3] B. Papirmeister, in: B. Papirmeister, A. J. Feister, S. I. Robinson and R. D. Ford (Eds.), *Medical Defense Against Mustard Gas: Toxic Mechanisms and Pharmacological Implications*, CRC Press, Boca Raton, FL, 1991.
- [4] F.M. Cowan, C.A. Broomfield, Putative roles of inflammation in the dermatopathology of sulfur mustard. *Cell Biol Toxicol* 9(3) (1993) 201-213.
- [5] Q. Gu, D. Wang, Y. Gao, J. Zhou, R. Peng, Y. Cui, G. Xia, Q. Qing, H. Yang, J. Liu, M. Zhao, Expression of MMP1 in surgical and radiation-impaired wound healing and its effects on the healing process. *J Environ Pathol Toxicol Oncol* 21(1) (2002) 71-78.
- [6] Y.P. Han, T.L. Tuan, H. Wu, M. Hughes, W.L. Garner, TNF-alpha stimulates activation of pro-MMP2 in human skin through NF-(kappa)B mediated induction of MT1-MMP. *J Cell Sci* 114(Pt 1) (2001) 131-139.
- [7] W.M. Holleran, R.E. Galaray, W.N. Gao, D. Levy, P.C. Tang, P.M. Elias, Matrix metalloproteinase inhibitors reduce phorbol ester-induced cutaneous inflammation and hyperplasia. *Arch Dermatol Res* 289(3) (1997) 138-144.
- [8] C.D. Lindsay, E. Gentilhomme, J.D. Mathieu, The use of doxycycline as a protectant against sulphur mustard in HaCaT cells. *J Appl Toxicol* 28(5) (2008) 665-673.
- [9] R. Mohan, S.K. Chintala, J.C. Jung, W.V. Villar, F. McCabe, L.A. Russo, Y. Lee, B.E. McCarthy, K.R. Wollenberg, J.V. Jester, M. Wang, H.G. Welgus, J.M. Shipley, R.M. Senior, M.E. Fini, Matrix metalloproteinase gelatinase B (MMP-9) coordinates and effects epithelial regeneration. *J Biol Chem* 277(3) (2002) 2065-2072.
- [10] P. Paquet, B.V. Nussgens, G.E. Pierard, C.M. Lapiere, Gelatinases in drug-induced toxic epidermal necrolysis. *Eur J Clin Invest* 28(7) (1998) 528-532.
- [11] J.C. Powers, C.M. Kam, K.M. Ricketts, R.P. Casillas, Cutaneous protease activity in the mouse ear vesicant model. *J Appl Toxicol* 20 Suppl 1 (2000) S177-182.

- [12] C.L. Sabourin, M.M. Danne, K.L. Buxton, R.P. Casillas, J.J. Schlager, Cytokine, chemokine, and matrix metalloproteinase response after sulfur mustard injury to weanling pig skin. *J Biochem Mol Toxicol* 16(6) (2002) 263-272.
- [13] M.P. Shakarjian, P. Bhatt, M.K. Gordon, Y.C. Chang, S.L. Casbohm, T.L. Rudge, R.C. Kiser, C.L. Sabourin, R.P. Casillas, P. Ohman-Strickland, D.J. Riley, D.R. Gerecke, Preferential expression of matrix metalloproteinase-9 in mouse skin after sulfur mustard exposure. *J Appl Toxicol* 26(3) (2006) 239-246.
- [14] J.F. Woessner, Jr., A.M. Dannenberg, Jr., P.J. Pula, M.G. Selzer, C.L. Ruppert, K. Higuchi, A. Kajiki, M. Nakamura, N.M. Dahms, J.S. Kerr, et al., Extracellular collagenase, proteoglycanase and products of their activity, released in organ culture by intact dermal inflammatory lesions produced by sulfur mustard. *J Invest Dermatol* 95(6) (1990) 717-726.
- [15] U. Wormser, B. Brodsky, R. Reich, Topical treatment with povidone iodine reduces nitrogen mustard-induced skin collagenolytic activity. *Arch Toxicol* 76(2) (2002) 119-121.
- [16] K.B. Yancey, The pathophysiology of autoimmune blistering diseases. *J Clin Invest* 115(4) (2005) 825-828.
- [17] T. Kadar, S. Dachir, L. Cohen, R. Sahar, E. Fishbine, M. Cohen, J. Turetz, H. Gutman, H. Buch, R. Brandeis, V. Horwitz, A. Solomon, A. Amir, Ocular injuries following sulfur mustard exposure-Pathological mechanism and potential therapy. *Toxicology* (2008).
- [18] D.R. Gerecke, M. Chen, S.S. Isukapalli, M.K. Gordon, Y.C. Chang, W. Tong, I.P. Androulakis, P.G. Georgopoulos, Differential gene expression profiling of mouse skin after sulfur mustard exposure: Extended time response and inhibitor effect. *Toxicol Appl Pharmacol* 234(2) (2009) 156-165.
- [19] J.F. Tarlton, C.J. Vickery, D.J. Leaper, A.J. Bailey, Postsurgical wound progression monitored by temporal changes in the expression of matrix metalloproteinase-9. *Br J Dermatol* 137(4) (1997) 506-516.
- [20] V.J. Uitto, J.D. Firth, L. Nip, L.M. Golub, Doxycycline and chemically modified tetracyclines inhibit gelatinase A (MMP-2) gene expression in human skin keratinocytes. *Ann N Y Acad Sci* 732 (1994) 140-151.
- [21] R. Hanemaaijer, H. Visser, P. Koolwijk, T. Sorsa, T. Salo, L.M. Golub, V.W. van Hinsbergh, Inhibition of MMP synthesis by doxycycline and chemically modified tetracyclines (CMTs) in human endothelial cells. *Adv Dent Res* 12(2) (1998) 114-118.
- [22] H.S. Kim, L. Luo, S.C. Pflugfelder, D.Q. Li, Doxycycline inhibits TGF-beta1-induced MMP-9 via Smad and MAPK pathways in human corneal epithelial cells. *Invest Ophthalmol Vis Sci* 46(3) (2005) 840-848.

- [23] D.Q. Li, Z. Chen, X.J. Song, L. Luo, S.C. Pflugfelder, Stimulation of matrix metalloproteinases by hyperosmolarity via a JNK pathway in human corneal epithelial cells. *Invest Ophthalmol Vis Sci* 45(12) (2004) 4302-4311.
- [24] B.L. Lokeshwar, MMP inhibition in prostate cancer. *Ann N Y Acad Sci* 878 (1999) 271-289.
- [25] B.L. Lokeshwar, M.G. Selzer, N.L. Block, Z. Gunja-Smith, Secretion of matrix metalloproteinases and their inhibitors (tissue inhibitor of metalloproteinases) by human prostate in explant cultures: reduced tissue inhibitor of metalloproteinase secretion by malignant tissues. *Cancer Res* 53(19) (1993) 4493-4498.
- [26] C.S. De Paiva, R.M. Corrales, A.L. Villarreal, W.J. Farley, D.Q. Li, M.E. Stern, S.C. Pflugfelder, Corticosteroid and doxycycline suppress MMP-9 and inflammatory cytokine expression, MAPK activation in the corneal epithelium in experimental dry eye. *Exp Eye Res* 83(3) (2006) 526-535.
- [27] A. Amir, J. Turetz, R. Brandeis, S. Dachir, L. Cohen, M. Cohen, E. Fishbeine, R. Sahar, T. Kadar, G. Schultz, Evaluation of Protease Inhibitors in Sulfur Mustard Ocular Injuries. *Medical Defense Bioscience Review*, Baltimore, MD, 2004.
- [28] T. Kadar, S. Dachir, L. Cohen, R. Sahar, E. Fishbine, M. Cohen, J. Turetz, H. Gutman, H. Buch, R. Brandeis, V. Horwitz, A. Solomon, A. Amir, Ocular injuries following sulfur mustard exposure-Pathological mechanism and potential therapy. *Toxicology* doi:10.1016/j.tox.2008.10.026 (2008).
- [29] C. Guignabert, L. Taysse, J.H. Calvet, E. Planus, S. Delamanche, S. Galiacy, M.P. d'Ortho, Effect of doxycycline on sulfur mustard-induced respiratory lesions in guinea pigs. *Am J Physiol Lung Cell Mol Physiol* 289(1) (2005) L67-74.
- [30] Z. Degim, Use of microparticulate systems to accelerate skin wound healing. *J Drug Target* 16(6) (2008) 437-448.
- [31] N.A. Peppas, P. Bures, W. Leobandung, H. Ichikawa, Hydrogels in pharmaceutical formulations. *Eur J Pharm Biopharm* 50(1) (2000) 27-46.
- [32] D. Eisenbud, H. Hunter, L. Kessler, K. Zulkowski, Hydrogel wound dressings: where do we stand in 2003? *Ostomy Wound Manage* 49(10) (2003) 52-57.
- [33] J.H. Lee, Y.M. Ju, D.M. Kim, Platelet adhesion onto segmented polyurethane film surfaces modified by addition and crosslinking of PEO-containing block copolymers. *Biomaterials* 21(7) (2000) 683-691.
- [34] K.D. Park, Y.S. Kim, D.K. Han, Y.H. Kim, E.H. Lee, H. Suh, K.S. Choi, Bacterial adhesion on PEG modified polyurethane surfaces. *Biomaterials* 19(7-9) (1998) 851-859.

- [35] H.Q. Le, S.J. Knudsen, Exposure to a First World War blistering agent. *Emerg Med J* 23(4) (2006) 296-299.
- [36] R. Aghanouri, M. Ghanei, J. Aslani, H. Keivani-Amine, F. Rastegar, A. Karkhane, Fibrogenic cytokine levels in bronchoalveolar lavage aspirates 15 years after exposure to sulfur mustard. *Am J Physiol Lung Cell Mol Physiol* 287(6) (2004) L1160-1164.
- [37] S. Khateri, M. Ghanei, S. Keshavarz, M. Soroush, D. Haines, Incidence of lung, eye, and skin lesions as late complications in 34,000 Iranians with wartime exposure to mustard agent. *J Occup Environ Med* 45(11) (2003) 1136-1143.
- [38] F. Azizi, A. Keshavarz, F. Roshanzamir, M. Nafarabadi, Reproductive function in men following exposure to chemical warfare with sulphur mustard. *Med War* 11(1) (1995) 34-44.
- [39] R.A. Case, A.J. Lea, Mustard gas poisoning, chronic bronchitis, and lung cancer; an investigation into the possibility that poisoning by mustard gas in the 1914-18 war might be a factor in the production of neoplasia. *Br J Prev Soc Med* 9(2) (1955) 62-72.
- [40] S.M. Somani, S.R. Babu, Toxicodynamics of sulfur mustard. *Int J Clin Pharmacol Ther Toxicol* 27(9) (1989) 419-435.
- [41] J.S. Graham, K.J. Smith, E.H. Braue, J.L. Martin, P.A. Matterson, F.S. Tucker, C.G. Hurst, B.E. Hackley, Improved healing of sulfur mustard-induced cutaneous lesions in the weanling pig by pulsed CO₂ laser debridement. *J Toxicol Cutan Ocul Toxicol* 16(4) (1997) 275-295.
- [42] M. Balali-Mood, M. Hefazi, Comparison of early and late toxic effects of sulfur mustard in Iranian veterans. *Basic Clin Pharmacol Toxicol* 99(4) (2006) 273-282.
- [43] J.S. Graham, R.P. Chilcott, P. Rice, S.M. Milner, C.G. Hurst, B.I. Maliner, Wound healing of cutaneous sulfur mustard injuries: strategies for the development of improved therapies. *J Burns Wounds* 4 (2005) e1.
- [44] M. Balali-Mood, M. Hefazi, The pharmacology, toxicology, and medical treatment of sulphur mustard poisoning. *Fundam Clin Pharmacol* 19(3) (2005) 297-315.
- [45] A. Richardt, M. Blum, *Decontamination of Warfare Agents: Enzymatic Methods for the Removal of B/C Weapons*, Wiley-VCH, Weinheim, Germany, 2008.
- [46] C.M. Pechura, D.P. Rall, *Veterans at Risk: The Health Effects of Mustard Gas and Lewisite*, National Academy Press, Washington, DC, 1993.
- [47] W.J. Geeraets, S. Abedi, R.V. Blanke, Acute corneal injury by mustard gas. *South Med J* 70(3) (1977) 348-350.

- [48] J.L. Willems, Clinical management of mustard gas casualties. *Ann. Med. Milita* 3(suppl.) (1989) 1–61.
- [49] K. Kehe, L. Szinicz, Medical aspects of sulphur mustard poisoning. *Toxicology* 214(3) (2005) 198-209.
- [50] K.J. Smith, C.G. Hurst, R.B. Moeller, H.G. Skelton, F.R. Sidell, Sulfur mustard: its continuing threat as a chemical warfare agent, the cutaneous lesions induced, progress in understanding its mechanism of action, its long-term health effects, and new developments for protection and therapy. *J Am Acad Dermatol* 32(5 Pt 1) (1995) 765-776.
- [51] J.L. Willems, Clinical management of mustard gas casualties. *Annal Med Mil* 3 (1989) 1–60.
- [52] B. Papirmeister, C.L. Gross, J.P. Petrali, H.L. Meier, Pathology produced by sulfur mustard in human skin grafts on athymic nude mice. II. Ultrastructural changes. *J. Toxicol. Cutaneous Ocul. Toxicol* 3 (1984.) 393–408.
- [53] J.P. Petrali, S.B. Oglesby, T.A. Justus, Morphologic effects of sulfur mustard on a human skin equivalent. *J. Toxicol. Cutaneous Ocul. Toxicol Ocul. Toxicol.* 10 (1991) 315–324.
- [54] M. Shohrati, M. Peyman, A. Peyman, M. Davoudi, M. Ghanei, Cutaneous and ocular late complications of sulfur mustard in Iranian veterans. *Cutan Ocul Toxicol* 26(2) (2007) 73-81.
- [55] J. Emmmler, M.I. Hermanns, D. Steinritz, H. Kreppel, C.J. Kirkpatrick, W. Bloch, L. Szinicz, K. Kehe, Assessment of alterations in barrier functionality and induction of proinflammatory and cytotoxic effects after sulfur mustard exposure of an in vitro coculture model of the human alveolo-capillary barrier. *Inhal Toxicol* 19(8) (2007) 657-665.
- [56] M. Jafari, R. Rezaie, The effect of sulfur mustard on glutathione level and activation of glutathione-related enzymes in heart of rats. *Toxicology letters* 180(Supplement 1) (2008) S35.
- [57] D.B. Ludlum, P. Austin-Ritchie, M. Hagopian, T.Q. Niu, D. Yu, Detection of sulfur mustard-induced DNA modifications. *Chem Biol Interact* 91(1) (1994) 39-49.
- [58] D.B. Ludlum, W.P. Tong, J.R. Mehta, M.C. Kirk, B. Papirmeister, Formation of O6-ethylthioethyldeoxyguanosine from the reaction of chloroethyl ethyl sulfide with deoxyguanosine. *Cancer Res* 44(12 Pt 1) (1984) 5698-5701.
- [59] D. Yu, T.Q. Niu, P. Austin-Ritchie, D.B. Ludlum, A 32P-postlabeling method for detecting unstable N-7-substituted deoxyguanosine adducts in DNA. *Proc Natl Acad Sci U S A* 91(15) (1994) 7232-7236.

- [60] A.R. Crathorn, J.J. Roberts, Mechanism of the cytotoxic action of alkylating agents in mammalian cells and evidence for the removal of alkylated groups from deoxyribonucleic acid. *Nature* 211(5045) (1966) 150-153.
- [61] A. Burkle, Physiology and pathophysiology of poly(ADP-ribosyl)ation. *Bioessays* 23(9) (2001) 795-806.
- [62] M.E. Martens, W.J. Smith, The role of NAD⁺ depletion in the mechanism of sulfur mustard-induced metabolic injury. *Cutan Ocul Toxicol* 27(1) (2008) 41-53.
- [63] A.A. Pieper, A. Verma, J. Zhang, S.H. Snyder, Poly (ADP-ribose) polymerase, nitric oxide and cell death. *Trends Pharmacol Sci* 20(4) (1999) 171-181.
- [64] C.M. Arroyo, C.A. Broomfield, B.E. Hackley, Jr., The role of interleukin-6 (IL-6) in human sulfur mustard (HD) toxicology. *Int J Toxicol* 20(5) (2001) 281-296.
- [65] C.M. Arroyo, D.L. Burman, D.W. Kahler, M.R. Nelson, C.M. Corun, J.J. Guzman, M.A. Smith, E.D. Purcell, B.E. Hackley, Jr., S.D. Soni, C.A. Broomfield, TNF- α expression patterns as potential molecular biomarker for human skin cells exposed to vesicant chemical warfare agents: sulfur mustard (HD) and Lewisite (L). *Cell Biol Toxicol* 20(6) (2004) 345-359.
- [66] C.M. Arroyo, R.J. Schafer, E.M. Kurt, C.A. Broomfield, A.J. Carmichael, Response of normal human keratinocytes to sulfur mustard: cytokine release. *J Appl Toxicol* 20 Suppl 1 (2000) S63-72.
- [67] C.M. Arroyo, R.L. Von Tersch, C.A. Broomfield, Activation of alpha-human tumour necrosis factor (TNF- α) by human monocytes (THP-1) exposed to 2-chloroethyl ethyl sulphide (H-MG). *Hum Exp Toxicol* 14(7) (1995) 547-553.
- [68] X. Gao, R. Ray, Y. Xiao, P.E. Barker, P. Ray, Inhibition of sulfur mustard-induced cytotoxicity and inflammation by the macrolide antibiotic roxithromycin in human respiratory epithelial cells. *BMC Cell Biol* 8 (2007) 17.
- [69] S. Greenberg, P. Kamath, J. Petrali, T. Hamilton, J. Garfield, J.A. Garlick, Characterization of the initial response of engineered human skin to sulfur mustard. *Toxicol Sci* 90(2) (2006) 549-557.
- [70] U. Wormser, R. Langenbach, S. Peddada, A. Sintov, B. Brodsky, A. Nyska, Reduced sulfur mustard-induced skin toxicity in cyclooxygenase-2 knockout and celecoxib-treated mice. *Toxicol Appl Pharmacol* 200(1) (2004) 40-47.
- [71] S. Macha, A.K. Mitra, P. Hughes, in: A. K. Mitra (Eds.), *Overview of Ocular Drug Delivery: Ophthalmic Drug Delivery Systems*, Informa Healthcare, New York, NY, 2003.
- [72] S.D. Klyce, Electrical profiles in the corneal epithelium. *J Physiol* 226(2) (1972) 407-429.

- [73] M.R. Prausnitz, J.S. Noonan, Permeability of cornea, sclera, and conjunctiva: a literature analysis for drug delivery to the eye. *J Pharm Sci* 87(12) (1998) 1479-1488.
- [74] H. Sasaki, K. Yamamura, T. Mukai, K. Nishida, J. Nakamura, M. Nakashima, M. Ichikawa, Enhancement of ocular drug penetration. *Crit Rev Ther Drug Carrier Syst* 16(1) (1999) 85-146.
- [75] P.M. Hughes, O. Olejnik, J.E. Chang-Lin, C.G. Wilson, Topical and systemic drug delivery to the posterior segments. *Adv Drug Deliv Rev* 57(14) (2005) 2010-2032.
- [76] D.M. Maurice, in: M. F. Saettone, M. Bucci, P. Speiser (Eds.), *Ophthalmic drug delivery: biopharmaceutical, technological, and clinical aspects*, Liviana press, Padova, 1987.
- [77] S.S. Anumolu, Y. Singh, D. Gao, S. Stein, P.J. Sinko, Design and evaluation of novel fast forming pilocarpine-loaded ocular hydrogels for sustained pharmacological response. *J Control Release* 137(2) (2009) 152-159.
- [78] S.S. Chrai, J.R. Robinson, Corneal permeation of topical pilocarpine nitrate in the rabbit. *Am J Ophthalmol* 77(5) (1974) 735-739.
- [79] T.F. Vandamme, L. Brobeck, Poly(amidoamine) dendrimers as ophthalmic vehicles for ocular delivery of pilocarpine nitrate and tropicamide. *J Control Release* 102(1) (2005) 23-38.
- [80] B.K. Nanjawade, F.V. Manvi, A.S. Manjappa, In situ-forming hydrogels for sustained ophthalmic drug delivery. *J Control Release* 122(2) (2007) 119-134.
- [81] J.W. Sieg, J.R. Robinson, Vehicle effects on ocular drug bioavailability II: Evaluation of pilocarpine. *J Pharm Sci* 66(9) (1977) 1222-1228.
- [82] Y.W. Chien, B.E. Cabana, S.E. Mares, *Novel Drug Delivery Systems: Fundamentals, Development Concepts and Biomedical Assessments*, Marcel Dekker Inc, NY, 1982.
- [83] M.A. Kass, D.W. Meltzer, M. Gordon, D. Cooper, J. Goldberg, Compliance with topical pilocarpine treatment. *Am J Ophthalmol* 101(5) (1986) 515-523.
- [84] V.H. Lee, J.R. Robinson, Topical ocular drug delivery: recent developments and future challenges. *J Ocul Pharmacol* 2(1) (1986) 67-108.
- [85] J.W. Sieg, J.R. Robinson, Vehicle effects on ocular drug bioavailability i: evaluation of fluorometholone. *J Pharm Sci* 64(6) (1975) 931-936.
- [86] A. Zimmer, J. Kreuter, Microspheres and nanoparticles used in ocular delivery systems. *Adv Drug Deliv Rev* 16 (1995) 61-73.

- [87] P. Simamora, S.R. Nadkarni, Y.C. Lee, S.H. Yalkowsky, Controlled delivery of pilocarpine. 2. In vivo evaluation of gelfoam device. *Int J Pharm* 170 (1998) 209-214.
- [88] G. Banker, C. Rhodes, *Modern Pharmaceutics*, Marcel Dekker Inc, NY, 2002.
- [89] D. Gupta, *Glaucoma Diagnosis and Management: Diagnosis and Management*, Lippincott Williams & Wilkins, Baltimore, MD, 2005.
- [90] H. Trommer, R.H. Neubert, Overcoming the stratum corneum: the modulation of skin penetration. A review. *Skin Pharmacol Physiol* 19(2) (2006) 106-121.
- [91] P.W. Wertz, Lipids and barrier function of the skin. *Acta Derm Venereol Suppl (Stockh)* 208 (2000) 7-11.
- [92] A. Misra, J. Nanchahal, Use of gauze soaked in povidone iodine for dressing acute open wounds. *Plast Reconstr Surg* 111(6) (2003) 2105-2107.
- [93] G.J. Motta, C.T. Milne, L.Q. Corbett, Impact of antimicrobial gauze on bacterial colonies in wounds that require packing. *Ostomy Wound Manage* 50(8) (2004) 48-62.
- [94] J.S. Boateng, K.H. Matthews, H.N. Stevens, G.M. Eccleston, Wound healing dressings and drug delivery systems: a review. *J Pharm Sci* 97(8) (2008) 2892-2923.
- [95] C. Dealey, Role of hydrocolloids in wound management. *Br J Nurs* 2(7) (1993) 358, 360, 362 passim.
- [96] A. Fukunaga, H. Naritaka, R. Fukaya, M. Tabuse, T. Nakamura, Our method of povidone-iodine ointment and gauze dressings reduced catheter-related infection in serious cases. *Dermatology* 212 Suppl 1 (2006) 47-52.
- [97] J. Fletcher, Understanding wound dressings: hydrocolloids. *Nurs Times* 101(46) (2005) 51.
- [98] M. Ramos-e-Silva, M.C. Ribeiro de Castro, New dressings, including tissue-engineered living skin. *Clin Dermatol* 20(6) (2002) 715-723.
- [99] J.R. Robinson, V.H.L. Lee, *Controlled Drug Delivery: Fundamentals and Applications*, Informa Health Care, New York, 1987.
- [100] J.W. Lee, J.H. Park, J.R. Robinson, Bioadhesive-based dosage forms: the next generation. *J Pharm Sci* 89(7) (2000) 850-866.
- [101] R. Langer, Polymeric delivery systems for controlled drug release. *Chem Eng Commun* 6 (1980) 1-48.
- [102] L. Brannon-Peppas, *Preparation and characterization of crosslinked hydrophilic networks*, Elsevier, Amsterdam, 1990.

- [103] N.A. Peppas, A.G. Mikos, Preparation methods and structure of hydrogels, CRC press, Boca Raton, FL, 1986.
- [104] N.A. Peppas, A.R. Khare, Preparation, structure and diffusional behavior of hydrogels in controlled release. *Adv. Drug Del. Rev* 11(1-2) (1993) 1-35.
- [105] N.A. Peppas, Physiologically responsive gels. *J. Bioact. Compat. Polym* 6 (1991) 241-246.
- [106] R. Jeyanthi, K.P. Rao, In vivo biocompatibility of collagen-poly(hydroxyethyl methacrylate) hydrogels. *Biomaterials* 11(4) (1990) 238-243.
- [107] K.Y. Lee, D.J. Mooney, Hydrogels for tissue engineering. *Chem Rev* 101(7) (2001) 1869-1879.
- [108] A.S. Hoffman, Hydrogels for biomedical applications. *Adv Drug Deliv Rev* 54(1) (2002) 3-12.
- [109] P. Gupta, K. Vermani, S. Garg, Hydrogels: from controlled release to pH-responsive drug delivery. *Drug Discov Today* 7(10) (2002) 569-579.
- [110] K.E. Uhrich, S.M. Cannizzaro, R.S. Langer, K.M. Shakesheff, Polymeric systems for controlled drug release. *Chem Rev* 99(11) (1999) 3181-3198.
- [111] M.V. Natsu, J.P. Sardinha, I.J. Correia, M.H. Gil, Controlled release gelatin hydrogels and lyophilisates with potential application as ocular inserts. *Biomed Mater* 2(4) (2007) 241-249.
- [112] M. Hamidi, A. Azadi, P. Rafiei, Hydrogel nanoparticles in drug delivery. *Adv Drug Deliv Rev* 60(15) (2008) 1638-1649.
- [113] C.C. Lin, A.T. Metters, Hydrogels in controlled release formulations: network design and mathematical modeling. *Adv Drug Deliv Rev* 58(12-13) (2006) 1379-1408.
- [114] A.S. Hickey, N.A. Peppas, Mesh size and diffusive characteristics of semicrystalline poly(vinyl alcohol) membranes prepared by freezing/thawing techniques. *J. Membr. Sci.* 107(3) (1995) 229-237.
- [115] N.A. Peppas, E.W. Merrill, PVA hydrogels: reinforcement of radiation-crosslinked networks by crystallization. *J Polym Sci Polym Chem Ed* 14(2) (1976) 441-457.
- [116] N.A. Peppas, E.W. Merrill, Differential scanning calorimetry of crystallized PVA hydrogels. *J. Appl. Polym. Sci* 20(6) (1976) 1457-1465.
- [117] N.A. Peppas, N.K. Mongia, Ultrapure poly(vinyl alcohol) hydro gels with mucoadhesive drug delivery characteristics. *Eur. J. Pharm. Biopharm.* 43(1) (1997) 51-58.

- [118] S.R. Stauffer, N.A. Peppas, Poly(vinyl alcohol) hydrogels prepared by freezing–thawing cyclic processing. *Polymer* 33(18) (1992) 3932-3936.
- [119] K. Kamath, K. Park, Biodegradable hydrogels in drug delivery. *Adv. Drug Deliv. Rev* 11(1-2) (1993) 59-84.
- [120] K. Park, W.S.W. Shalaby, H. Park, *Biodegradable Hydrogels For Drug Delivery*, Technomic, Lancaster, PA, 1993.
- [121] W.E. Hennink, S.J. De Jong, G.W. Bos, T.F. Veldhuis, C.F. van Nostrum, Biodegradable dextran hydrogels crosslinked by stereocomplex formation for the controlled release of pharmaceutical proteins. *Int J Pharm* 277(1-2) (2004) 99-104.
- [122] Y. Liu, N.E. Vrana, P.A. Cahill, G.B. McGuinness, Physically crosslinked composite hydrogels of PVA with natural macromolecules: Structure, mechanical properties, and endothelial cell compatibility. *J Biomed Mater Res B Appl Biomater* (2009).
- [123] E. de Souza Costa-Junior, M.M. Pereira, H.S. Mansur, Properties and biocompatibility of chitosan films modified by blending with PVA and chemically crosslinked. *J Mater Sci Mater Med* 20(2) (2009) 553-561.
- [124] S.Q. Liu, P.L. Ee, C.Y. Ke, J.L. Hedrick, Y.Y. Yang, Biodegradable poly(ethylene glycol)-peptide hydrogels with well-defined structure and properties for cell delivery. *Biomaterials* 30(8) (2009) 1453-1461.
- [125] T. Hoare, D. Kohane, Hydrogels in drug delivery: Progress and challenges. *Polymer* 49(8) (2008) 1993-2007.
- [126] A.T. Metters, C. Lin, Biodegradable hydrogels: Tailoring properties and function through chemistry and structure In: J.Y.Wong and J.D.Bronzino (Eds.), *Biomaterials*, CRC press, Boca Raton, FL., 2007.
- [127] D. Kanjickal, S. Lopina, M.M. Evanco-Chapman, S. Schmidt, D. Donovan, Improving delivery of hydrophobic drugs from hydrogels through cyclodextrins. *J Biomed Mater Res A* 74(3) (2005) 454-460.
- [128] T. Kecik, J. Szlaski, L. Portacha, P. Lewandowski, B. Marchlewska, I. Pacak, Studies of releasing rate of pilocarpine hydrochloride from hydrogel eye ointments. *Klin Oczna* 95(7) (1993) 263-264.
- [129] G.H. Hsiue, J.A. Guu, C.C. Cheng, Poly(2-hydroxyethyl methacrylate) film as a drug delivery system for pilocarpine. *Biomaterials* 22(13) (2001) 1763-1769.
- [130] S. Miyazaki, S. Suzuki, N. Kawasaki, K. Endo, A. Takahashi, D. Attwood, In situ gelling xyloglucan formulations for sustained release ocular delivery of pilocarpine hydrochloride. *Int J Pharm* 229(1-2) (2001) 29-36.

- [131] H.R. Lin, K.C. Sung, W.J. Vong, In situ gelling of alginate/pluronic solutions for ophthalmic delivery of pilocarpine. *Biomacromolecules* 5(6) (2004) 2358-2365.
- [132] S.D. Desai, J. Blanchard, In vitro evaluation of pluronic F127-based controlled-release ocular delivery systems for pilocarpine. *J Pharm Sci* 87(2) (1998) 226-230.
- [133] S. Kumar, B.O. Haglund, K.J. Himmelstein, In situ-forming gels for ophthalmic drug delivery. *J Ocul Pharmacol* 10(1) (1994) 47-56.
- [134] S. Cohen, E. Lobel, A. Trevigoda, Y. Peled, A novel in situ-forming ophthalmic drug delivery system from alginates undergoing gelation in the eye. *J Control Release* 44(2-3) (1997) 201-208.
- [135] K. Anseth, A. Metters, S. Bryant, P. Martens, H. Jennifer, C. Bowman, In situ forming degradable networks and their application in tissue engineering and drug delivery. *J Control Release* 78(1-3) (2002) 199-209.
- [136] X. Huang, C.S. Brazel, On the importance and mechanisms of burst release in matrix-controlled drug delivery systems. *J Control Release* 73(2-3) (2001) 121-136.
- [137] N.A. Peppas, K.B. Keys, M. Torres-Lugo, A.M. Lowman, Poly(ethylene glycol)-containing hydrogels in drug delivery. *J Control Release* 62(1-2) (1999) 81-87.
- [138] N.A. Peppas, Y. Huang, M. Torres-Lugo, J.H. Ward, J. Zhang, Physicochemical foundations and structural design of hydrogels in medicine and biology. *Annu Rev Biomed Eng* 2 (2000) 9-29.
- [139] A.M. Lowman, N.A. Peppas, Solute transport analysis in pH-responsive, complexing hydrogels of poly(methacrylic acid-g-ethylene glycol). *J Biomater Sci Polym Ed* 10(9) (1999) 999-1009.
- [140] L. Serra, J. Domenech, N.A. Peppas, Drug transport mechanisms and release kinetics from molecularly designed poly(acrylic acid-g-ethylene glycol) hydrogels. *Biomaterials* 27(31) (2006) 5440-5451.
- [141] M. Sen, A. Yakar, Controlled release of antifungal drug terbinafine hydrochloride from poly(N-vinyl 2-pyrrolidone/itaconic acid) hydrogels. *Int J Pharm* 228(1-2) (2001) 33-41.
- [142] O. Garcia, R.M. Trigo, M.D. Blanco, J.M. Teijon, Influence of degree of crosslinking on 5-fluorouracil release from poly(2-hydroxyethyl methacrylate) hydrogels. *Biomaterials* 15(9) (1994) 689-694.
- [143] V.S. Rudraraju, C.M. Wyandt, Rheology of Microcrystalline Cellulose and Sodiumcarboxymethyl Cellulose hydrogels using a controlled stress rheometer: part II. *Int J Pharm* 292(1-2) (2005) 63-73.

- [144] J. Li, Z. Xu, Physical characterization of a chitosan-based hydrogel delivery system. *J Pharm Sci* 91(7) (2002) 1669-1677.
- [145] A. Lippacher, R.H. Muller, K. Mader, Investigation on the viscoelastic properties of lipid based colloidal drug carriers. *Int J Pharm* 196(2) (2000) 227-230.
- [146] A. Lippacher, R.H. Muller, K. Mader, Liquid and semisolid SLN dispersions for topical application: rheological characterization. *Eur J Pharm Biopharm* 58(3) (2004) 561-567.
- [147] J. Carlfors, K. Edsman, R. Petersson, K. Jornving, Rheological evaluation of Gelrite in situ gels for ophthalmic use. *Eur J Pharm Sci* 6(2) (1998) 113-119.
- [148] V. Jones, T. Milton, When and how to use hydrocolloid dressings. *Nurs Times* 96(4 Suppl) (2000) 5-7.
- [149] S. Thomas, P. Hay, Fluid handling properties of hydrogel dressings. *Ostomy Wound Manage* 41(3) (1995) 54-56, 58-59.
- [150] S. Bale, V. Banks, S. Haglestein, K.G. Harding, A comparison of two amorphous hydrogels in the debridement of pressure sores. *J Wound Care* 7(2) (1998) 65-68.
- [151] D. Colin, P.A. Kurring, C. Yvon, Managing sloughy pressure sores. *J Wound Care* 5(10) (1996) 444-446.
- [152] M. Flanagan, The efficacy of a hydrogel in the treatment of wounds with non-viable tissue. *J Wound Care* 4(6) (1995) 264-267.
- [153] S. Thomas, M. Fear, Comparing two dressings for wound debridement. *J Wound Care* 2(5) (1993) 272-274.
- [154] H.J. Yoo, H.D. Kim, Synthesis and properties of waterborne polyurethane hydrogels for wound healing dressings. *J Biomed Mater Res B Appl Biomater* 85(2) (2008) 326-333.
- [155] W.H. Eaglstein, S.C. Davis, A.L. Mehle, P.M. Mertz, Optimal use of an occlusive dressing to enhance healing. Effect of delayed application and early removal on wound healing. *Arch Dermatol* 124(3) (1988) 392-395.
- [156] G.D. Winter, Formation of the scab and the rate of epithelization of superficial wounds in the skin of the young domestic pig. *Nature* 193 (1962) 293-294.
- [157] G.D. Winter, J.T. Scales, Effect of air drying and dressings on the surface of a wound. *Nature* 197 (1963) 91-92.
- [158] F. Yoshii, Y. Zhanshan, K. Isobe, K. Shinozaki, K. Makuuchi, Electron beam crosslinked PEO and PEO/PVA hydrogels for wound dressing. *Radiation physics and chemistry* 55 (1999) 133-138.

- [159] A. Tong, The identification and treatment of slough. *J Wound Care* 8(7) (1999) 338-339.
- [160] R. Pudner, Amorphous hydrogel dressings in wound management. *J Community Nursing* 15(6) (2001) 43-46.
- [161] S. Thomas, I.M. Leigh, Wound dressings. In: D.J. Leaper, K.G. Harding (eds.), *Wounds: biology and management*, Oxford University Press, Oxford, 1998.
- [162] L.G. Ovington, The well-dressed wound: an overview of dressing types. *Wounds* 10(Suppl A): (1998) 1A-11A.
- [163] J.L. Gates, G.A. Holloway, A comparison of wound environments. *Ostomy Wound Manage* 38(8) (1992) 34-37.
- [164] G.D. Mulder, Cost-effective managed care: gel versus wet-to-dry for debridement. *Ostomy Wound Manage* 41(2) (1995) 68-70, 72, 74 passim.
- [165] B. Cable, M. Stewart, J. Davis, Nipple wound care: a new approach to an old problem. *J Hum Lact* 13(4) (1997) 313-318.
- [166] H. Hollinworth, Pain relief. *Nurs Times* 97(28) (2001) 63-66.
- [167] J.S. Lozano, E.Y. Chay, J. Healey, R. Sullenberger, J.K. Klarlund, Activation of the epidermal growth factor receptor by hydrogels in artificial tears. *Exp Eye Res* 86(3) (2008) 500-505.
- [168] C.P. Lin, M. Boehnke, Influences of methylcellulose on corneal epithelial wound healing. *J Ocul Pharmacol Ther* 15(1) (1999) 59-63.
- [169] Q. Garrett, P.A. Simmons, S. Xu, J. Vehige, Z. Zhao, K. Ehrmann, M. Willcox, Carboxymethylcellulose binds to human corneal epithelial cells and is a modulator of corneal epithelial wound healing. *Invest Ophthalmol Vis Sci* 48(4) (2007) 1559-1567.
- [170] C. Pratoomsoot, H. Tanioka, K. Hori, S. Kawasaki, S. Kinoshita, P.J. Tighe, H. Dua, K.M. Shakesheff, F.R. Rose, A thermoreversible hydrogel as a biosynthetic bandage for corneal wound repair. *Biomaterials* 29(3) (2008) 272-281.
- [171] S.W. Shalaby, K.J.L. Burg, *Polyethylene glycol-based copolyesters: Absorbable and biodegradable polymers*, CRC Press, Boca Raton, FL, 2004.
- [172] J.M. Harris, Introduction to biotechnical and biomedical applications of poly(ethylene glycol). In: J.M. Harris (Ed.), *Poly(ethylene glycol) Chemistry: Biotechnical and Biomedical Applications*, Plenum press, New York, NY, 1992.
- [173] M. Zacchigna, G. Di Luca, V. Maurich, E. Boccu, Syntheses, chemical and enzymatic stability of new poly(ethylene glycol)-acyclovir prodrugs. *Farmaco* 57(3) (2002) 207-214.

- [174] E.W. Merrill, Poly(ethylene oxide) star molecules: synthesis, characterization, and applications in medicine and biology. *J Biomater Sci Polym Ed* 5(1-2) (1993) 1-11.
- [175] K.B. Keys, F.M. Andreopoulos, N.A. Peppas, Poly(ethylene glycol) Star Polymer Hydrogels. *Macromolecules* 31(23) (1998) 8149–8156.
- [176] N.B. Graham, Poly(ethylene oxide) and related hydrogels. In: N.A. Peppas (Ed.), *Hydrogels in Medicine and Pharmacy*, CRC press, Boca Raton, FL, 1987.
- [177] A. Apicella, B. Cappello, M.A. Del Nobile, M.I. La Rotonda, G. Mensitieri, L. Nicolais, Poly(ethylene oxide) (PEO) and different molecular weight PEO blends monolithic devices for drug release. *Biomaterials* 14(2) (1993) 83-90.
- [178] N. Belcheva, R. Stamenova, C. Tsvetanov, Crosslinked poly(ethylene oxide) for drug release systems. *Macromol. Symp* 103 (1996) 193–211.
- [179] D.M. Maurice, in: M. F. Saettone, M. Bucci and P. Speiser (Eds.), *Ophthalmic drug delivery: biopharmaceutical, technological, and clinical aspects*, Vol. 11, Liviana Press, Padova, 1987, pp. 19-26.
- [180] Y. Ali, K. Lehmussaari, Industrial perspective in ocular delivery. *Adv Drug Deliv Rev* 58 (2006) 1258-1268.
- [181] B. Katzung, *Basic and clinical pharmacology*, McGraw Hill Professional, Chicago, IL, 2004.
- [182] S.K. Gupta, R. Agarwal, N.D. Galpalli, S. Srivastava, S.S. Agrawal, R. Saxena, Comparative efficacy of pilocarpine, timolol and latanoprost in experimental models of glaucoma. *Methods Find Exp Clin Pharmacol* 29(10) (2007) 665-671.
- [183] R. Lazare, M. Horlington, Pilocarpine levels in the eyes of rabbits following topical application. *Exp Eye Res* 21(3) (1975) 281-287.
- [184] B. Qiu, S. Stefanos, J. Ma, A. Lalloo, B.A. Perry, M.J. Leibowitz, P.J. Sinko, S. Stein, A hydrogel prepared by in situ cross-linking of a thiol-containing poly(ethylene glycol)-based copolymer: a new biomaterial for protein drug delivery. *Biomaterials* 24(1) (2003) 11-18.
- [185] S.K. Murthy, N. Ravi, Hydrogels as potential probes for investigating the mechanism of lenticular presbyopia. *Curr Eye Res* 22(5) (2001) 384-393.
- [186] M. Suzuki, M. Yumoto, M. Kimura, H. Shirai, K. Hanabusa, A family of low-molecular-weight hydrogelators based on L-lysine derivatives with a positively charged terminal group. *Chemistry* 9(1) (2003) 348-354.
- [187] OECD, Test No. 405: Acute Eye Irritation/Corrosion. vol 1, no 4 (2002) 1-14.

- [188] S. W. Shalaby and M. Shalaby, Polyethylene glycol-based copolyesters: Absorbable and biodegradable polymers, CRC Press, Boca Raton, FL, 2004, pp. 39-58.
- [189] R. Greenwald, PEG drugs: an overview. *J Control Release* 74 (2001) 159-171.
- [190] Y. Singh, M. Palombo, P. Sinko, Recent trends in targeted anticancer prodrug and conjugate design. *Curr Med Chem* 15 (2008) 1802-1826.
- [191] Y. Singh, N. Spinelli, E. Defrancq, Chemical strategies for oligonucleotide-conjugate synthesis. *Curr Org Chem* 12 (2008) 263-290.
- [192] M. Morpurgo, F. Veronese, D. Kachensky, J. Harris, Preparation and characterization of poly(ethylene glycol) vinyl sulfone. *Bioconj Chem* 7 (1996) 363-368.
- [193] H. Park, K. Park, D. Kim, Preparation and swelling behavior of chitosan-based superporous hydrogels for gastric retention application. *J Biomed Mater Res A* 76(1) (2006) 144-150.
- [194] H. Tan, C.R. Chu, K.A. Payne, K.G. Marra, Injectable in situ forming biodegradable chitosan-hyaluronic acid based hydrogels for cartilage tissue engineering. *Biomaterials* (2009).
- [195] J. Crank, *The Mathematics of Diffusion*, Oxford University Press, New York, NY, 1975.
- [196] L. Kenar, T. Karayilanoglu, A. Yuksel, O. Gunhan, S. Kose, B. Kurt, Evaluation of protective ointments used against dermal effects of nitrogen mustard, a vesicant warfare agent. *Mil Med* 170(1) (2005) 1-6.
- [197] J.C. Dacre, M. Goldman, Toxicology and pharmacology of the chemical warfare agent sulfur mustard. *Pharmacol Rev* 48(2) (1996) 289-326.
- [198] U. Wormser, Toxicology of mustard gas. *Trends Pharmacol Sci* 12(4) (1991) 164-167.
- [199] N.S. Gould, C.W. White, B.J. Day, A role for mitochondrial oxidative stress in sulfur mustard analog 2-chloroethyl ethyl sulfide-induced lung cell injury and antioxidant protection. *J Pharmacol Exp Ther* 328(3) (2009) 732-739.
- [200] P.A. Jowsey, F.M. Williams, P.G. Blain, DNA damage, signalling and repair after exposure of cells to the sulphur mustard analogue 2-chloroethyl ethyl sulphide. *Toxicology* 257(3) (2009) 105-112.
- [201] C. Karacsonyi, N. Shanmugam, E. Kagan, A clinically relevant in vitro model for evaluating the effects of aerosolized vesicants. *Toxicol Lett* 185(1) (2009) 38-44.
- [202] Y. Morad, E. Banin, E. Averbukh, E. Berenshtein, A. Obolensky, M. Chevion, Treatment of ocular tissues exposed to nitrogen mustard: beneficial effect of zinc

desferrioxamine combined with steroids. *Invest Ophthalmol Vis Sci* 46(5) (2005) 1640-1646.

[203] N. Tewari-Singh, S. Rana, M. Gu, A. Pal, D.J. Orlicky, C.W. White, R. Agarwal, Inflammatory biomarkers of sulfur mustard analog 2-chloroethyl ethyl sulfide-induced skin injury in SKH-1 hairless mice. *Toxicol Sci* 108(1) (2009) 194-206.

[204] G.Q. Wang, Z.F. Xia, Tissue injury by hot fluid containing nitrogen mustard. *Burns* 33(7) (2007) 923-926.

[205] L.R. Barrows, Antineoplastic and immunoactive drugs. In: A.R. Gennaro (Eds.), *Remington: The Science and Practice of Pharmacy*, Mack Publishing Company, Easton, PA, 1995.

[206] B.A. Chabner, C.J. Allegra, G.A. Curt, P. Calabresi, Antineoplastic agents. In: J.G. Hardman, L.E. Limbird, P.B. Molinoff, R.W. Ruddon and A.G. Gilman (Eds.), *Goodman & Gilman's The Pharmacological Basis of Therapeutics*, McGraw-Hill, New York, NY, 1996.

[207] M. Sharma, R. Vijayaraghavan, A. Gautam, DRDE-07 and its analogues as promising cytoprotectants to nitrogen mustard (HN-2)-An alkylating anticancer and chemical warfare agent. *Toxicol Lett* (2009).

[208] A.M. Evens, M. Hutchings, V. Diehl, Treatment of Hodgkin lymphoma: the past, present, and future. *Nat Clin Pract Oncol* 5(9) (2008) 543-556.

[209] H. Tesch, M. Sieber, V. Diehl, Treatment of advanced stage Hodgkin's disease. *Oncology* 60(2) (2001) 101-109.

[210] U. Tirelli, E. Vaccher, M. Spina, A. Carbone, Hodgkin's disease: clinical presentation and treatment. *Cancer Treat Res* 104 (2001) 247-265.

[211] N. Apisarnthanarax, R. Talpur, M. Duvic, Treatment of cutaneous T cell lymphoma: current status and future directions. *Am J Clin Dermatol* 3(3) (2002) 193-215.

[212] S.R. Parker, B. Bradley, Treatment of cutaneous T-cell lymphoma/mycosis fungoides. *Dermatol Nurs* 18(6) (2006) 566-570, 573-565.

[213] C. Berthelot, A. Rivera, M. Duvic, Skin directed therapy for mycosis fungoides: a review. *J Drugs Dermatol* 7(7) (2008) 655-666.

[214] Y.H. Kim, Management with topical nitrogen mustard in mycosis fungoides. *Dermatol Ther* 16(4) (2003) 288-298.

[215] B.D. Smith, L.D. Wilson, Management of mycosis fungoides: Part 2. Treatment. *Oncology (Williston Park)* 17(10) (2003) 1419-1428; discussion 1430, 1433.

- [216] U. Wormser, B. Brodsky, B.S. Green, R. Arad-Yellin, A. Nyska, Protective effect of povidone-iodine ointment against skin lesions induced by sulphur and nitrogen mustards and by non-mustard vesicants. *Arch Toxicol* 71(3) (1997) 165-170.
- [217] J.A. Hartley, Selectivity in alkylating agent-DNA interactions, In: S. Neidle, M. Waring (Eds.), *Molecular aspects of anticancer drug-DNA interactions*, CRS press, Boca Raton, FL, 1993.
- [218] K.J. Smith, W.J. Smith, T. Hamilton, H.G. Skelton, J.S. Graham, C. Okerberg, R. Moeller, B.E. Hackley, Jr., Histopathologic and immunohistochemical features in human skin after exposure to nitrogen and sulfur mustard. *Am J Dermatopathol* 20(1) (1998) 22-28.
- [219] A. Anwar, M. Gu, S. Brady, L. Qamar, K. Behbakht, Y.G. Shellman, R. Agarwal, D.A. Norris, L.D. Horwitz, M. Fujita, Photoprotective effects of bucillamine against UV-induced damage in an SKH-1 hairless mouse model. *Photochem Photobiol* 84(2) (2008) 477-483.
- [220] R.R. Bell, R.W. Dunstan, N.K. Khan, Skin wound healing in the SKH-1 female mouse following inducible nitric oxide synthase inhibition. *Br J Dermatol* 157(4) (2007) 656-661.
- [221] Y.C. Chang, C.L. Sabourin, S.E. Lu, T. Sasaki, K.K. Svoboda, M.K. Gordon, D.J. Riley, R.P. Casillas, D.R. Gerecke, Upregulation of gamma-2 laminin-332 in the mouse ear vesicant wound model. *J Biochem Mol Toxicol* 23(3) (2009) 172-184.
- [222] T.P. Amadeu, B. Coulomb, A. Desmouliere, A.M. Costa, Cutaneous wound healing: myofibroblastic differentiation and in vitro models. *Int J Low Extrem Wounds* 2(2) (2003) 60-68.
- [223] J.S. Graham, R.S. Stevenson, L.W. Mitcheltree, M. Simon, T.A. Hamilton, R.R. Deckert, R.B. Lee, Improved wound healing of cutaneous sulfur mustard injuries in a weanling pig model. *J Burns Wounds* 5 (2006) e7.
- [224] I. Kurokawa, H. Mizutani, K. Kusumoto, S. Nishijima, M. Tsujita-Kyutoku, N. Shikata, A. Tsubura, Cytokeratin, filaggrin, and p63 expression in reepithelialization during human cutaneous wound healing. *Wound Repair Regen* 14(1) (2006) 38-45.
- [225] C.E. Pullar, A. Rizzo, R.R. Isseroff, beta-Adrenergic receptor antagonists accelerate skin wound healing: evidence for a catecholamine synthesis network in the epidermis. *J Biol Chem* 281(30) (2006) 21225-21235.
- [226] L.E. Reynolds, F.J. Conti, R. Silva, S.D. Robinson, V. Iyer, R. Rudling, B. Cross, E. Nye, I.R. Hart, C.M. Dipersio, K.M. Hodivala-Dilke, alpha3beta1 integrin-controlled Smad7 regulates reepithelialization during wound healing in mice. *J Clin Invest* 118(3) (2008) 965-974.

- [227] M. Blaha, W. Bowers, Jr., J. Kohl, D. DuBose, J. Walker, IL-1-related cytokine responses of nonimmune skin cells subjected to CEES exposure with and without potential vesicant antagonists. *In Vitro Mol Toxicol* 13(2) (2000) 99-111.
- [228] M. Blaha, W. Bowers, Jr., J. Kohl, D. DuBose, J. Walker, A. Alkhyat, G. Wong, Effects of CEES on inflammatory mediators, heat shock protein 70A, histology and ultrastructure in two skin models. *J Appl Toxicol* 20 Suppl 1 (2000) S101-108.
- [229] J.F. Dillman, 3rd, K.L. McGary, J.J. Schlager, An inhibitor of p38 MAP kinase downregulates cytokine release induced by sulfur mustard exposure in human epidermal keratinocytes. *Toxicol In Vitro* 18(5) (2004) 593-599.
- [230] M.A. Isidore, M.P. Castagna, K.E. Steele, R.K. Gordon, M.P. Nambiar, A dorsal model for cutaneous vesicant injury by 2-chloroethyl ethyl sulfide using C57BL/6 mice. *Cutan Ocul Toxicol* 26(3) (2007) 265-276.
- [231] R.K. Kan, C.M. Pleva, T.A. Hamilton, D.R. Anderson, J.P. Petrali, Sulfur mustard-induced apoptosis in hairless guinea pig skin. *Toxicol Pathol* 31(2) (2003) 185-190.
- [232] V. Paromov, Z. Suntres, M. Smith, W.L. Stone, Sulfur mustard toxicity following dermal exposure: role of oxidative stress, and antioxidant therapy. *J Burns Wounds* 7 (2007) e7.
- [233] K.M. Ricketts, C.T. Santai, J.A. France, A.M. Graziosi, T.D. Doyel, M.Y. Gazaway, R.P. Casillas, Inflammatory cytokine response in sulfur mustard-exposed mouse skin. *J Appl Toxicol* 20 Suppl 1 (2000) S73-76.
- [234] J.V. Rogers, Y.W. Choi, R.C. Kiser, M.C. Babin, R.P. Casillas, J.J. Schlager, C.L. Sabourin, Microarray analysis of gene expression in murine skin exposed to sulfur mustard. *J Biochem Mol Toxicol* 18(6) (2004) 289-299.
- [235] D.S. Rosenthal, C.M. Simbulan-Rosenthal, S. Iyer, A. Spoonde, W. Smith, R. Ray, M.E. Smulson, Sulfur mustard induces markers of terminal differentiation and apoptosis in keratinocytes via a Ca^{2+} -calmodulin and caspase-dependent pathway. *J Invest Dermatol* 111(1) (1998) 64-71.
- [236] C.L. Sabourin, J.P. Petrali, R.P. Casillas, Alterations in inflammatory cytokine gene expression in sulfur mustard-exposed mouse skin. *J Biochem Mol Toxicol* 14(6) (2000) 291-302.
- [237] U. Wormser, B. Brodsky, E. Proscura, J.F. Foley, T. Jones, A. Nyska, Involvement of tumor necrosis factor- α in sulfur mustard-induced skin lesion; effect of topical iodine. *Arch Toxicol* 79(11) (2005) 660-670.
- [238] G.S. Berenson, G.E. Burch, Studies of diffusion of water through dead human skin; the effect of different environmental states and of chemical alterations of the epidermis. *Am J Trop Med Hyg* 31(6) (1951) 842-853.

- [239] C.J. Morgan, A.G. Renwick, P.S. Friedmann, The role of stratum corneum and dermal microvascular perfusion in penetration and tissue levels of water-soluble drugs investigated by microdialysis. *Br J Dermatol* 148(3) (2003) 434-443.
- [240] M.R. Rosen, *Delivery System Handbook for Personal Care and Cosmetic Products: Technology, Applications and Formulations* (Personal Care and Cosmetic Technology), William Andrew Publishing, Maryland Heights, MO, 2006.
- [241] P.D. Blanc, The legacy of war gas. *Am J Med* 106(6) (1999) 689-690.
- [242] R.N. Saladi, E. Smith, A.N. Persaud, Mustard: a potential agent of chemical warfare and terrorism. *Clin Exp Dermatol* 31(1) (2006) 1-5.
- [243] J. Borak, F.R. Sidell, Agents of chemical warfare: sulfur mustard. *Ann Emerg Med* 21(3) (1992) 303-308.
- [244] M. Ghanei, A.A. Harandi, Long term consequences from exposure to sulfur mustard: a review. *Inhal Toxicol* 19(5) (2007) 451-456.
- [245] W.J. Smith, M.A. Dunn, Medical defense against blistering chemical warfare agents. *Arch Dermatol* 127(8) (1991) 1207-1213.
- [246] T. Kadar, S. Dachir, L. Cohen, R. Sahar, E. Fishbine, M. Cohen, J. Turetz, H. Gutman, H. Buch, R. Brandeis, V. Horwitz, A. Solomon, A. Amir, Ocular injuries following sulfur mustard exposure--pathological mechanism and potential therapy. *Toxicology* 263(1) (2009) 59-69.
- [247] E.K. Akpek, A. Merchant, V. Pinar, C.S. Foster, Ocular rosacea: patient characteristics and follow-up. *Ophthalmology* 104(11) (1997) 1863-1867.
- [248] D. Dursun, M.C. Kim, A. Solomon, S.C. Pflugfelder, Treatment of recalcitrant recurrent corneal erosions with inhibitors of matrix metalloproteinase-9, doxycycline and corticosteroids. *Am J Ophthalmol* 132(1) (2001) 8-13.
- [249] J.A. Seedor, H.D. Perry, T.F. McNamara, L.M. Golub, D.F. Buxton, D.S. Guthrie, Systemic tetracycline treatment of alkali-induced corneal ulceration in rabbits. *Arch Ophthalmol* 105(2) (1987) 268-271.
- [250] D.M. Maurice, S. Mishima, Ocular pharmacokinetics, in: M. L. Sears (Ed.), *Handbook of experimental pharmacology*, Springer Verlag, Berlin-Heidelberg, 1984.
- [251] A. Urtti, Challenges and obstacles of ocular pharmacokinetics and drug delivery. *Adv Drug Deliv Rev* 58(11) (2006) 1131-1135.
- [252] A. Urtti, J.D. Pipkin, G.S. Rork, T. Sendo, U. Finne, A.J. Repta, Controlled drug delivery devices for experimental ocular studies with timolol. 2. Ocular and systemic absorption in rabbits. *Int. J. Pharm* 61 (1990) 241-249.

- [253] M. Hornof, E. Toropainen, A. Urtti, Cell culture models of the ocular barriers. *Eur J Pharm Biopharm* 60(2) (2005) 207-225.
- [254] M.W. Grinstaff, Designing hydrogel adhesives for corneal wound repair. *Biomaterials* 28(35) (2007) 5205-5214.
- [255] K. Hori, C. Sotozono, J. Hamuro, K. Yamasaki, Y. Kimura, M. Ozeki, Y. Tabata, S. Kinoshita, Controlled-release of epidermal growth factor from cationized gelatin hydrogel enhances corneal epithelial wound healing. *J Control Release* 118(2) (2007) 169-176.
- [256] R.M. Palmer, M.B. McDonald, A corneal lens/shield system to promote postoperative corneal epithelial healing. *J Cataract Refract Surg* 21(2) (1995) 125-126.
- [257] H. Sheardown, H. Clark, C. Wedge, R. Apel, D. Rootman, Y.L. Cheng, A semi-solid drug delivery system for epidermal growth factor in corneal epithelial wound healing. *Curr Eye Res* 16(3) (1997) 183-190.
- [258] D. Gupta, C.H. Tator, M.S. Shoichet, Fast-gelling injectable blend of hyaluronan and methylcellulose for intrathecal, localized delivery to the injured spinal cord. *Biomaterials* 27(11) (2006) 2370-2379.
- [259] D.M. Foreman, S. Pancholi, J. Jarvis-Evans, D. McLeod, M.E. Boulton, A simple organ culture model for assessing the effects of growth factors on corneal re-epithelialization. *Exp Eye Res* 62(5) (1996) 555-564.
- [260] A. Lendlein, R. Langer, Biodegradable, elastic shape-memory polymers for potential biomedical applications. *Science* 296(5573) (2002) 1673-1676.
- [261] G. Hermanson, Bioconjugate techniques, 2nd Edition, Elsevier Science & Technology Books, Burlington, MA, 2008.
- [262] E. Mannermaa, K.S. Vellonen, A. Urtti, Drug transport in corneal epithelium and blood-retina barrier: emerging role of transporters in ocular pharmacokinetics. *Adv Drug Deliv Rev* 58(11) (2006) 1136-1163.
- [263] R. Campbell, P. Caroline, Lens Adhesion and RGP Daily Wear. *Contact Lens Spectrum* Jan (1) (1996) 1-2.
- [264] S. Eiden, S. Cristina, Adherence of Daily Wear RGP Contact Lenses. *Contact Lens Spectrum* Feb(1) (1996) 1-6.
- [265] G.M. Gordon, D.R. Ledee, W.J. Feuer, M.E. Fini, Cytokines and signaling pathways regulating matrix metalloproteinase-9 (MMP-9) expression in corneal epithelial cells. *J Cell Physiol* 221(2) (2009) 402-411.
- [266] D.A. Morgan, Wound management products in the Drug Tariff. *The Pharmaceutical Journal* 263(7072) (1999) 820-825.

- [267] D.A. Morgan, Alginate dressings. Part 1: Historical aspects. *J Tissue Viabil* 7 (1997) 4-9.
- [268] L. Mi, W. Gong, P. Nelson, L. Martin, T.W. Sawyer, Hypothermia reduces sulphur mustard toxicity. *Toxicol Appl Pharmacol* 193(1) (2003) 73-83.
- [269] T.W. Sawyer, P. Nelson, I. Hill, J.D. Conley, K. Blohm, C. Davidson, T.W. Sawyer, Therapeutic effects of cooling swine skin exposed to sulfur mustard. *Mil Med* 167(11) (2002) 939-943.
- [270] T.W. Sawyer, D. Risk, Effect of lowered temperature on the toxicity of sulphur mustard in vitro and in vivo. *Toxicology* 134(1) (1999) 27-37.
- [271] S.S. Anumolu, A.S. DeSantis, A.R. Menjoge, R.A. Hahn, J.A. Beloni, M.K. Gordon, P.J. Sinko, Doxycycline loaded poly(ethylene glycol) hydrogels for healing vesicant-induced ocular wounds. *Biomaterials* 31(5) (2010) 964-974.
- [272] K.M. Huh, Y.H. Bae, Sythesis and characterization of poly(ethylene glycol)/poly(L-lactic acid) alternatng multiblock copolymers. *Polymer* 40(22) (1999) 6147-6155.
- [273] C. Qiao, S. Jiang, D. Dong, X. Ji, L. An, B. Jiang, The Critical Lowest Molecular Weight for PEG to Crystallize in Cross-Linked Networks. *Macromol. Rapid Commun.* 25 (2004) 659-663.
- [274] M. Ash, I. Ash, Handbook of preservatives, Synapse Information Resources, Inc., Endicott, New York, 2004.
- [275] C.V. Uglea, Oligomer technology and applications, CRC press, Boca Raton, FL, 1998.
- [276] D.S. Jones, C.R. Irwin, A.D. Woolfson, J. Djokic, V. Adams, Physicochemical characterization and preliminary in vivo efficacy of bioadhesive, semisolid formulations containing flurbiprofen for the treatment of gingivitis. *J Pharm Sci* 88(6) (1999) 592-598.
- [277] M. Shibayama, H. Takahashia, H. Yamaguchia, S. Sakuraia, S. Nomura, Isothermal crystallization of end-linked poly(tetrahydrofuran) networks. *Polymer* 35(14) (1994) 2944-2951.
- [278] C. Ferrero, A. Munoz-Ruiz, M.R. Jimenez-Castellanos, Fronts movement as a useful tool for hydrophilic matrix release mechanism elucidation. *Int J Pharm* 202(1-2) (2000) 21-28.
- [279] J.M. Llabot, R.H. Manzo, D.A. Allemandi, Drug release from carbomer:carbomer sodium salt matrices with potential use as mucoadhesive drug delivery system. *Int J Pharm* 276(1-2) (2004) 59-66.

- [280] D.L. Munday, P.J. Cox, Compressed xanthan and karaya gum matrices: hydration, erosion and drug release mechanisms. *Int J Pharm* 203(1-2) (2000) 179-192.
- [281] J.K. Tessmar, A.M. Gopferich, Customized PEG-derived copolymers for tissue-engineering applications. *Macromol Biosci* 7(1) (2007) 23-39.
- [282] J. Crank, G.S.E. Park, *Diffusion in polymers*, Academic Press, London and New York, 1968.
- [283] P.L. Ritger, N.A. Peppas, A simple equation for description of solute release. II. Fickian and anomalous release from swellable devices. *J Control Release* 5 (1987) 37-42.
- [284] J. Siepmann, F. Lecomte, R. Bodmeier, Diffusion-controlled drug delivery systems: calculation of the required composition to achieve desired release profiles. *J Control Release* 60(2-3) (1999) 379-389.
- [285] R.W. Korsmeyer, R. Gurney, E. Doelker, P. Buri, N.A. Peppas, Mechanism of solute release from porous hydrophilic polymers. *Int J Pharm* 15 (1983) 25-35.
- [286] J.L. Hambrook, D.J. Howells, C. Schock, Biological fate of sulphur mustard (1,1'-thiobis(2-chloroethane)): uptake, distribution and retention of ³⁵S in skin and in blood after cutaneous application of ³⁵S-sulphur mustard in rat and comparison with human blood in vitro. *Xenobiotica* 23(5) (1993) 537-561.
- [287] S. Popiel, Z. Witkiewicz, M. Chrzanowski, Sulfur mustard destruction using ozone, UV, hydrogen peroxide and their combination. *J Hazard Mater* 153(1-2) (2008) 37-43.

10 CURRICULUM VITA

Siva Naga Sree Priya Anumolu

January 1981: Born in Vijayawada, Andhra Pradesh, India.

May 2003: Bachelor of Pharmacy, Nagarjuna University, Andhra Pradesh, India.

January 2010: Ph.D., Pharmaceutical Science, Rutgers University, New Brunswick, NJ.

Publications

Research articles

- **S. S. Anumolu**, Y. Singh, D. Gao, S. Stein and P. J. Sinko, “Design and evaluation of novel fast forming pilocarpine-loaded ocular hydrogels for sustained pharmacological response”, Journal of Controlled Release (2009), 137(2), 152-159.
- **S. S. Anumolu**, A. S. DeSantis, A. R. Menjoge, R. A. Hahn, J. A. Beloni, M. K. Gordon and P. J. Sinko, “Doxycycline loaded poly(ethylene glycol) hydrogels for healing vesicant-induced ocular wounds”, Biomaterials (2010), 31(5), 964-974.

Patent application

- P. J. Sinko, S. Stein, A. Menjoge, S. Gunaseelan, **S. S. Anumolu** and R. Navath, “Spray-on hydrogel comprising crosslinkable water soluble PEG polymers for dressings”, PCT Int. Appl. 2008, WO 2008133918 A1 20081106 AN 2008:1338746.